REPORT 72-8687

75°K VUILLEUMIER CRYOGENIC REFRIGERATOR

C. W. Browning
W. S. Miller
V. L. Potter
The Garrett Corporation
AiResearch Manufacturing Co.
2525 West 190th Street
Torrance, California

November 1972

Final Report for Task IV Model Fabrication

Prepared for

GODDARD SPACE FLIGHT CENTER
Greenbelt, Maryland 20771

REPORT 72-8687

75°K VUILLEUMIER CRYOGENIC REFRIGERATOR

C. W. Browning
W. S. Miller
V. L. Potter
The Garrett Corporation
AiResearch Manufacturing Co.
2525 West 190th Street
Torrance, California

November 1972

Final Report for Task IV Model Fabrication

Prepared for

GODDARD SPACE FLIGHT CENTER
Greenbelt, Maryland 20771

PREFACE

GENERAL

The 75°K Vuilleumier Cryogenic Refrigerator Program was administered by the Goddard Space Flight Center, Greenbelt, Maryland, under Contract No. NAS 5-21096. The NASA technical monitor for this contract was Mr. Max Gasser.

The analytical, fabrication and test program activities were completed by the AiResearch Manufacturing Company, a division of The Garrett Corporation, in Torrance, California. The program manager was C. W. Browning and the program engineer was D. K. Yoshikawa. Major contributors to this Task IV effort were V. L. Potter, mechanical design and model fabrication; C. W. Browning, thermodynamics and heat transfer; and W. Miller, thermodynamics and heat transfer.

OBJECTIVE

NASA earlier completed a systems feasibility study (Contract No. NAS 5-21039 of the Integrated Cryogenic Isotope Cooling Engine (ICICLE) system. In this ICICLE concept, a central cooling device provides all the refrigeration to sensors positioned remotely at various locations in the spacecraft. The cooling device configuration investigated during the study consisted of a heat-driven VM refrigerator.

The objective of the AiResearch program is to further evaluate the feasibility of the ICICLE concept through development of an engineering model of a VM refrigerator.

SCOPE OF WORK

The VM cryogenic engine program consists of six major tasks: (1) Task I, Preliminary Design; (2) Task II, Analytical and Test Programs; (3) Task III, Model Specification; (4) Task IV, Model Fabrication; (5) Task V, Heat Pipe Interface Designs and Specifications; and (6) Task VI, Ambient Heat Pipe.

This technical report describes the Task IV (Model Fabrication) phase of the VM cryogenic refrigerator program. The general requirement of the refrigerator is to produce 5 watts of cooling at 75°K after operating 2 to 5 years in a space environment. These Task IV accomplishments provide the basis for verifying that the required cooling will be attained.

Other reports already published during this program are: Final Report for Task I - Preliminary Design, AiResearch Report 70-6854; and Final Report for Task II - Analytical and Test Program, AiResearch Report 72-8497.

CONTENTS

CONTENTS (Cont)

ILLUSTRATIONS

ILLUSTRATIONS (Cont)

ILLUSTRATIONS (Cont)

TABLES

SECTION I

INTRODUCTION AND SUMMARY

INTRODUCTION

The progressing development of meterological and communication spacecraft requires increasingly sophisticated sensing devices. A coexisting requirement is the development of cryogenic refrigeration; the sensitivity and performance of certain advanced sensing devices is enhanced when cooled to cryogenic temperatures, while others must be cooled to cryogenic temperatures in order to function.

Most NASA space applications for cryogenic refrigeration require operational lifetimes of 1 to 5 years. State-of-the-art VM refrigerators, however, have life expectancies far less than the minimum acceptable for space applications. For this reason, NASA undertook the development of a long life cryogenic refrigeration system compatible with spacecraft requirements. The heat driven Vuilleumier (VM) cycle was the refrigeration system selected for development because of the following characteristics that are potentially advantageous for space applications: (1) long operating life due to low working stresses placed on bearings and internal seals, (2) use of thermal energy as the source of energy to drive the system, (3) small size and weight, (4) moderate efficiencies for low cooling capacity systems, and (5) low noise and vibration levels.

Government funded efforts in this area have shown significant progress in demonstrating most of the characteristics listed above. The main characteristic remaining to be demonstrated is long operating life. To demonstrate the feasibility of VM refrigerators for NASA applications, Contract NAS 5-21096 was entered into in November 1969 between AiResearch and the NASA Goddard Space Flight Center. The contract covered design, development and fabrication of an engineering model VM refrigerator. The primary design requirement of the unit being developed was long operating life, with a 2 year operating life specified as a minimum requirement and a 5 year life as a design goal.

The program under Contract No. NAS 5-21096 consisted of the following major tasks:

Task I	Preliminary Design
Task II	Analytical and Test Program
Task III	Model Specification
Task IV	Model Fabrication
Task V	Heat Pipe Interface Drawing and Specifications
Task VI	Ambient Heat Pipe

This report describes the Task IV effort which consisted of fabrication of the refrigerator, according to the design evolved in Task II, and performing the necessary tests to verify that the unit defined by the model specification (Task III) met with the expected high degree of success. Task V and Task VI were concerned with design and development of heat pipes for supplying heat to, or rejecting heat from, the VM refrigerator as well as coupling the refrigeration load to the refrigerator.

A brief description of the refrigerator design and the test system used during this program is given in Section 2 of this report. The design has several unique features which enhance its thermal and long life capabilities. The most outstanding of these are summarized below:

- Inorganic bearings provide minimum contamination of the working fluid as wear occurs
- Noncontacting dynamic internal seals are not subject to wear
- Monel cold regenerator provides nearly optimum thermal properties at cryogenic temperatures
- Extended-surface, forced-convection heat exchangers provide maximum heat transfer performance with minimum working fluid pressure drop
- Flow distributors located at critical points assure uniform working fluid distribution in the heat transfer devices

The test data, operating conditions, and design point performance verification are presented in Section 3. Section 3 also provides cross plots of the data which allow determination of off design performance over a wide range of operating parameters.

SUMMARY

Test results presented in this report show conclusively that the GSFC 5-watt Vuilleumier cryogenic refrigerator exceeds the required design point performance. There is also every indication that the required performance will be attained after a period of 2 years of continuous operation. In addition, the thermal efficiency is believed to be the maximum ever attained with a Vuilleumier cycle refrigerator: 36.7 watts input power per watt of cooling at $75^{0}K$. This high thermal efficiency, of course, is in part due to the high cooling capacity of the unit compared with other available units. The losses are more easily minimized in larger scale units.

Bearing run in friction prevented operation of the engine at design speed during the tests described herein. No other mechanical problems were encountered and the machine operated properly upon first assembly. Design point performance was attained at reduced engine speed and hot end temperature, thus indicating a performance margin.

This program has developed and verified the design concepts required for production of a long-life, flight-type Vuilleumier cryogenic refrigerator. No problems are envisioned in extending this technology to flight hardware capable of two to five years of unattended operation.

The Vuilleumier cryogenic refrigerator described in this report has been shipped to GSFC, where it will undergo further performance and endurance testing.

SECTION 2

SYSTEM DESCRIPTION

INTRODUCTION

This section provides a complete description of assemblies and components that make up the VM refrigerator. A general description of the complete VM machine, including performance characteristics, is followed by a detailed description of all mechanical assemblies and components. The functional effect of the various mechanical parts of the machine on the operating fluid medium completes the section.

VM REFRIGERATOR CHARACTERISTICS

General Hardware Description

The GSFC VM refrigerator (Figures 2-1, 2-2) is a gas cycle, reciprocating machine, intended to operate continuously for five years at a design speed of 400 rpm. Figure 2-2 shows the refrigerator assembly prior to, and after, installation of the drive motor and cooling subassembly.

The primary energy input to the refrigerator is thermal energy in the form of radiant heat, but moving components (two displacers) are also required so that the VM cycle will function properly. The moving components are two displacers (hot and cold) driven by connecting rods attached to a crankshaft (Figure 2-1). Crankshaft throws are arranged 90-degrees apart so that the hot displacer is leading the cold displacer. The crankshaft is driven by an electric motor magnetically coupled to one end of the shaft. The displacers travel inside cylinders surrounded by packed-bed regenerators which in turn, are enclosed in pressure shells joined to the crankshaft housing, making the entire assembly pressure tight.

The displacers are arranged in a horizontally opposed configuration, simplifying crankcase and sump heat exchanger analysis and mechanical design and minimizing the interaction between the hottest and coldest parts of the system.

The primary energy input to the refrigerator is at an interface at the hot end of the machine. For this design, an electric heater is used to simulate the end of the heat pipe. In a spacecraft application, energy would be transferred to the hot end of the machine through a high-temperature heat pipe from the spacecraft heat source.

Proper operation of the VM cycle also depends on rejecting heat in the crankcase-sump region. The refrigerator rejects heat to water cooling coils that interface with the crankcase and sump heat exchanger. These water cooling coils replace the ammonia heat pipes which would be used in a flight-type system.

The refrigeration heat load is absorbed at the cold end via the cold-end heat exchanger. For test purposes, the refrigeration load is generated by a

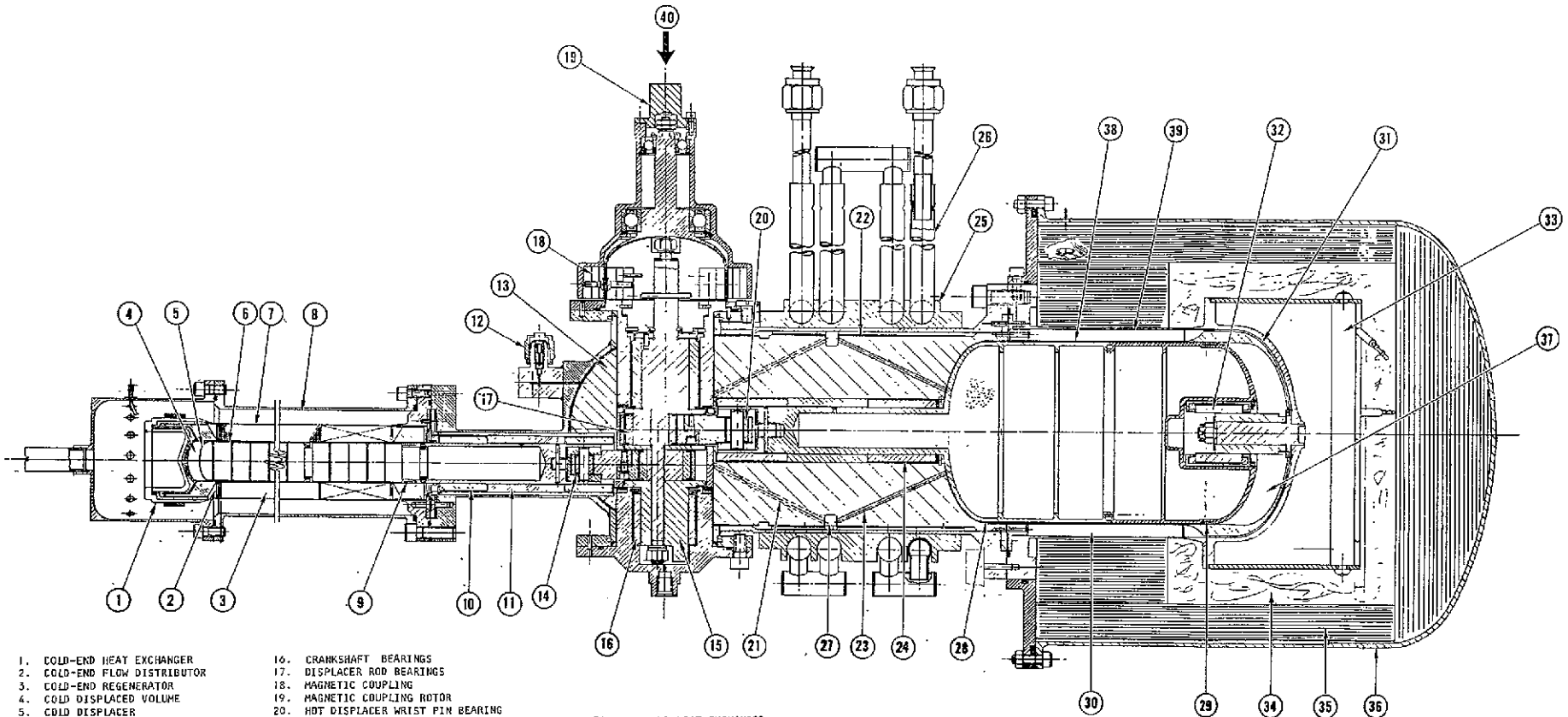

1. COLD-END HEAT EXCHANGER
2. COLD-END FLOW DISTRIBUTOR
3. COLD-END REGENERATOR
4. COLD DISPLACED VOLUME
5. COLD DISPLACER
6. INNER WALL COLD REGENERATOR
7. OUTER WALL COLD REGENERATOR
8. DEWAR OUTER WALL
9. COLD-END SEAL
10. COLD-END LINEAR BEARINGS
11. BEARING SUPPORT
12. FILL VALVE
13. SUMP FILLER BLOCK
14. COLD DISPLACER WRIST PIN BEARING
15. CRANKSHAFT ASSEMBLY
16. CRANKSHAFT BEARINGS
17. DISPLACER ROD BEARINGS
18. MAGNETIC COUPLING
19. MAGNETIC COUPLING ROTOR
20. HOT DISPLACER WRIST PIN BEARING
21. PORTS TO CRANKCASE SUMP
22. SUMP HEAT EXCHANGER
23. PORTS TO BACKSIDE OF HOT DISPLACER
24. HOT END LINEAR BEARINGS
25. COPPER COOLING COLLAR
26. WATER COOLING TUBES
27. SUMP HEAT EXCHANGER FLOW DISTRIBUTION SLOT
28. HOT DISPLACER
29. HOT-END SEAL
30. HOT-END REGENERATOR
31. HOT-END HEAT EXCHANGER
32. HOT-END BEARING
33. HOT-END HEATER
34. MIN-K INSULATION
35. FIBERGLASS INSULATION
36. HOT-END INSULATION VACUUM JACKET
37. HOT DISPLACED VOLUME
38. INNER WALL HOT REGENERATOR
39. OUTER WALL HOT REGENERATOR
40. POINT OF LABORATORY MOTOR SHAFT INPUT POWER

L- 73758

Figure 2-1. GSFC 5-Watt, 75°K, Vuilleumier Cryogenic Refrigerator

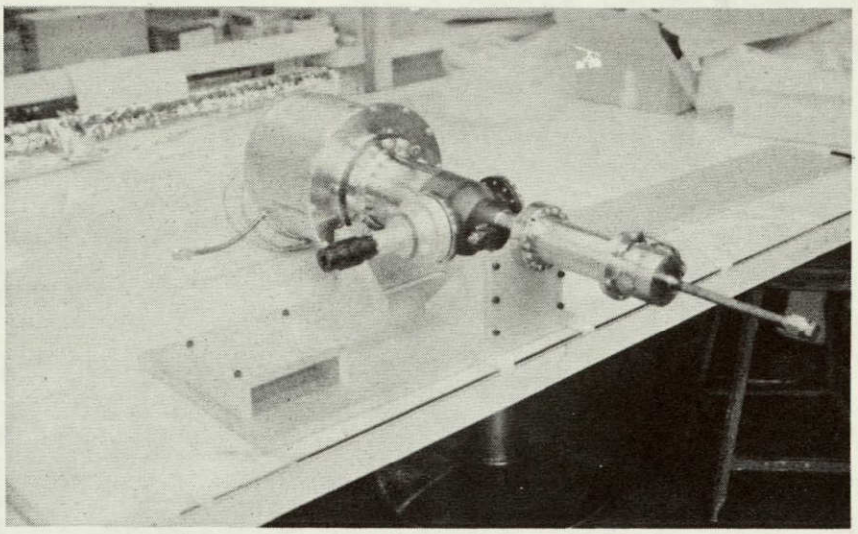

a. VM Refrigerator Prior to Installation of Drive Motor and Cooling Subassembly.

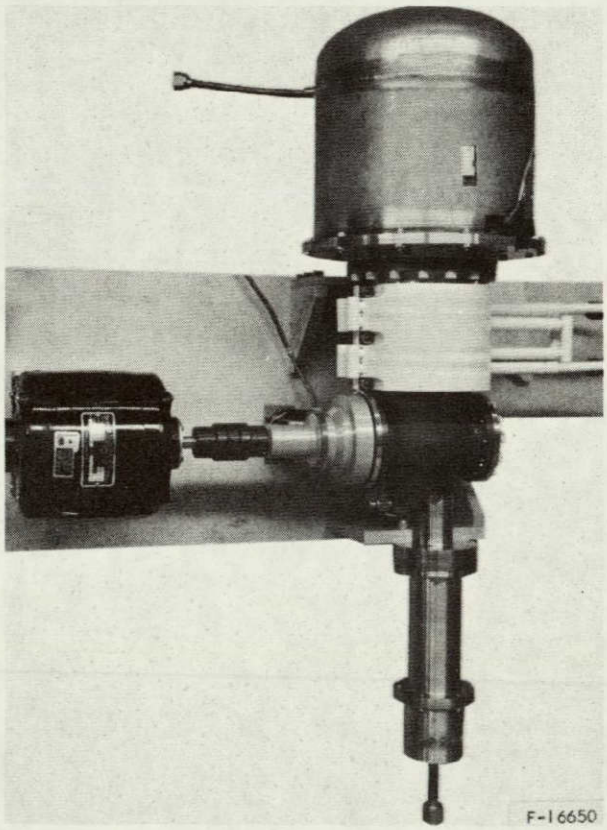

F-16928

b. VM Refrigerator with Drive Motor and Cooling Subassembly Installed

Figure 2-2. GSFC 5-Watt, 75°K VM Cryogenic Refrigerator Assembly

small resistance-type heater attached to the exterior surface of the cold-end heat exchanger. In a spacecraft system, the cold-end heat exchanger would interface with a cryogenic heat pipe, providing the thermal link to the devices being cooled.

Performance and Design Summary

The major performance and design parameters for the GSFC VM refrigerator are summarized in Table 2-I.

COMPONENT DETAIL DESCRIPTIONS

The following paragraphs briefly describe the major mechanical components of the VM refrigerator.

Crankshaft Assembly

Crankshaft design is based on the need to install full journal bearings in the main support area as well as the connecting rods. This was accomplished by a take-apart design--fabricating one connecting rod and one main bearing journal as a removable component. In this way, the main support and a connecting rod bearing could be inserted as a full bearing rather than split halves. The removable bearing surfaces are retained in place by a machined-screw stud and nut arrangement. When all members of the crankshaft are installed, the nut is torqued down on the screw stud, with all bearing surfaces retained in their proper position by strategically located dowel pins. All materials of construction consist of PH 13-8 Mo with flame sprayed tungsten carbide in those areas requiring wear resistance. The assembled crankshaft is shown in Figure 2-3.

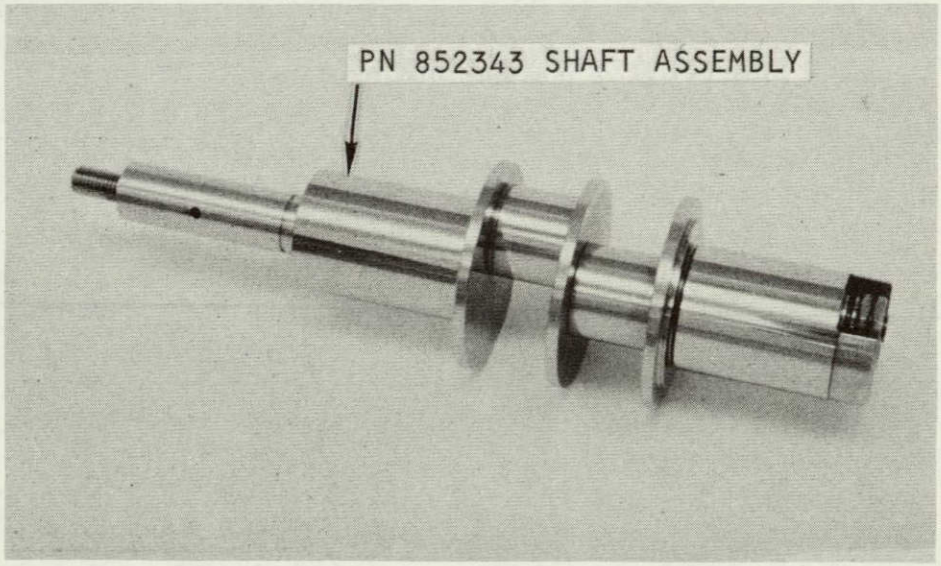

Figure 2-3. Assembled Crankshaft

TABLE 2-I

GSFC VUILLEUMIER REFRIGERATOR
PERFORMANCE AND DESIGN SUMMARY NOMINAL VALUES

WORKING FLUID	Helium
TEMPERATURES	
Interfaces	
Cold End Interface	130°R (72.2°K)
Sump Interface	600°R (333.3°K)
Hot End Interface	1660°R (922.2°K)
Gas	
Cold End	125°R (69.4°K)
Sump	620°R (344.4°K)
Hot End	1630°R (905.6°K)
PRESSURES	
Charge Gas Pressure at 535°R	550 psia (37.44 atm)
Maximum Cycle Pressure	800 psia (54.46 atm)
Minimum Cycle Pressure	682 psia (46.43 atm)
THERMAL INPUT/OUTPUT	
Net Cold End Refrigeration	23.87 Btu/hr (7.0 w)
Cold End Insulation Loss	0.375 Btu/hr (0.11 w)
Total Hot End Input Power	1011.0 Btu/hr (296.5 w)
Hot End Insulation Loss	78.43 Btu/hr (23 w)
Hot End Input Less Insulation Loss	932.6 Btu/hr (273.5 w)
Motor Input Power	32 w
Heat Rejection Rate	1041.8 Btu/hr (305.5 w)
DRIVE MOTOR POWER INPUT	
Speed	400 rpm
Shaft Power	16 w
Electrical Input Power	32 w max.
COLD DISPLACER SPECIFICATIONS	
Length	5.0 in. (12.7 cm)
Bore	0.840 in. (2.134 cm)
Stroke	0.45 in. (1.14 cm)
Displaced Volume	0.2511 $in.^3$ (4.115 cm^3)

HOT DISPLACER SPECIFICATIONS	
Length	6.08 in. (15.44 cm)
Bore	3.86 in. (9.8 cm)
Stroke	0.60 in. (1.52 cm)
Displaced Volume	6.841 $in.^3$ (112.1 cm^3)
COLD REGENERATOR SPECIFICATIONS	
NOTE: Cold regenerator consists of 2 sections: (1) Sump end with screens and (2) Cold end with spheres.	
Sump End	
Configuration	Annular
Matrix Material	Monel screen, 150 mesh
Inside Diameter	0.874 in. (2.22 cm)
Outside Diameter	1.554 in. (3.95 cm)
Frontal Area	1.297 $in.^2$ (8.37 cm^2)
Length	1.87 in. (4.75 cm)
Matrix Hydraulic Diameter	0.00791 in. (0.0201 cm)
Matrix Surface/Volume Ratio	367 $\frac{in.^2}{in.^3}$ (144.5 $\frac{cm^2}{cm^3}$)
Void Fraction	0.725
Cold End	
Configuration	Annular
Matrix Material	Monel spheres. 0.0075 in. dia (0.01905 cm)
Inside Diameter	0.874 in. (2.22 cm)
Outside Diameter	1.554 in. (3.95 cm)
Frontal Area	1.297 $in.^2$ (8.37 cm^2)
Length	2.53 in. (6.43 cm)
Matrix Hydraulic Diameter	0.003197 in. (0.00812 cm)
Matrix Surface/Volume Ratio	488.5 $\frac{in.^2}{in.^3}$ (192.3 $\frac{cm^2}{cm^3}$)
Void Fraction	0.39
HOT REGENERATOR SPECIFICATIONS	
Configuration	Annular
Matrix Material	Stainless Steel, 100 mesh
Inside Diameter	3.85 in. (9.78 cm)

HOT REGENERATOR SPECIFICATIONS--Continued	
Outside Diameter	4.37 in. (11.10 cm)
Frontal Area	3.18 $in.^2$ (20.52 cm^2)
Length	3.3 in. (8.38 cm)
Matrix Hydraulic Diameter	0.01132 in. (0.0287 cm)
Matrix Surface/Volume Ratio	256 $\frac{in.^2}{in.^3}$ (100.7 $\frac{cm^2}{cm^3}$)
Void Fraction	.725
DEAD VOLUMES	
Cold End at 125°R	0.16438 $in.^3$ (2.694 cm^3)
Sump at 620°R	8.804 $in.^3$ (144.27 cm^3)
Hot end at 1630°R	2.050 $in.^3$ (33.59 cm^3)
Cold Regenerator at 372°R	3.112 $in.^3$ (51.00 cm^3)
Hot Regenerator at 1125°R	8.140 $in.^3$ (133.39 cm^3)
HEAT TRANSFER CHARACTERISTICS	
Cold Heat Exchanger	
Maximum Pressure Drop	0.615 $lb/in.^2$ (0.0419 atm)
Conductance (ηhA)	15.68 Btu/hr-°R (8.277 w/°K)
Hot Heat Exchanger	
Maximum Pressure Drop	0.155 $lb/in.^2$ (0.0106 atm)
Conductance (ηhA)	48.84 Btu/hr-°R (25.78 w/°K)
Sump Heat Exchanger	
Maximum Pressure Drop	0.012 $lb/in.^2$ (0.00082 atm)
Conductance (ηhA)	113 Btu/hr-°R (59.65 w/°K)

Magnetic Drive Rotors

The crankshaft is driven by a motor, magnetically coupled to the crankshaft. The inner magnetic rotor (Figure 2-4) is attached to one end of the crankshaft. When coupled magnetically with the outer magnetic rotor (Figure 2-5), the crankshaft is driven without the need for a rotating shaft seal to retain the helium operating fluid. The rotor itself is fabricated from an aluminum alloy with a nickel plated carbon steel inner magnet keeper ring pressed into it. Alnico -9 permanent magnets are attached at eight points. Each magnet is terminated in a carbon steel pole piece conforming to the contour of the pressure dome wall in order to minimize the gap between the magnet and the wall. This procedure assures the maximum magnetic coupling between the driven and driving magnet pairs.

To minimize the eddy current losses resulting from magnet pairs rotating around the cylindrical section of the pressure dome, heat treated Inconel 718 is utilized for maximum strength. This allows for a clearance of only a few thousandths of an inch between the magnet pole pieces and pressure wall. The outer rotor is constructed in the same manner as the inner except that it is mounted on a stud machined into the pressure dome. The bearings utilized for the outer rotor are conventional sealed, grease-packed type.

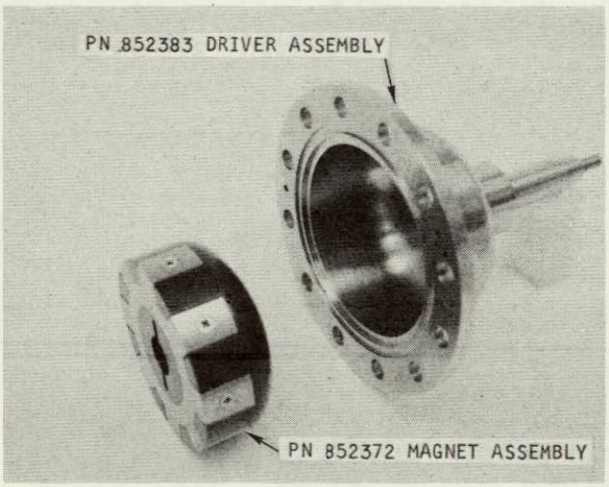

Figure 2-4. Inner Magnetic Rotor Assembly

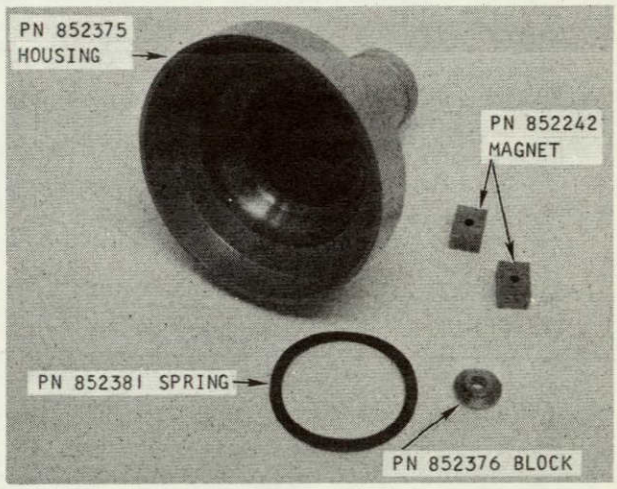

Figure 2-5. Outer Magnetic Rotor Assembly

Connecting Rods

The connecting rods are constructed of titanium alloy to minimize weight and provide high strength. In addition, the surfaces are tiodized to assure maximum anti-galling characteristics with respect to the insertion of the bearings at both ends and the assembly screw, located in the center of the rod. The screw was required to allow fabricating the rod in two pieces which in turn allows the final assembly of the displacers to the crankshaft by merely dropping the displacer into its respective cylinder, installing the connecting rod/bearing subassembly onto the crankshaft and inserting the connecting rod retention screw. Figure 2-6 shows the two pieces of a connecting rod.

Displacers

Both displacers are cylindrical in shape, enclosed by domes on the outboard ends. The cylindrical inboard ends have rod bearings for the connecting rods that attach the displacers to the crankshaft. The displacers travel in linear bearings that support the displacer during its back-and-forth movement. The hot-end displacer dome is designed with an additional linear bearing at the hot end to support the larger size.

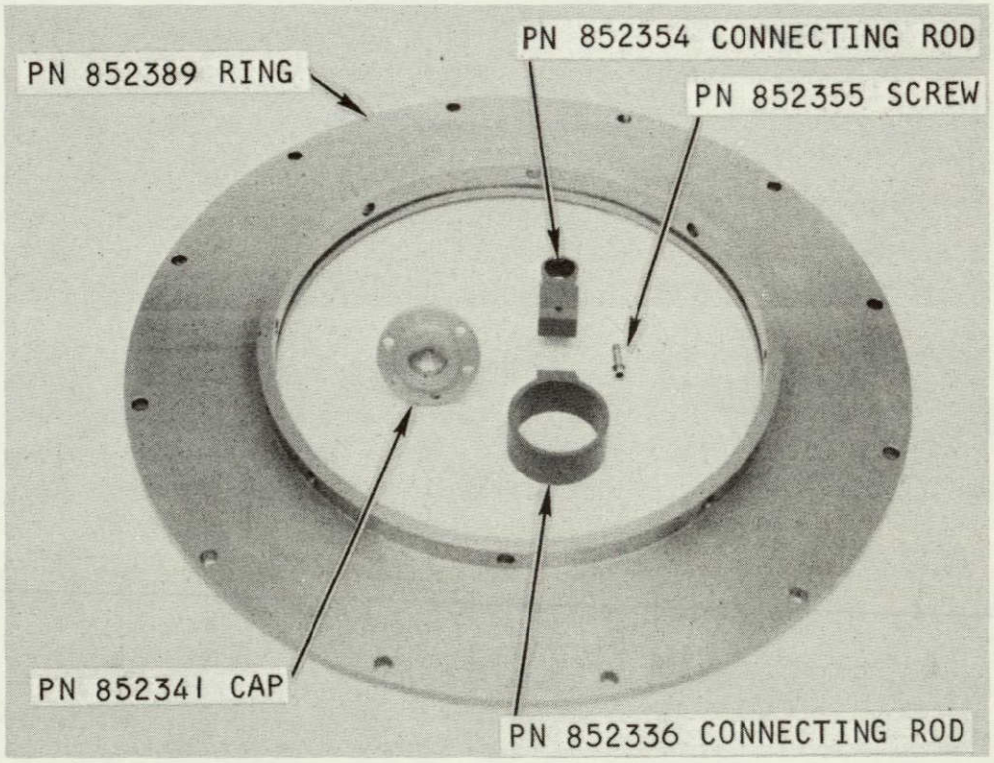

Figure 2-6. Connecting Rod Components

1. Hot Displacer

The helium gas is shuttled through the hot regenerator by hot displacer movement. The displacer consists of a heat treated Inconel 718 shell with intermittent integral reinforcing ribs. This allows minimizing displacer wall thickness to reduce the axial heat transfer and weight. The displacer is constructed so that the internal volume is hermetically sealed, isolating it from the active volume of the refrigerator. The displacer internal volume is filled with a low conductivity fiberous material (microquartz) to reduce convective heat transfer within the displacer. Prior to the final closure weld, the component is evacuated and backfilled with an argon-helium gas mixture. Helium is introduced as a tracer gas to allow a mass spectrometer leak check of the final closure weld and the argon for reduced heat transfer. Figure 2-7 shows the completed hot displacer assembly.

Two bearings are provided to support the displacer: one at the hot end and the other at the sump end. The shaft on the cold end of the displacer rides on the sump support bearing surface. This shaft is flame sprayed with tungsten carbide and matches the requirements of the mating Boeing Compact journal linear bearings. The connecting rod is connected through an adaptor that is bolted and pinned to the displacer, after shimming the displacer within the hot regnerator for proper clearance. The opposing hot end of the displacer has been fitted internally with a Boeing Compact bearing surface which mates with the shaft assembly contained within the pressure dome.

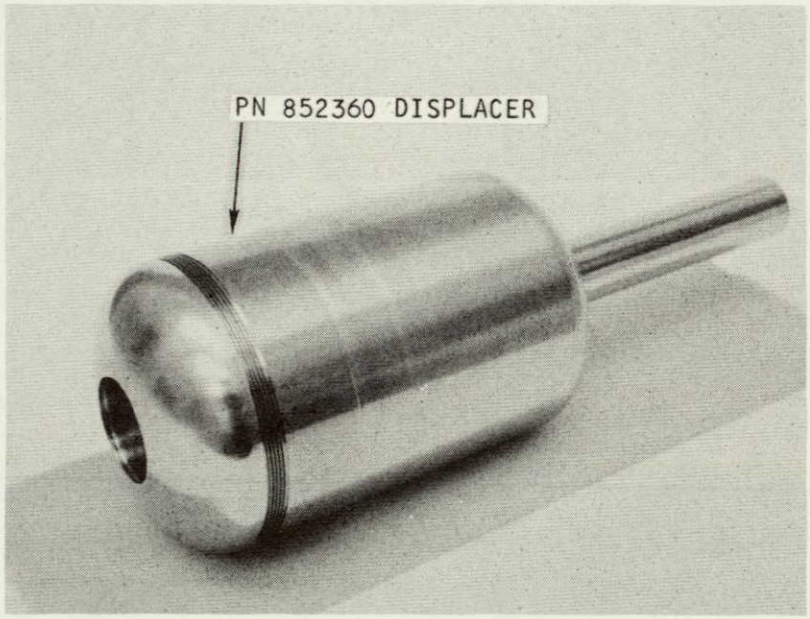

F-16932

Figure 2-7. Hot Displacer Assembly

2. Cold Displacer

Construction techniques and materials utilized in fabrication of the cold displacer are the same as those of the hot displacer. One exception is that three sections were initially machined, then welded together to form the entire displacer assembly. As with the hot displacer, the interior was packed with microquartz prior to final weld closeout and the shaft at the sump end has been flame sprayed with tungsten carbide to mate with the Boeing Compact bearing. This assembly and the inner wall of the cold regenerator are shown in Figure 2-8.

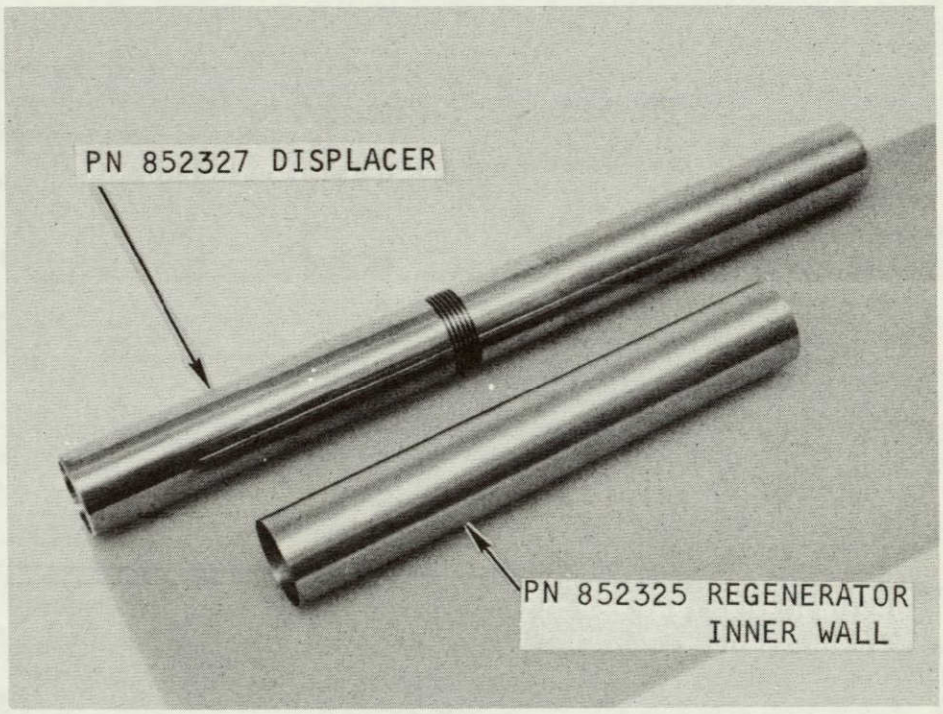

Figure 2-8. Cold Displacer Assembly and Cold Regnerator Inner Wall

Bearings

The bearings described below are shown in Figures 2-9 and 2-10.

1. Crankshaft Bearings

The crankshaft bearings, as with the hot and cold displacer bearings, utilize Boeing Compact 6-84-1 as the bearing surface. The bearing adjacent to the magnetic drive rotor has two thrust faces to accommodate the location of the crankshaft with respect to the sump housing and the respective displacers. The outboard bearing provides only radial support to the crankshaft thus allowing the shaft to float, seeking proper position as dictated by the inboard bearing. In both cases, the Boeing Compact has been fitted into PH 13-8 Mo shells to provide the needed protection.

Each main bearing is retained in an Inconel 718 housing attached either directly (outboard bearing) or indirectly (inboard bearing) to machined flanges on the sump section. These flanges are dowel pinned to the bearing housings for consistent orientation and positioning.

2. Wrist Pin Bearing

The connecting rod wrist pin bearings are also composed of Boeing Compact 6-84-1 encased in a PH 13-8 Mo sheath. The wrist pin itself is fine-finished tungsten carbide. This entire assembly is contained within an adaptor assembly that is threaded into the aft end of the respective displacer assemblies. The adaptor is shimmed into place after the displacer is located properly and is pinned to prevent rotation.

3. Hot Displacer Sump Bearing

This bearing is heat-shrunk into the aluminun sump-filler block and is also fitted with a snap ring retainer. This precaution compensates for the wide temperature range that the combination is subjected to. The bearing housing is fabricated from PH 13-8 Mo heat treated steel and the bearing is Boeing Compact 6-84-1. The mating surface on the hot displacer is flame sprayed with tungsten carbide. Two independent Boeing Compact bearing surfaces are provided to assure long life.

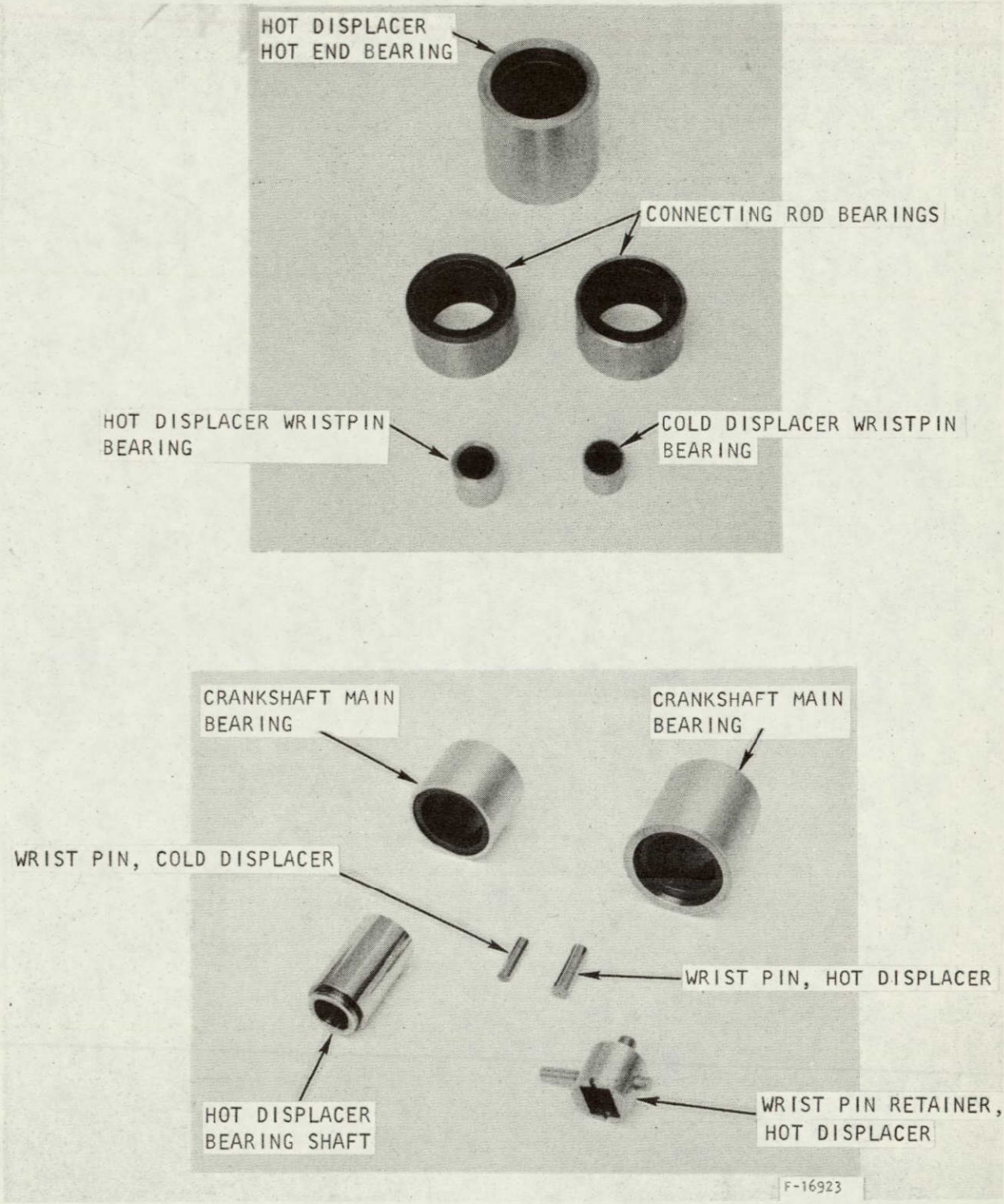

Figure 2-9. VM Refrigerator Bearings

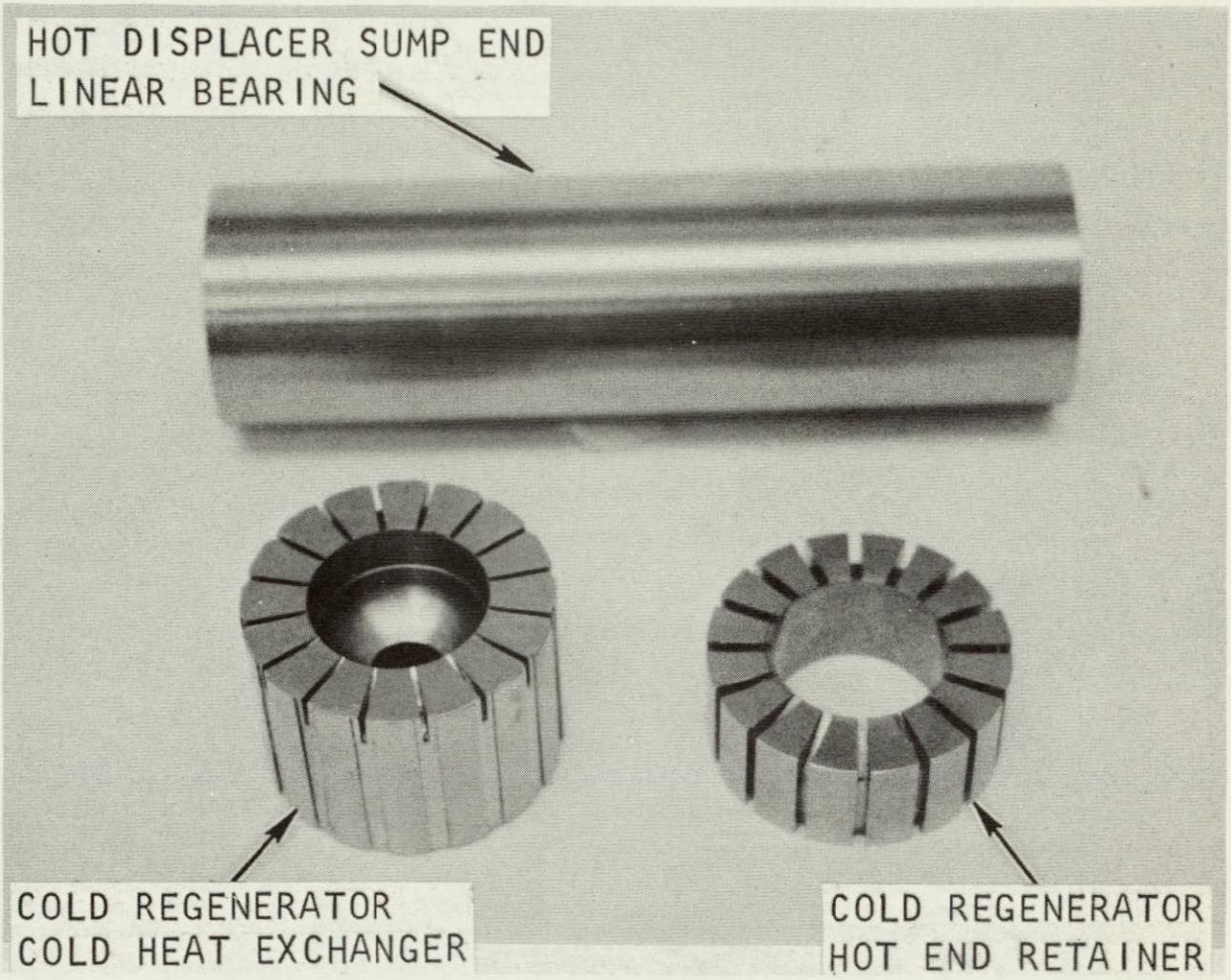

Figure 2-10. Hot Displacer Bearing, Cold-End Heat Exchanger, and Cold Regnerator Retainer

4. Hot Displacer Hot-End Bearing

The hot displacer hot end support consists of a sleeve of Boeing Compact 6-84-1, retained in the bore within the hot displacer. The mating surface is detonation flame-sprayed chrome carbide on a hardened Inconel 718 substrate. Both assemblies are retained in their relative positions by mechanical fasteners and are maintained in a fixed position by a spring retainer mechanism. The bearing is shown in Figure 2-11 prior to assembly into the hot displacer.

5. Cold Displacer Bearing

The final bearing in the system is utilized for cantilever support of the cold displacer. This bearing is also fabricated from Boeing Compact 6-84-1 with a PH 13-8 Mo case. In this case, however, the outside diameter of the bearing sheath is fitted with a series of axial grooves to provide a flow path from the sump section into the cold regenerator, Figure 2-12 shows the bearing inserted into the sump housing of the machine. The bearing is retained in the Inconel 718 portion of the sump assembly by a compression plate containing a series of flow passages corresponding to a flow redistribution annulus machined at the end of the bearing assembly. An additional flow distribution channel has been provided near the sump end of the bearing to assure adequate flow distribution and thus minimize thermal discontinuities.

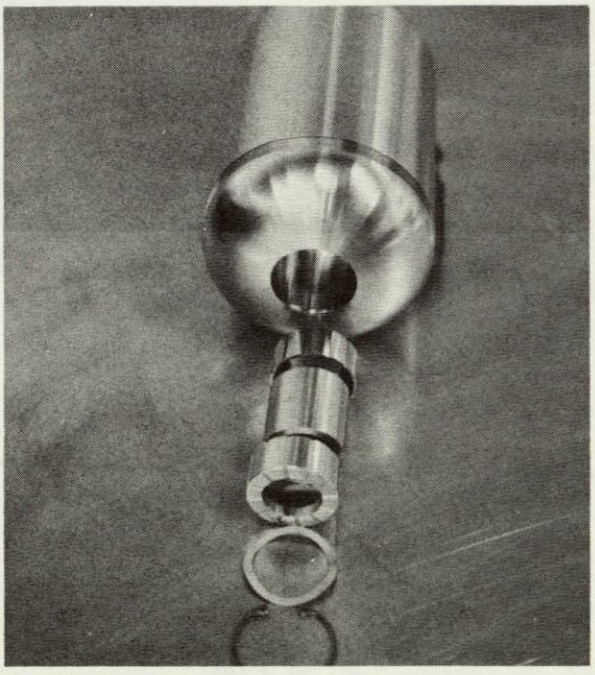

Figure 2-11. Hot-End Bearing and Displacer

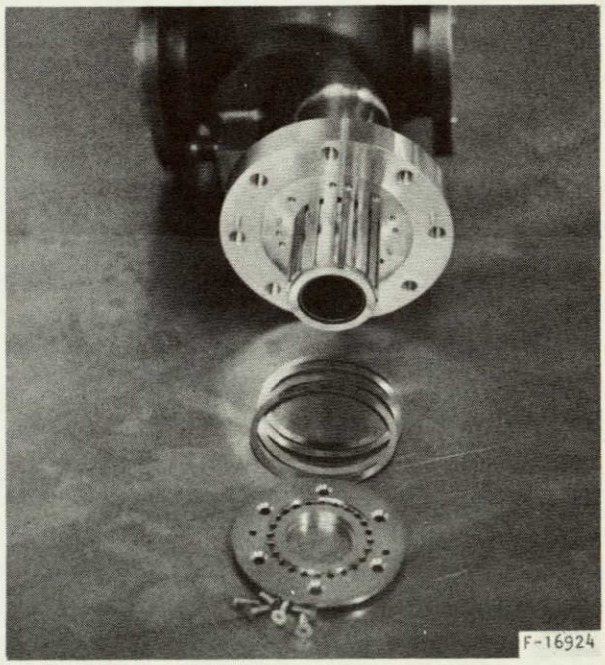

Figure 2-12. Cold Displacer Bearing

Cold Regenerator

The cold displacer regenerator is also an annular design utilizing a combination of screen and solid sphere packing. The screen used is shown in Figure 2-13. A constant compressive load is maintained on the packing material in order to eliminate orientation, packing, or thermal contraction problems. The inner wall of the regenerator forms the cylinder in which the cold displacer moves. This component has been fabricated from a 300 series stainless steel. The regenerator outer wall, which also forms the cold end pressure vessel wall, is composed of heat treated Inconel 718 with a thin cross section to minimize axial heat transfer.

Flow distribution plates are provided in the cold end of the regenerator to assure good flow and temperature distribution at the entrance to the regenerator. An extended heat transfer surface is also included to assure adequate heat transfer area at the cryogenic heat pipe interface located at the outer periphery of the extreme end of the cold cylinder.

Cold-End Pressure Dome

The cold-end pressure shell is a cylinder with a flange on one end and an intricate closure complex on the opposite. A vacuum jacket completely surrounds the cold-end pressure shell.

Cold End Insulation

Thermal protection of the cold end is accomplished by providing numerous wraps of aluminized mylar around the exterior surface of the cold regenerator and cold heat exchanger. A vacuum dewar, placed around the entire assembly, provides the low pressure necessary to optimize the performance of this multi-layer insulation. The materials utilized for the vacuum jacket are stainless steel for fabrication simplicity and high-vacuum integrity.

Hot Regenerator

The hot displacer regenerator is an annular design which contains stainless steel screen packing. The screen packing material is shown in Figure 2-13. The inner diameter of the annular regenerator also serves as the cylinder wall for the hot displacer. The hot end of the inner liner is an integral part of the hot regenerator. This element is fabricated from Inconel 718, heat treated for high strength and long term thermal stability. The packing material of the regenerator is maintained under a constant uniform load by a spring member located at the sump--hot displacer interface flange.

Hot-End Pressure Dome

Heat from the thermal source is transferred through the Inconel 718 wall of the pressure dome to the helium gas circulating within the hot-end heat exchanger. The Inconel pressure vessel provides an integral mounting structure for the hot bearing which supports the hot end of the hot displacer. The material has been heat treated to provide an optimized stress level and heat transfer combination. This element of the machine is shown in Figure 2-14.

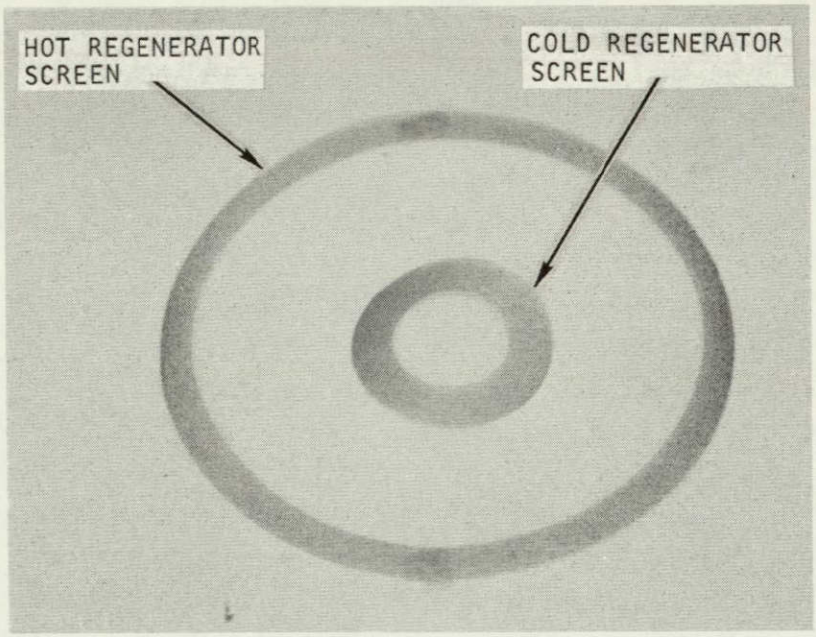

Figure 2-13. Hot and Cold Regenerator Screen Packing

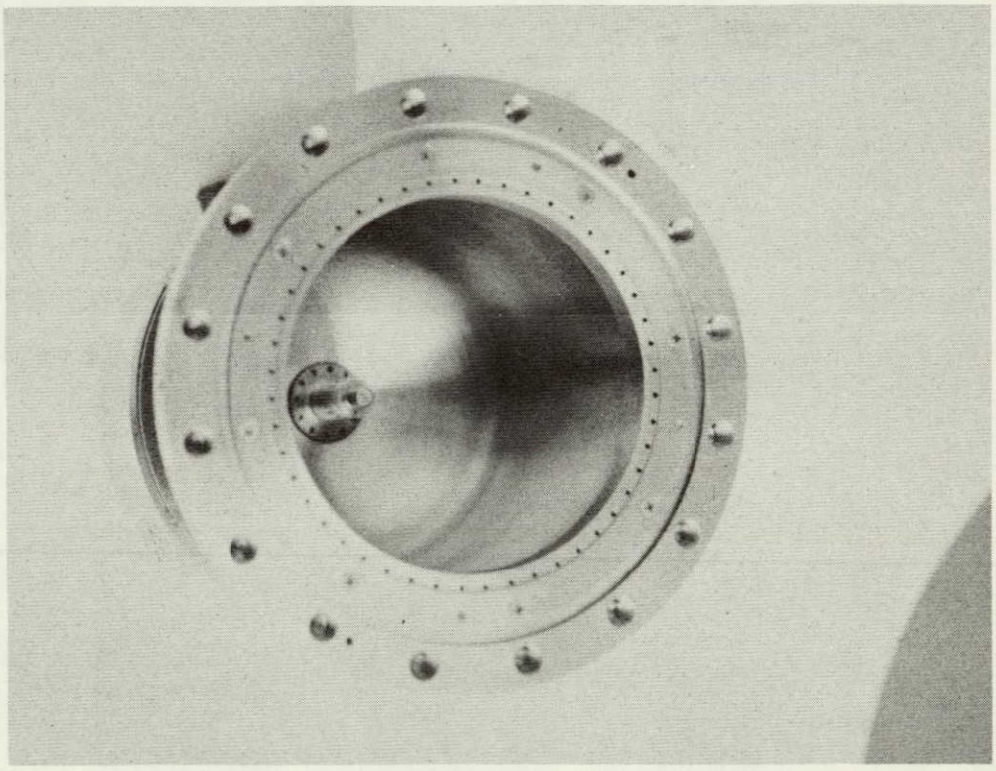

F-16931

Figure 2-14. Hot-End Pressure Dome

Hot-End Vacuum Jacket

Thermal isolation of the 1200°F source for the hot end is provided by an evacuated laminated insulation system composed of Johns Manville Min-K immediately surrounding the highest temperature portion followed by fiberglass blankets. A stainless steel cylinder provides physical protection of these insulation elements as well as a leak proof outer vacuum shell and is terminated at the hot displacer dome flange.

Instrumentation for the hot end is brought through the insulation layers and terminated at glass to metal seals located in the lower portion of the vacuum barier. In addition to instrumentation, additional conductors supply operating power for the hot end heater.

Hot-End Heater

The hot-end heater, which simulates the hot heat pipe that would be used in the spaceflight configuration of the refrigerator, provides the primary energy input to the machine. The heater is a Cal-Rod heating element enclosed in a stainless steel sheath which is coiled and brazed to an Inconel 718 disc. The Inconel 718 disc is physically separated from the hot-end heat exchanger to simulate the condenser-end of the hot heat pipe. The heater and disc assembly is shown in Figure 2-15.

Sump Subassembly

The main sump housing of the refrigerator is a multipiece unit of welded and heat treated Inconel 718. The sump housing is shown in Figure 2-16. The sump consists principally of the main cylindrical section (terminated in a hemispherical dome) with two smaller cylinders that protrude from the sides. Flanges, welded to the cylinders, act as the main crankshaft support members. Each support member is fitted with a pressure dome that also functions as a support for the main crankshaft bearings. An integral part of one dome is a thin-walled cylindrical section through which a magnetic coupling drives the crankshaft via a laboratory type motor. Eddy current losses through this thin cylindrical section are minimized by utilizing heat treated Inconel 718.

Each entry into the sump area of the machine is fitted with a flange and threaded insert retention system for easy access. This was considered necessary to maintain maximum flexibility in this prototype VM and satisfy the requirement for removal and replacement of components for rapid evaluation.

An offset-fin copper heat exchanger is brazed to the interior surface of the cylindrical section of the sump enhancing heat transfer to the outer surface of the sump section, and from there the rejection of waste heat to an

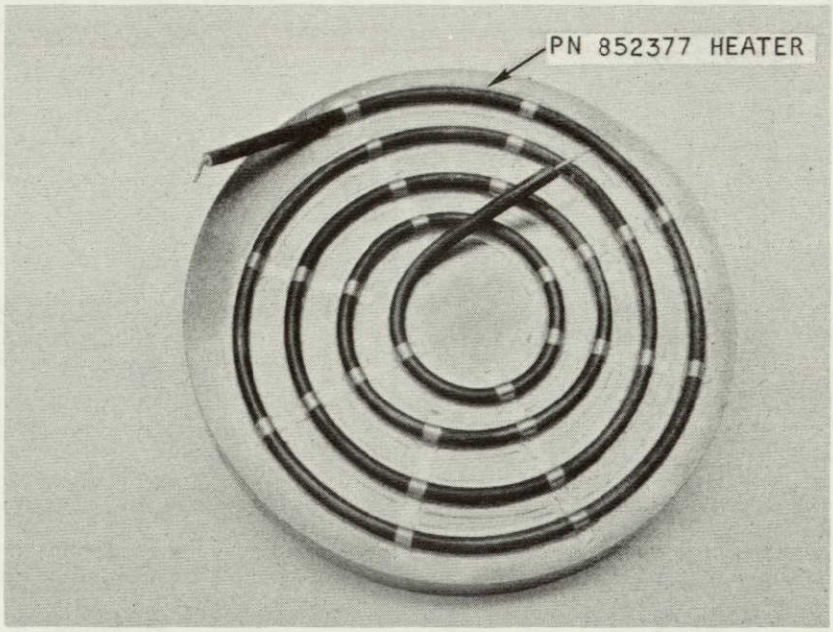

Figure 2-15. Hot-End Heater and Disc Assembly

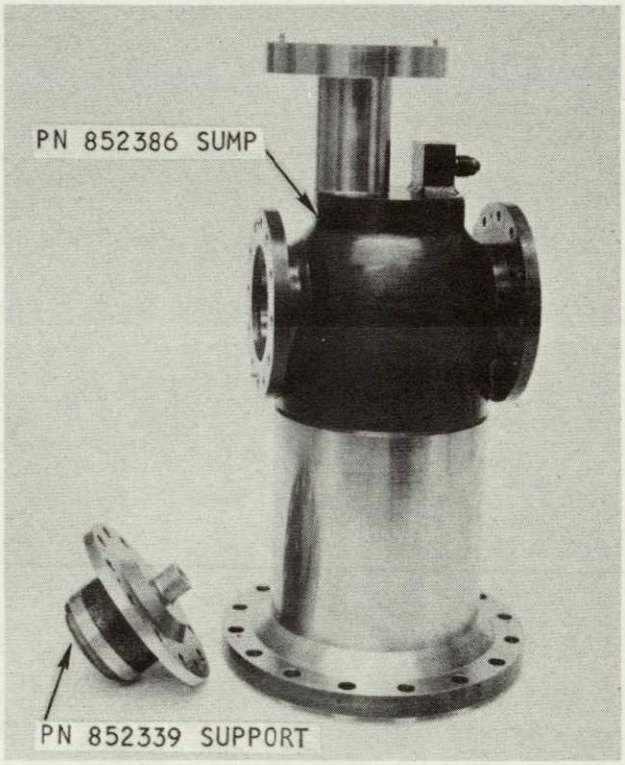

F-16921

Figure 2-16. Sump Housing

ambient heat pipe or laboratory cooling collar system. This heat exchanger is shown in Figure 2-17. The heat transfer coefficient at the interface between the sump outer surface and the inside diameter of the heat pipe (or cooling collar) is improved by using an indium foil insert, 0.003 in. thick between the two surfaces.

The bearing support member for the cold displacer, the interface flange for the cold regenerator and pressure vessel, and the dewar vacuum jacket for the cold-end heat exchanger are machined on the domed end of the sump. A system filler and shutoff valve, and a port for introduction of a minimized volume pressure transducer, are located adjacent to the cold displacer bearing housing.

Sump Filler Block

Dead volume in the VM sump section is reduced by an aluminum filler block fitted in this section. The block acts as the inner annulus surface for the heat exchanger area, supports or contains the hot displacer ambient temperature bearing and acts as the flow distributor in the transition from the full sump diameter to that of the cold displacer regenerator.

The filler block is fitted with a flow redistribution channel, minimizing radial thermal and flow maldistribution as a result of channeling. In addition, ports in the filler block duct gas from the aft portion of the hot displacer and crankshaft areas into the main gas flow streams thereby minimizing pressure drop.

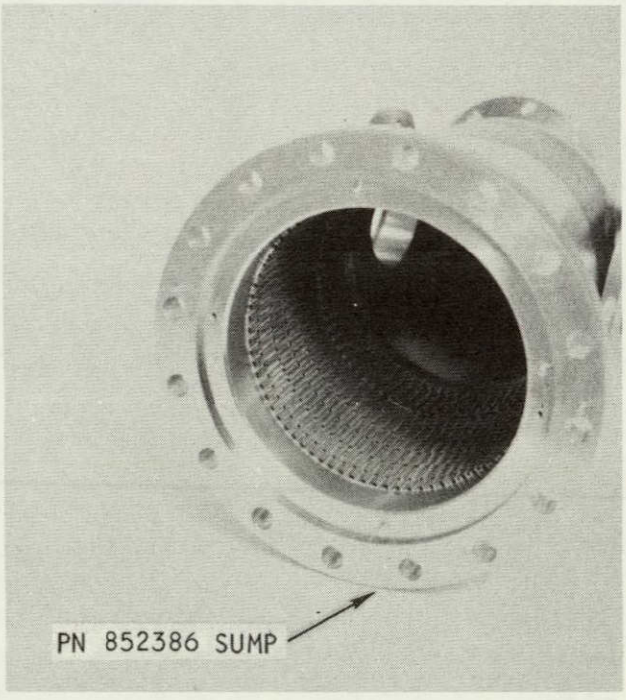

F-16922

Figure 2-17. Sump Housing with Heat Exchanger Installed

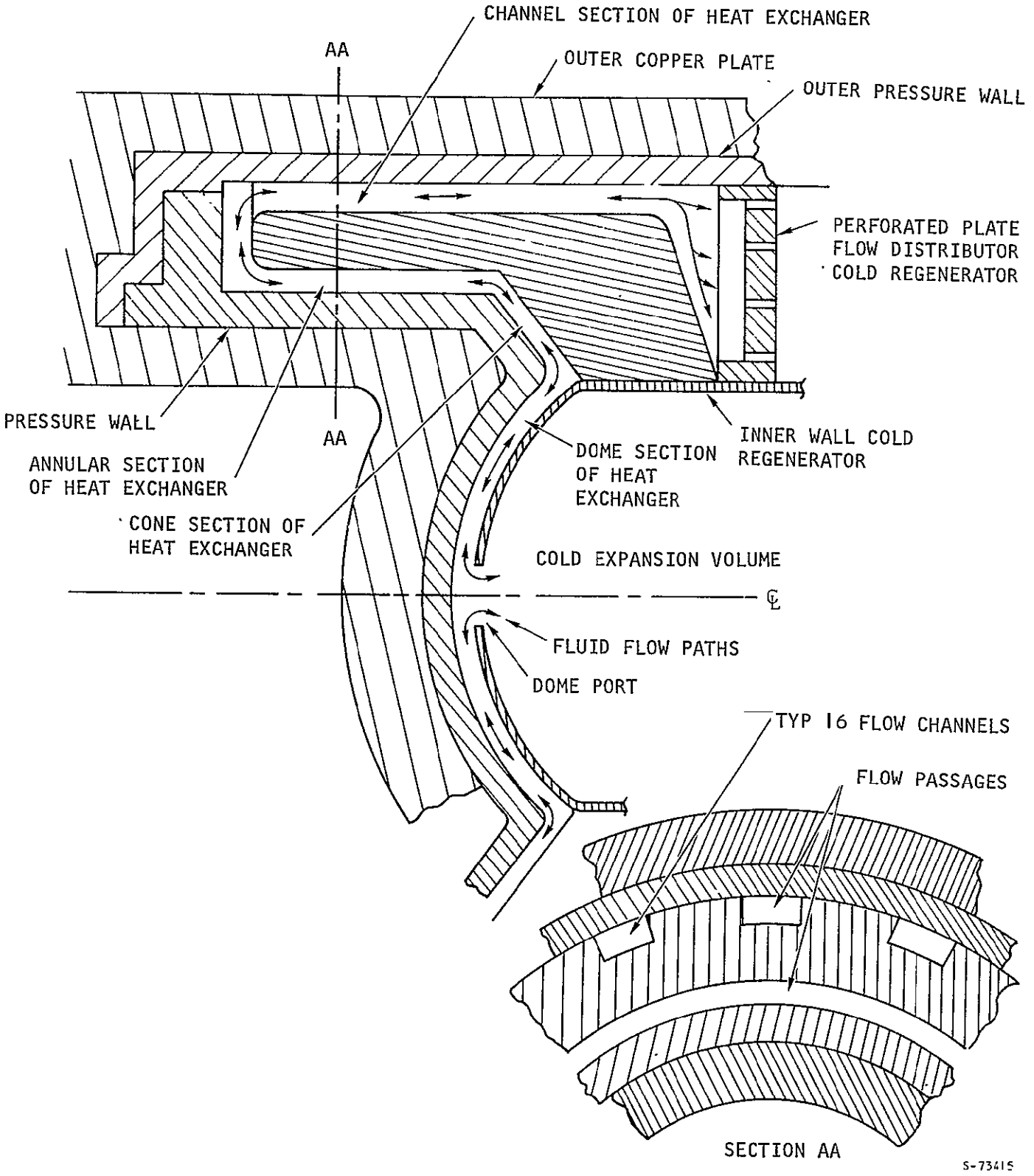

Figure 2-18. Cold End Heat Exchanger Configuration

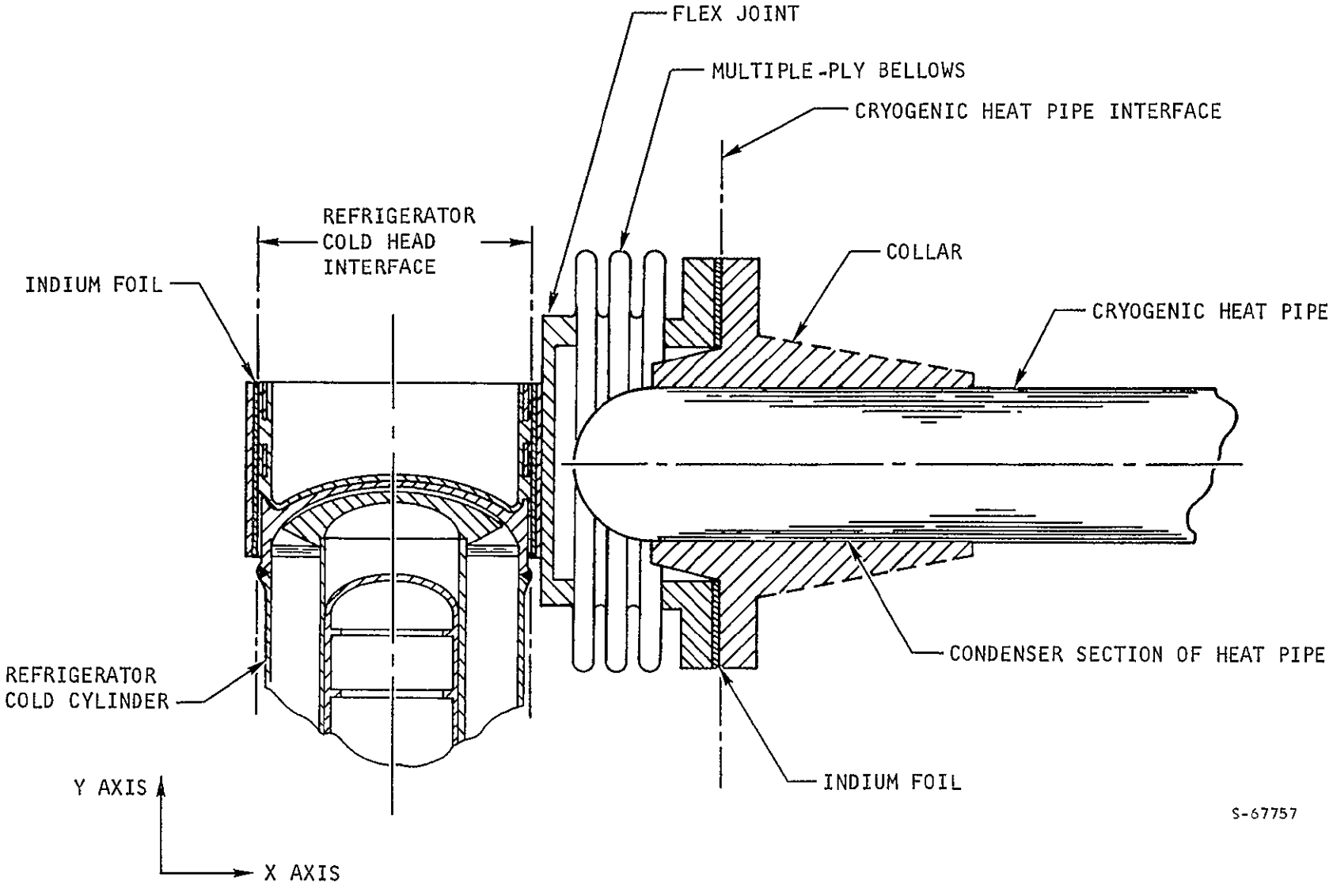

Figure 2-19 Interface Joint Design

The flow distributor (Figure 2-20) consists of a perforated plate with standoff rings that forms an annular cavity. The distributor is located between the cold-end heat exchanger and the low temperature end of the cold regenerator. The ratio of axial-to-circumferential pressure drop is adjusted to allow circumferential flow around the annular cavity in sufficient quantity to redistribute any non-uniformity in flow entering either face of the distributor.

The characteristics of the flow distributor are given in Table 2-2.

TABLE 2-2

COLD END FLOW DISTRIBUTOR CHARACTERISTICS

Parameter	Value
Dimensions	
Outside diameter, in.	1.552
Inside diameter, in.	0.880
Annular cavity depth, in.	0.045
Ring thickness, in.	0.025
Hole diameter, in.	0.020
Plate thickness, in.	0.040
Number of holes	80
Void volume, cu. in.	0.055
Pressure drop ratio $\frac{\Delta P_{axial}}{\Delta P_{circ}}$	12
Maximum axial pressure drop, psi	0.1

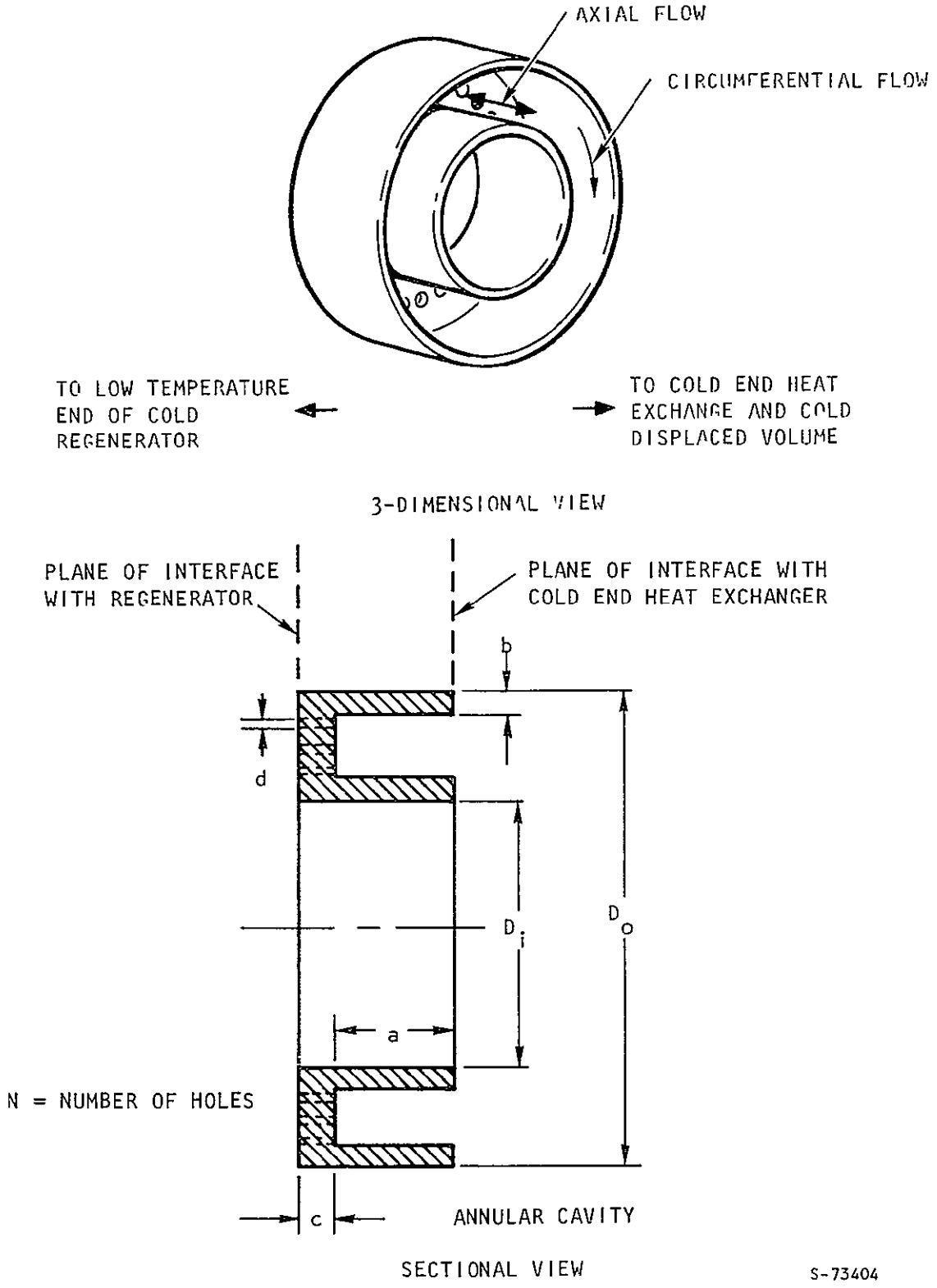

Figure 2-20. Cold End Flow Distributor Configuration

Cold Regenerator

The cold regenerator is one of the most important components of the VM refrigerator. The regenerator is used to cool incoming gas as it enters the cold expansion volume of the machine. The expansion process of the gas further reduces the gas temperature thereby providing the required cooling at the cold end. After absorbing heat from the refrigeration load, the gas then is exhausted through the regenerator where it regains previously stored energy. This exhaust process reestablishes the temperature profile in the regenerator for cooling the incoming gas during the next cycle.

An efficient regenerator performs the following functions: (1) absorbs heat from the gas stream while at nearly the same temperature as the gas, (2) stores this energy without significant temperature changes in a given locality, and (3) resupplies the energy to the gas stream when the flow reverses direction, again while as near as possible to the gas stream temperature. To accomplish these functions, the regenerator packing (1) is a material with a very large heat capacity relative to that of the gas, (2) has a high heat transfer coefficient, high thermal diffusivity as well as a large heat transfer area, and (3) is of a configuration that limits the amount of axial conduction through the packing and minimizes gas flow pressure drop.

The cold regenerator is an annular configuration with monel spheres as the matrix material. This configuration yields the best overall performance and monel has superior heat capacity as compared to other candidate materials.

The cold regenerator contains small diameter monel shot in the section of the regenerator toward the cold end heat exchanger. This shot size is 0.0075 in. diameter. The smaller diameter shot provides for increased heat transfer in the cold end of the regenerator.

The screen matrix packing used in the warm end of the cold regenerator reduces the pressure drop since gas density is relatively low in this section and the velocities correspondingly higher. Additionally, the influence of higher dead volume associated with the screen packing is less due to the low gas density. Shot used in the cold end provides maximum heat capacity per unit volume and minimizes the dead volume associated with the lower temperatures.

Design of Cold End Seals

The cold end seals function to control the rate of leakage which bypasses the cold regenerator. This function is critical since leakage past the seals can result in a significant loss in thermal performance. Seal leakage bypasses the regenerator by flowing through the annular space between the cold displacer and cold cylinder walls. At low leakage rates, the displacer and cylinder walls effectively regenerate the leakage fluid temperatures and the resulting thermal losses are small. As leakage rates increase, the walls can no longer function as an effective regenerator, and significant losses in overall thermal performance occur.

The cold end sealing system is shown in Figure 2-21. Seals incorporated in the cold end sealing system, from the cold end toward the sump end of the cold displacer, are as follows:

(a) An 0.945 in. long, close-fit annular seal with a clearance between the inner wall of the regenerator and the seal of 0.0025 in. maximum.

(b) A 5-groove labyrinth seal with a tip clearance of 0.0025 in., a groove spacing of 0.05 in., and a nominal tip width of 0.005 in.

(c) The first linear bearing which acts as an annular seal with a clearance of 0.0004 in. and a length of 1.0 in.

(d) The linear bearing support member which acts as an annular seal with a clearance of 0.0035 in. and a length of 1.69 in.

(e) The second linear bearing which is identical to the first.

The physical arrangement of the machine is such that these sealing elements are in series.

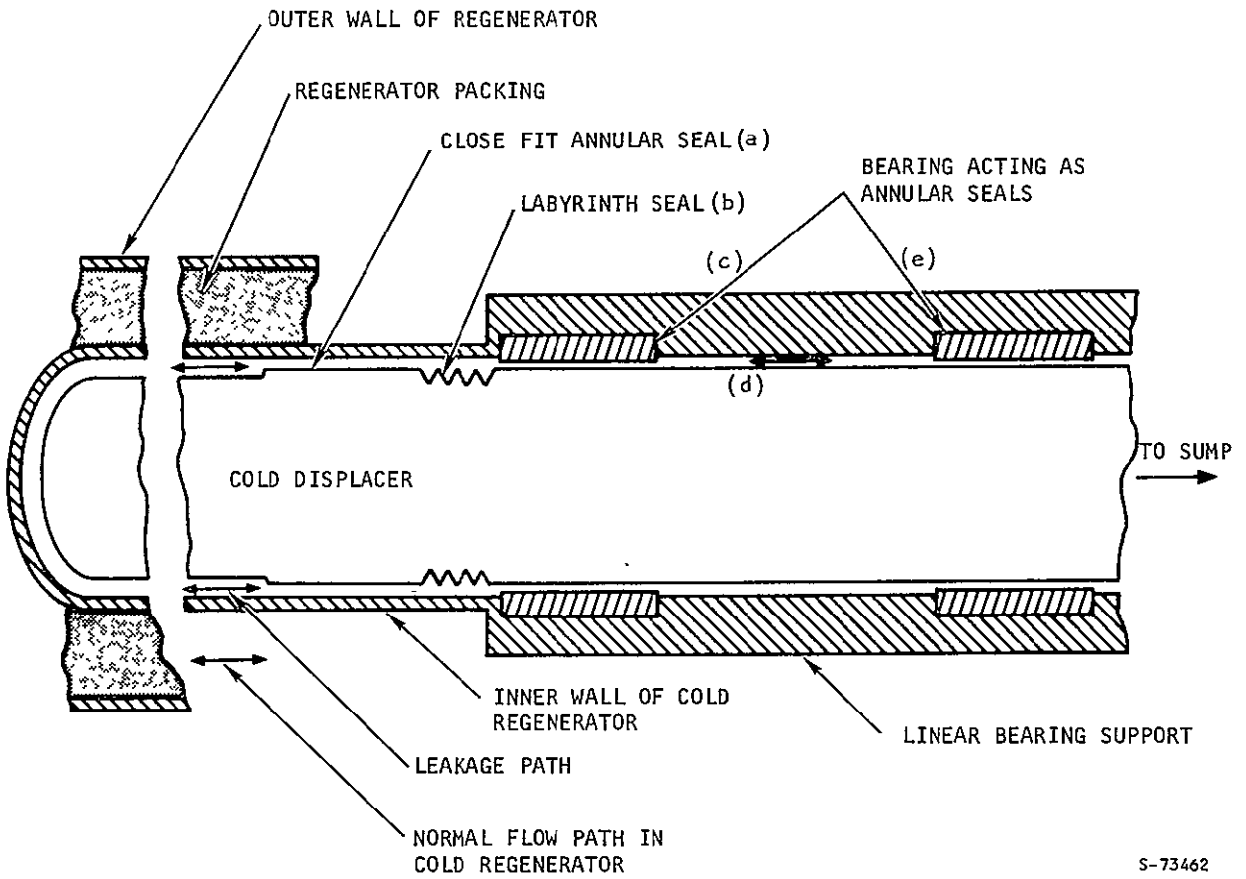

Figure 2-21. Cold Displacer Sealing Design Configuration

Hot Regenerator

The hot regenerator is an annular configuration similar to the cold regenerator and functions to regenerate the temperature of the working fluid as it cycles in the refrigerator between the hot end and sump active volumes.

The full screen matrix rather than a packed bed of spheres or a combination of screens and spheres, minimizes pressure drop, which is a major factor in the hot-end of the machine due to drive motor requirements.

Hot-End Heat Exchanger

The hot-end heat exchanger functions to transfer heat to the working fluid of the VM refrigerator, providing the energy input necessary to drive the system.

The hot-end heat exchanger configuration is shown in Figure 2-22.

Flow enters and exits the heat exchanger at it's interface with the hot displaced volume through ports cut in the heat exchanger inner wall. Considering flow from the hot volume, flow from the ports into the heat exchanger is initially radially outward around the dome of the refrigerator in flow passages between the pressure vessel wall and the heat exchanger inner wall. The number of flow passages increase at two points as the flow progresses radially outward. The number and size of passages--formed by ribs machined on the inner heat exchanger wall--promote high rates of heat transfer while maintaining a low pressure drop. From the heat exchanger dome section, the flow enters flow passages between ribs in the cylindrical section (Section A-A, Figure 2-22) and then passes on to the hot regenerator. For flow toward the hot volume, the flow paths described above are reversed.

Heat transfer to the working fluid is accomplished by both primary and secondary heat transfer surfaces. The primary heat transfer surface consists of segments of the pressure vessel wall which form the outer boundary of the flow passages in both the dome and cylindrical sections of the heat exchanger. Heat transfers directly into the working fluid from this surface. The secondary surface consists of the heat exchanger inner wall including the ribs. Here, heat is conducted from the exterior through the ribs to the inner wall and then into the working fluid. This secondary heat transfer surface is approximately 85 percent as effective as the primary surface.

Hot-End Seal Leakage

The hot-end seal functions to control the leakage rate of the working fluid which bypasses the hot regenerator. Leakage bypasses the regenerator by flowing through the annular space between the hot displacer and the inner wall of the regenerator. Excessive leakage results in a loss in thermal performance.

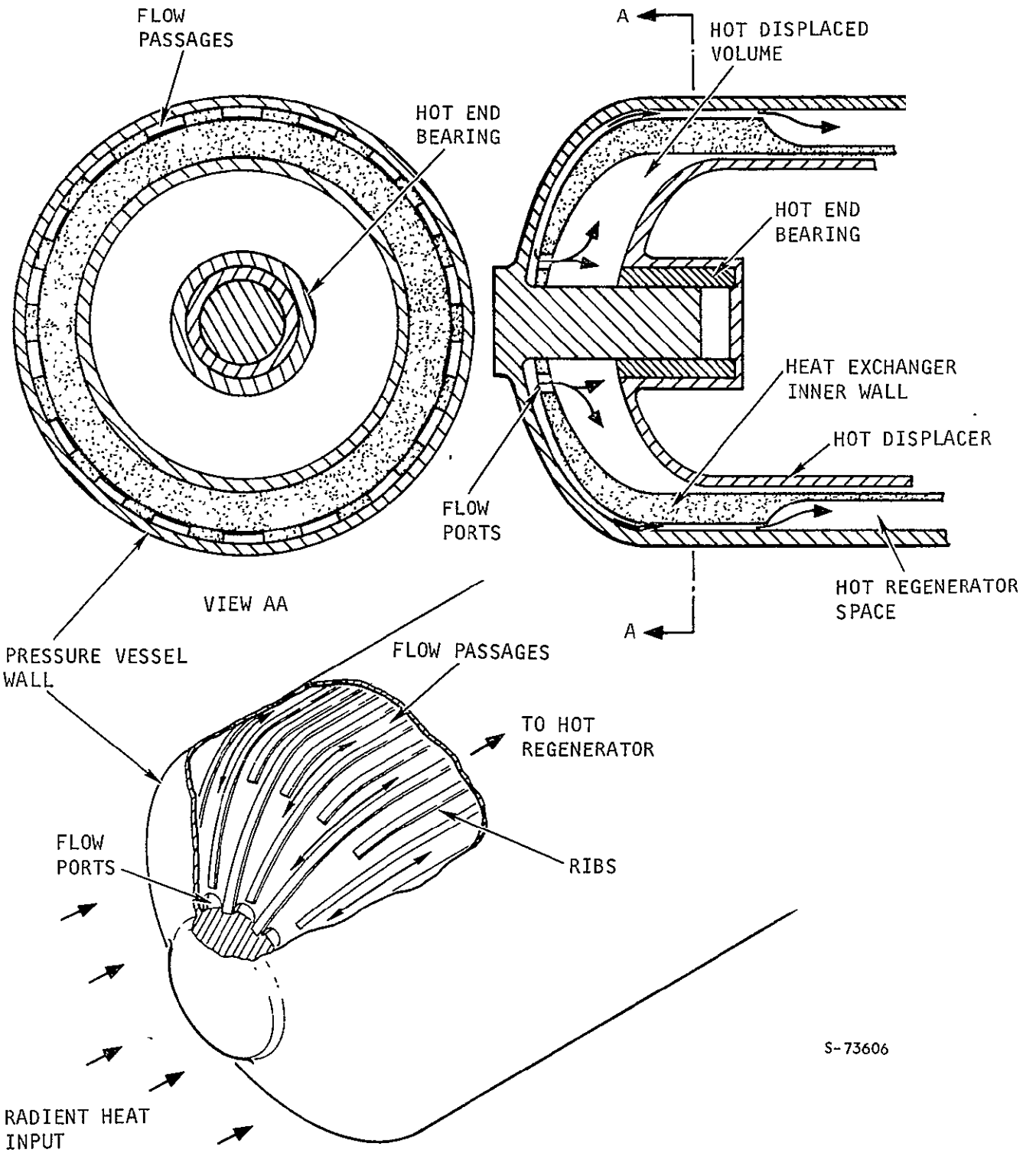

Figure 2-22. Hot-End Heat Exchanger

At low leakage rates, the hot displacer and cylinder walls effectively regenerate the leakage fluid temperature and the resulting thermal losses are small. As the leakage rates increase, the walls can no longer function as an effective regenerator; thus significant losses in overall thermal performance result.

The hot-end seal configuration (Figure 2-23) consists of the following two elements, from the hot end toward the sump end: (1) a 5-groove labyrinth seal with a tip clearance of 0.0025 in., a groove spacing of 0.05 in., and a nominal tip width of 0.005 in. and (2) a 1.0 in. long close fit annular seal with a clearance between the inner wall of the regenerator and the seal of 0.0025 in. maximum.

These sealing elements are similar to those used in the cold-end seal except for the diameter. One major difference is the use of linear bearings as part of the sealing system for the cold end. The bearings are not used in the hot-end seal and thus the performance of this seal is independent of wear (or operational time).

It should be noted that the seal is located in the highest temperature region possible within the machine. The leakage rate is an inverse function of the temperature; therefore, this location minimizes the leakage rate for a given seal configuration.

Hot-End Insulation Losses and Heater Temperature

The GSFC refrigerator hot-end is designed to simulate the interface between a VM refrigerator and a thermal power source, supplying energy to the refrigerator via a hot heat pipe. The hot-end interface and adjacent elements of the refrigerator are insulated from the surroundings to avoid excessive thermal losses from the hot-end of the machine.

The configuration of the hot-end insulation and heater assembly is shown in Figure 2-24. Heat is supplied to the refrigerator hot-end heat exchanger by a coiled resistance heater element brazed to the backside of an Inconel 718 plate (disc). The plate is physically separated from the hot-end heat exchanger to simulate the condenser-end of a hot heat pipe. The primary mode of heat exchange between the heater plate and hot-end heat exchanger is radiation; some heat is also transferred by conduction through the heater support.

In operation, the heat exchanger temperature will generally be somewhat below 1660°R and is never allowed to exceed this temperature due to structural limitations. Lower heat exchanger temperatures result in lower heater temperatures for the same input power level; thus the heater will never exceed 2000°R (1540°F). Since the heater elements can withstand continuous operation at 2060°R (1600°F), burn-out problems are avoided. The heater leads are terminated on the heater plate where good thermal contact can be maintained between the leads, heater element and plate. This prevents sections of the heater from reaching elevated temperatures (above that of the plate) as a result of being insulated from the plate and reduces potential burn-out problems;

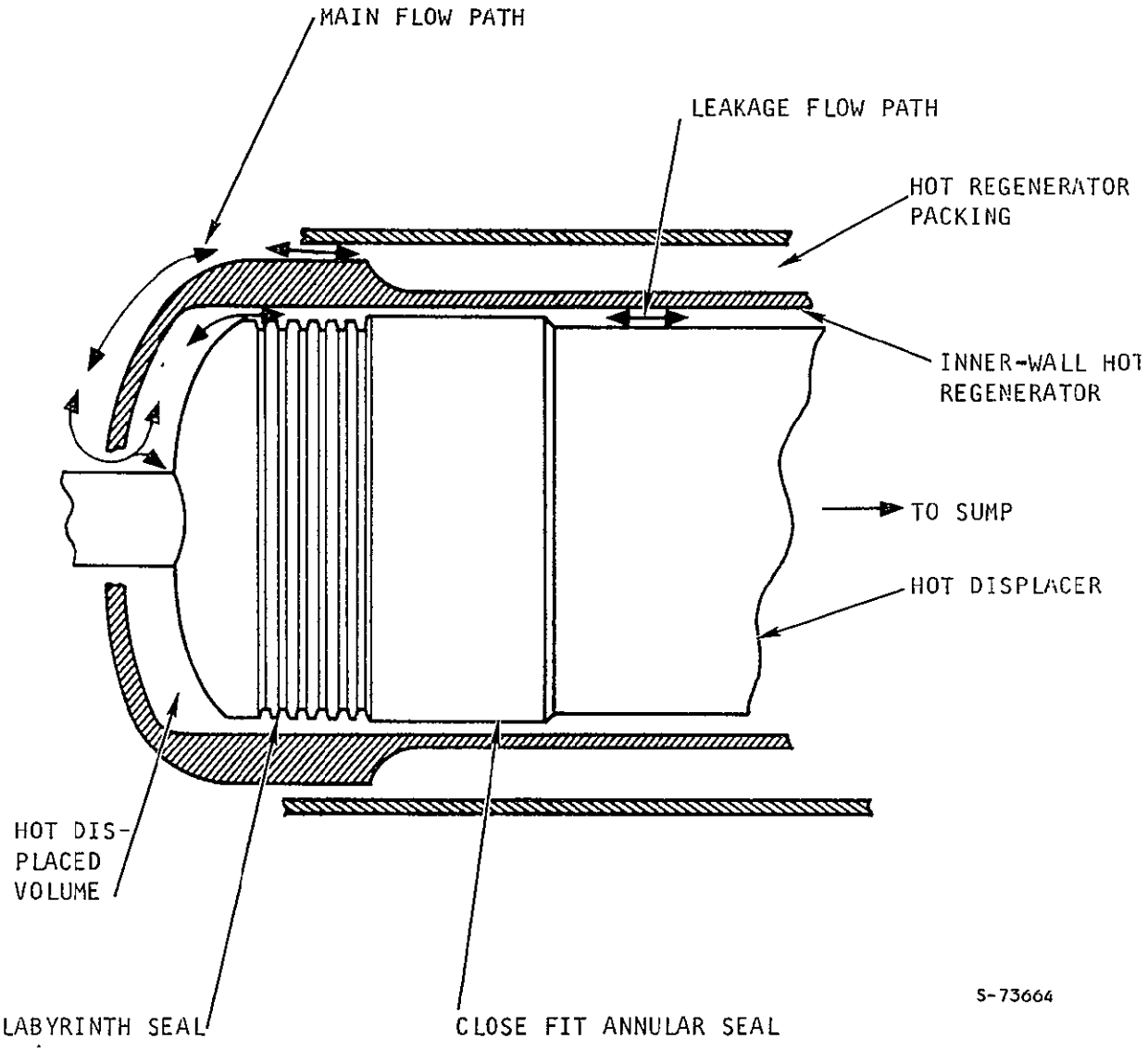

Figure 2-23. Hot-End Seal Configuration

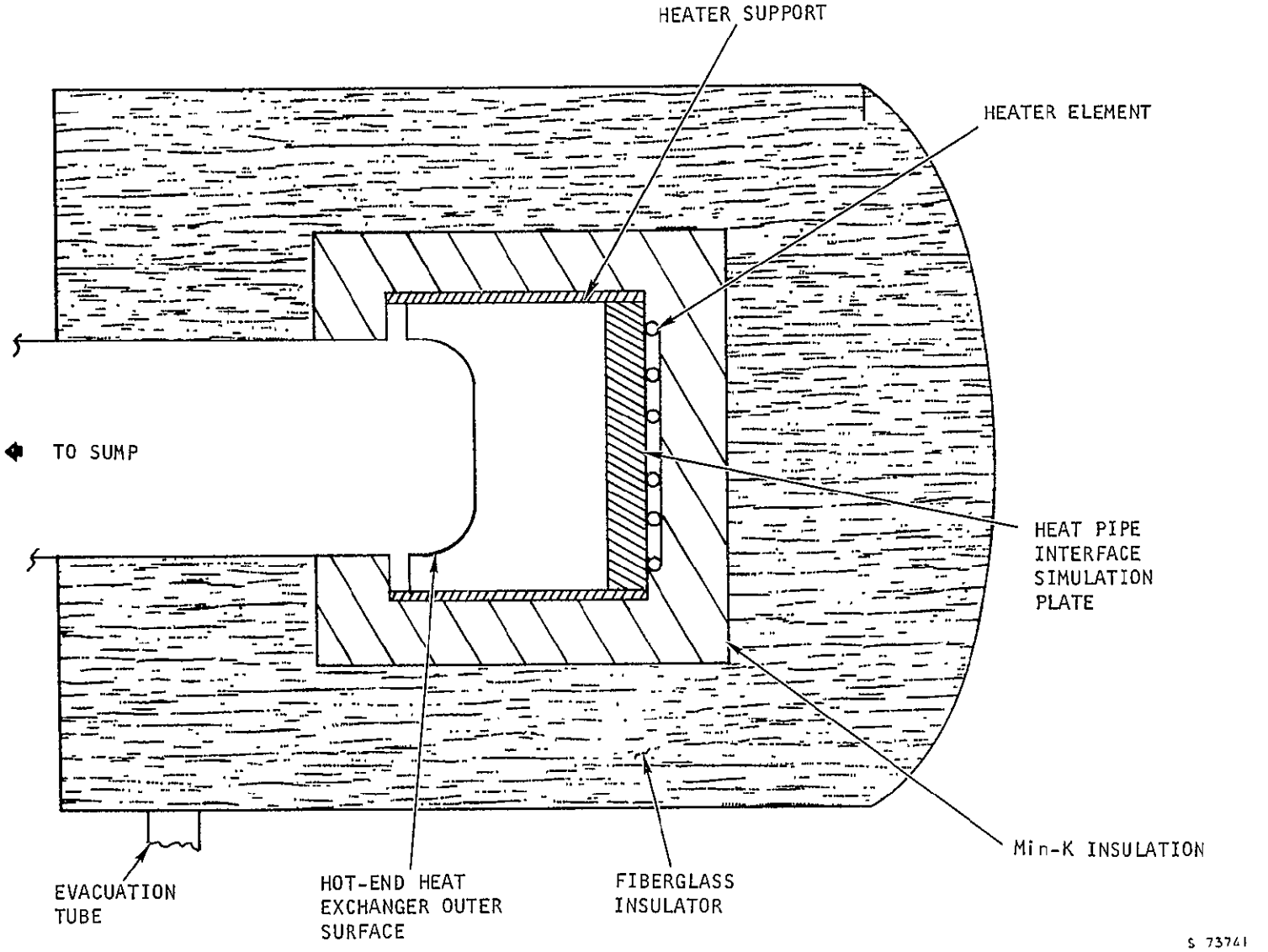

Figure 2-24. Hot-End Insulation and Heater Configuration

The insulation system consists of an inner layer of Min-K and an outer layer of fiberglass. Both insulation materials are contained within a sealed enclosure and dynamically pumped to maintain a vacuum environment. The Min-K is used in the high temperature region of the system due to it's excellent high temperature properties. The fiberglass is used in the lower temperature region due to it's lower thermal conductivity. The insulation system limits the hot-end insulation losses to 25 watts.

Sump Cooling Interface

To properly function, VM refrigerators must reject heat from the sump or crankcase region. The amount of heat that must be rejected is equal to the sum of: the hot-end input power; the refrigeration load; all losses; and the drive motor input power. In the GSFC 5-watt VM refrigerator, the heat rejection rate is between 325 to 370 watts.

In a spacecraft configuration, an ambient heat pipe assembly would be used to reject heat from the system. Water cooling coils replace this heat pipe assembly in the GSFC model VM. In adapting the refrigerator for water cooling, as much as possible of the heat pipe assembly to refrigerator interface design was retained.

The interface between the heat pipe assembly and refrigerator is shown in views a and b of Figure 2-25. In this design, heat is rejected from the sump heat exchanger through the sump pressure vessel wall to a copper collar which is clamped around the cylindrical section of the sump. This approach had four ammonia-filled heat pipes soldered to each half of the copper collar to transport the heat to a remote heat sink. Indium foil placed between the copper collar and sump pressure wall assured good thermal contact. The foil is maintained under a constant interface pressure of approximately 100 psi by bellville spring washers placed on the bolts which hold the collar halves together.

In adapting the refrigerator for water cooling, the copper collar interface was retained and the heat pipes (0.5 in. O.D.) replaced with coolant passages formed by soldering copper tubes (0.5 in. O.D.) to the copper collar. Water flow through the cooling system was set at 100 gal/hr (typical for laboratory water supplies). At a heat rejection rate of 400 watts which exceeds the maximum anticipated rejection rate the series flow arrangement shown in Figure 2-25 leads to an average temperature difference between the water and cooling collar of slightly greater than $3.0^{\circ}R$. The temperature rise of the water from it's inlet to exit is only $1.64^{\circ}R$. The small temperature differences were entirely consistent with the testing planned for the system.

Ambient Sump Heat Exchanger

The sump heat exchanger functions to transfer heat from the working fluid of the VM refrigerator for rejection from the system.

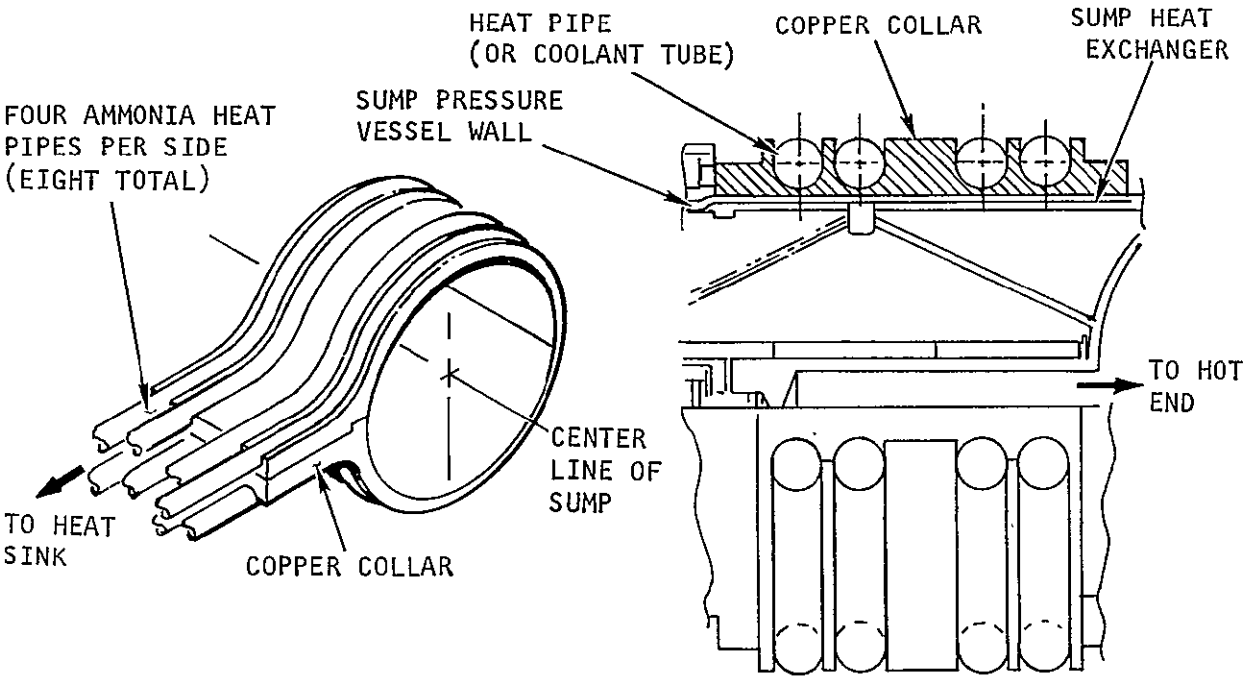

a. SUMP END OF ORIGINAL HEAT PIPE ASSEMBLY

b. CROSS SECTION OF SUMP INTERFACE

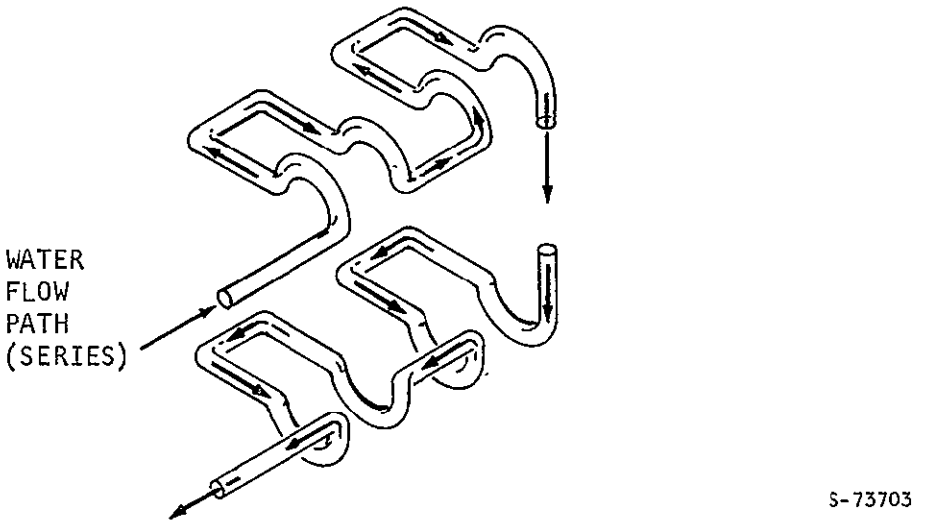

c. FLOW PATH OF WATER COOLANT TUBES TO REPLACE HEAT PIPES

Figure 2-25. Sump Cooling Interface Schematics

The annular shaped heat exchanger (Figure 2-26) is divided into two sections, with both sections being identical in configuration except for length. The heat transfer surface of each section is formed by brazing an offset copper plate-fin (Figure 2-27) to the inside surface of the cylindrical section of the sump pressure vessel wall. The cylindrical sump filler block fits inside the plate-fin thereby forming an annular passage forcing flow through the finned surface. At the right hand side, flow of the working fluid enters and exits Section I of the heat exchanger as it leaves and returns to the hot regenerator during the cyclic flow process. The average flow rate in this section of the heat exchanger is approximately 5 times that in Section 2; this accounts for the greater length (larger heat transfer surface) required for this section. At the other end of Section I of the heat exchanger, the flow enters and exits from a flow distribution passage cut into the sump filler block. This distribution passage or slot is supplied working fluid via ports that connect to the active cycle volumes in the crank case and behind the hot displacer as shown. The distribution slot provides uniform flow across the face of the heat exchanger.

On the left hand side of the figure, flow enters and exits Section 2 of the heat exchanger as it leaves and returns to the cold regenerator. This section of the heat exchanger is pneumatically connected to the cold regenerator via channels cut into the sump filler block (not shown in Figure 2-26) and passages in the cold-end linear bearing support. To provide uniform flow distribution at the left hand face of Section 2 of the heat exchanger, a secondary flow distribution slot is cut into the sump filler block as shown. The right hand of this section of the heat exchanger interfaces and shares the central flow distribution slot with the other section of the exchanger.

The path for heat transfer from both sections of the heat exchanger is from the gas to the plate fin surface, from the fined surface through the pressure vessel wall and on into the copper sump cooling collar. Indium foil is placed between the sump pressure vessel and the cooling collar; this foil is maintained under a 100 psi interface pressure to ensure good thermal contact. Heat is finally rejected from the system to cooling coils brazed into channels cut in the cooling collar. This collar was orginally designed to allow interfacing of the refrigerator with ammonia heat pipes but is interchangeably usable with simple water cooling coils.

Flow Distribution and Pressure Losses in the Sump Region

In the refrigerator sump region, flow passages are provided to pneumatically connect the active sump volume to the hot and cold volumes through the various heat transfer devices. These passages are described in the following paragraphs.

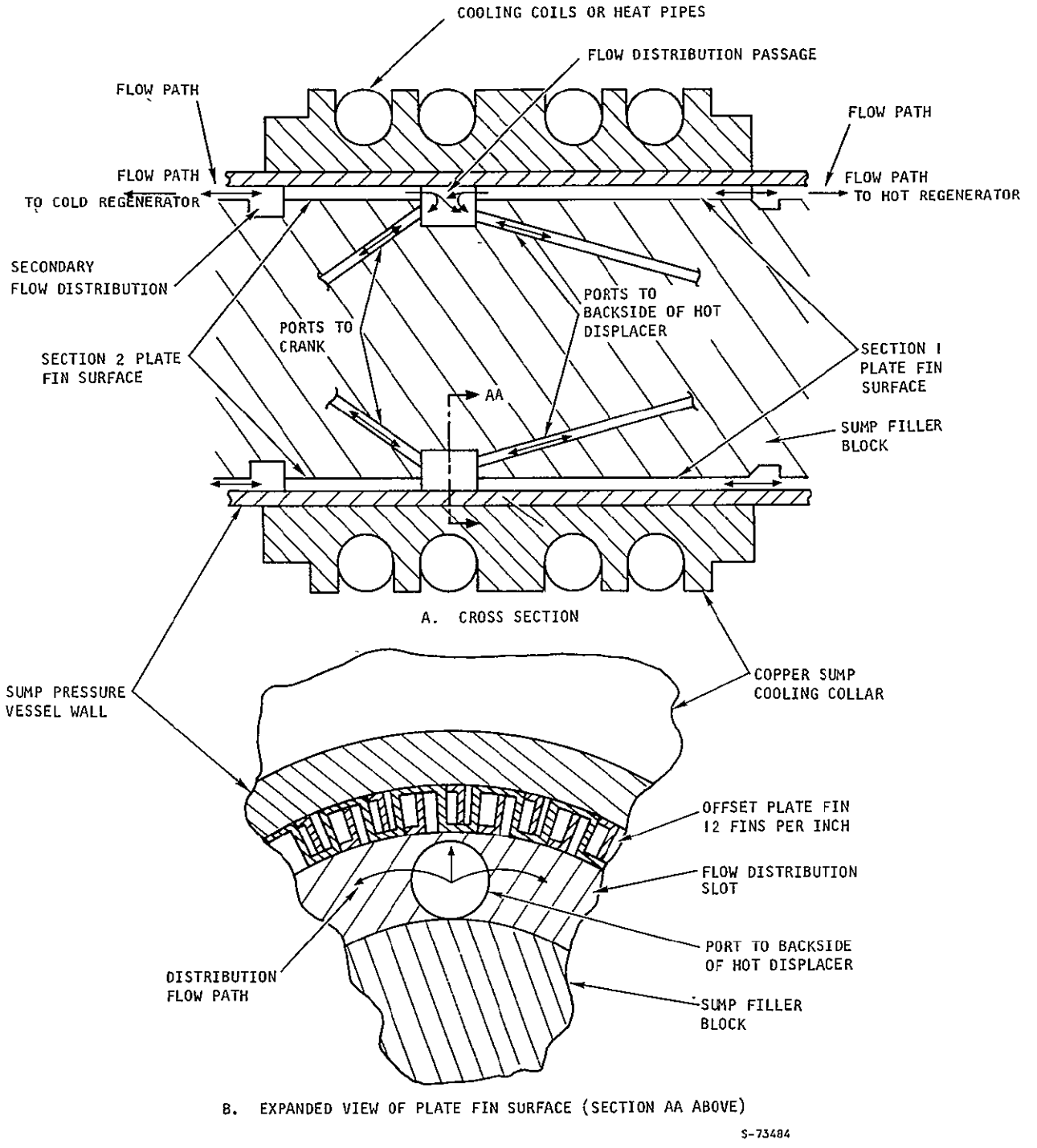

Figure 2-26. Sump Heat Exchanger Configuration

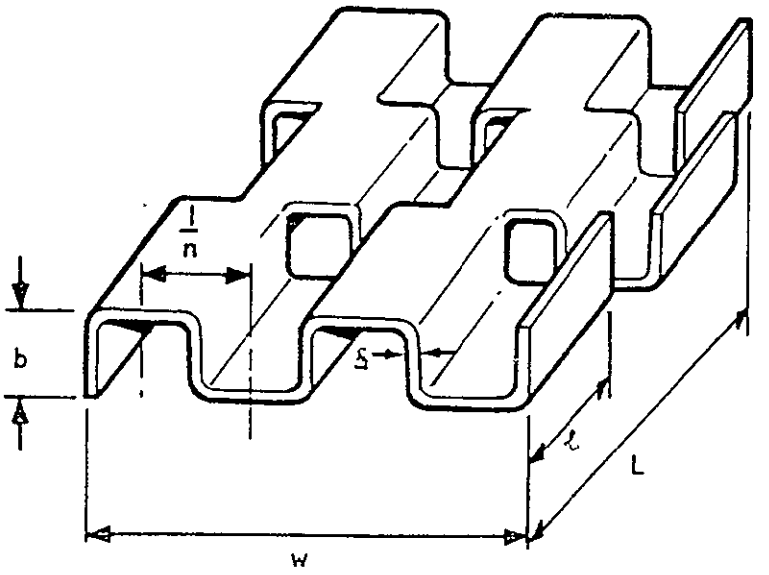

S-41922

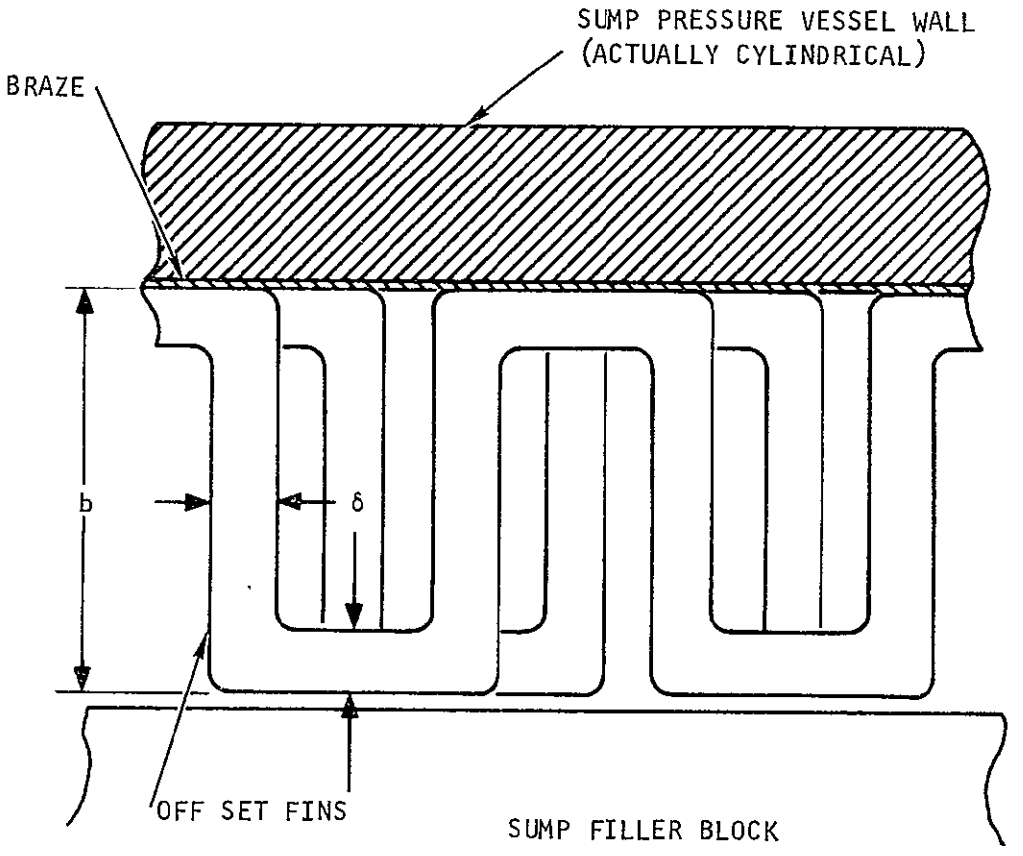

b. INSTALLED PLATE-FIN SURFACE

S-73483

Figure 2-27. Rectangular Offset Plate-Fin-VM Refrigerator Sump Heat Exchanger

1. Flow Distribution Around Sump Filler Block at Interfaces with Cold End and Section 2 of Ambient Heat Exchanger

Section 2 of the ambient heat exchanger receives flow from the cold end of the refrigerator via channels cut in the sump filler block. These channels, and the interface with the sump heat exchanger, are shown in Figure 2-28. The flow passages around the sump filler block are formed by chemical milled channels or slots in the block. The filler block is encased within the sump pressure vessel to provide enclosed flow passages as shown.

- Flow distribution and pressure drop in the channels around the surface of the sump filler block. These channels are not of equal length; some non-uniformity in flow between channels is excpected.
- Flow distribution in the distribution slot upstream of Section 2 of the sump heat exchanger.
- Pressure drop in the secondary distribution slot where the sump flow channels interface with flow passages in the linear bearing support.

2. Sump Filler Block Flow Channels

There are 10 channels in the sump filler block which direct flow between Section 2 of the heat exchanger and the cold regenerator redistributor.

3. Upstream Flow Distribution Slot

The distribution slot distributes flow around the face of Section 2 of the sump heat exchanger to provide even flow across the heat exchanger face.

4. Secondary Flow Distribution Slot

The secondary flow distribution slot is cut into the sump filler block to provide uniform flow distribution at the left side of heat exchanger Section 2. This is accomplished by taking a 45^0 cut of the edge of the sump filler block at the interface between the sump block and the bearing support. The triangular flow passage formed by this cut has a cross sectional flow area of four times that of the sump flow channels. Due to the short distance between sump channels and bearing support flow passages, the pressure drop in the interfacing flow passage is negligible.

Bearing Support Flow Passage Pressure Drop and Flow Distribution Slot Design

The flow passage configuration along the length of the bearing support, and the bearing support flow distribution slot, are shown in Figure 2-29. The flow passage provides the fluid connection between the cold end and the sump region. The distribution slot is included to ensure uniform distribution of flow to the cold regenerator.

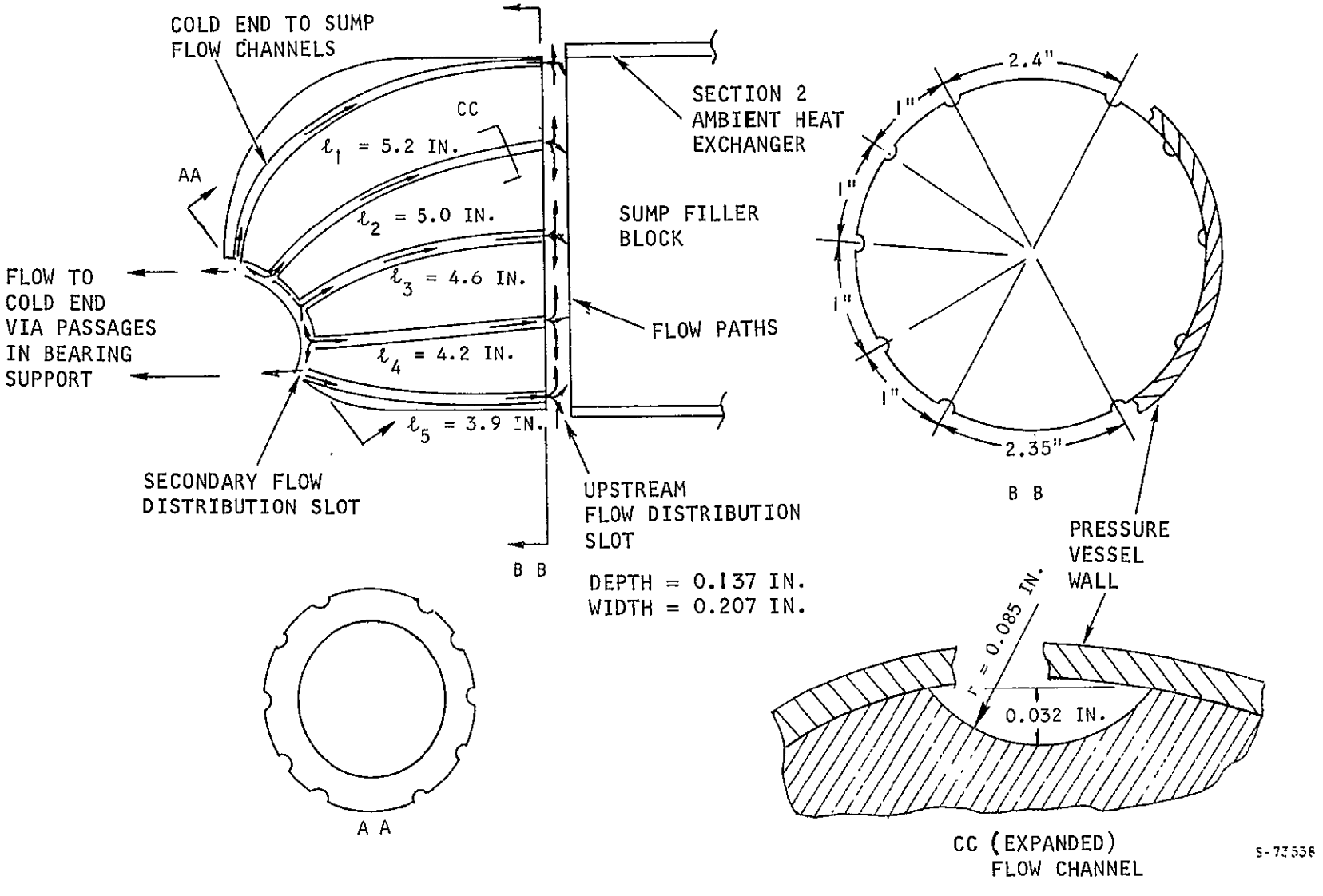

Figure 2-28. Sump Filler Block Flow Channels Toward Cold End

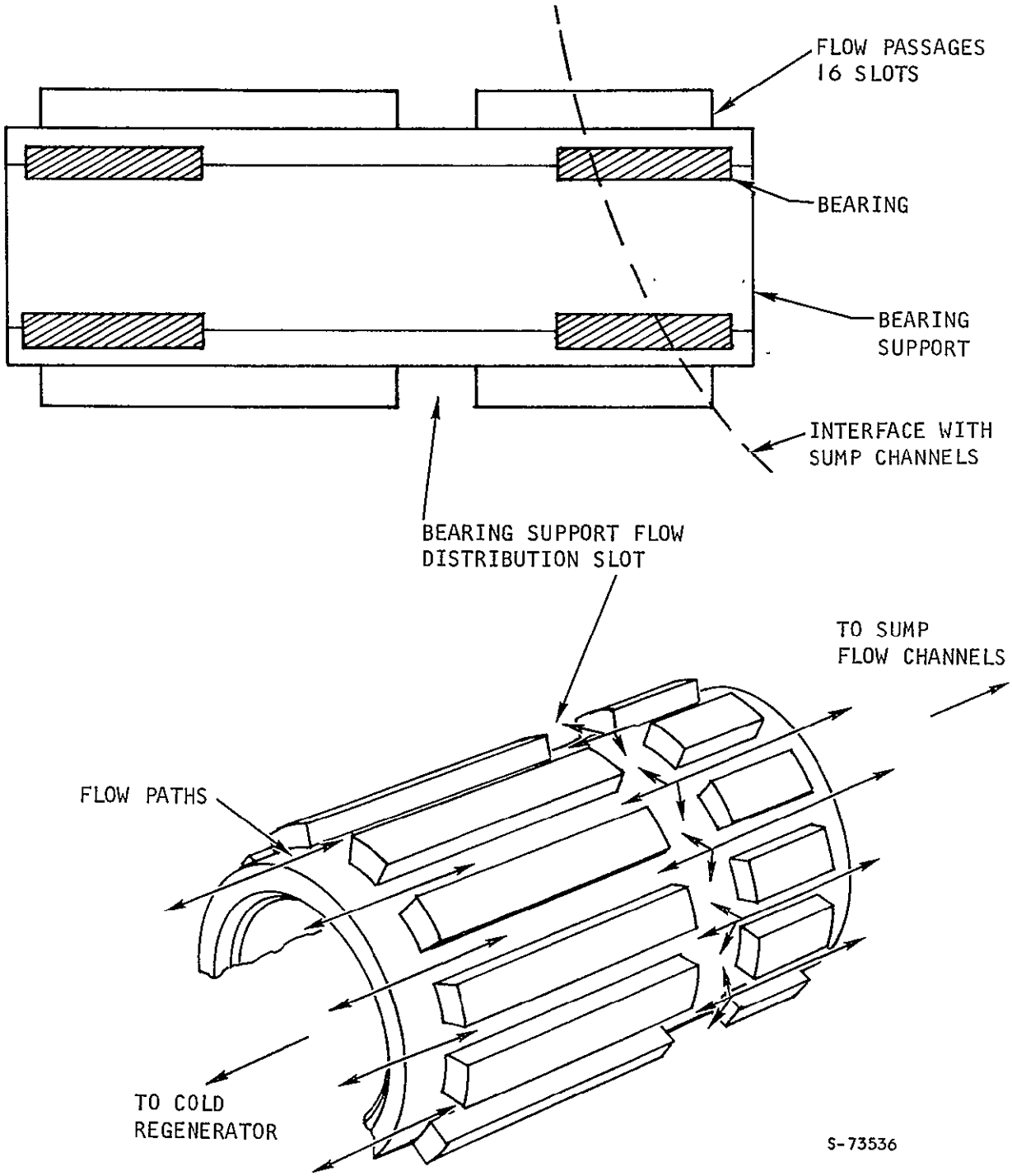

Figure 2-29. Bearing Support Flow Passages

1. Flow Passage Sizing and Axial Pressure Drop

Sixteen separate flow passages are provided for good flow distribution at the end of the passages.

2. Flow Distribution Slot

The flow distribution slot assures that flow in the sump flow channels is distributed uniformly to the cold regenerator. The slot depth is equal to the lengthwise flow passage depth of 0.05 in. to avoid unnecessary loss in the axial direction.

Ports to Active Sump Volumes

The basic GSFC VM refrigerator configuration has two active volumes in the sump region (Figure 2-30). These active volumes are plumbed to the hot and cold active volumes, through various heat transfer devices via ports drilled into the sump filler block as shown.

1. Ports to Backside of the Hot Displacer

For fabrication simplicity, a six-port configuration is provided for the ports to the backside of the hot displacer.

The port diameter is 0.160 in., this port diameter gives a pressure drop slightly below 0.5 psi and does not have an excessive void volume.

2. Ports to Crankcase Sump

Four ports are provided into the crankcase sump with a diameter of 0.1 in. These ports interface with the sump heat exchanger flow distribution slot.

Sump Heat Exchanger Flow Distribution Slot

The interface between the ambient sump heat exchanger, the ports into active sump volumes, and the flow distribution slot is shown in Figure 2-31. Figure 2-31 shows the orientation of the two sets of ports around the flow distribution slot. The function of this distribution slot, as previously discussed, is to distribute flow coming from the sump ports uniformly across the face of the sump heat exchanger.

Refrigerator Drive Motor

A simple laboratory motor drives the refrigerator; this provides a practical and flexible means for driving the refrigerator for the test program. To provide for operation at test conditions and bearing run-in, an oversized 1/4 h.p. laboratory motor was supplied with the refrigerator.

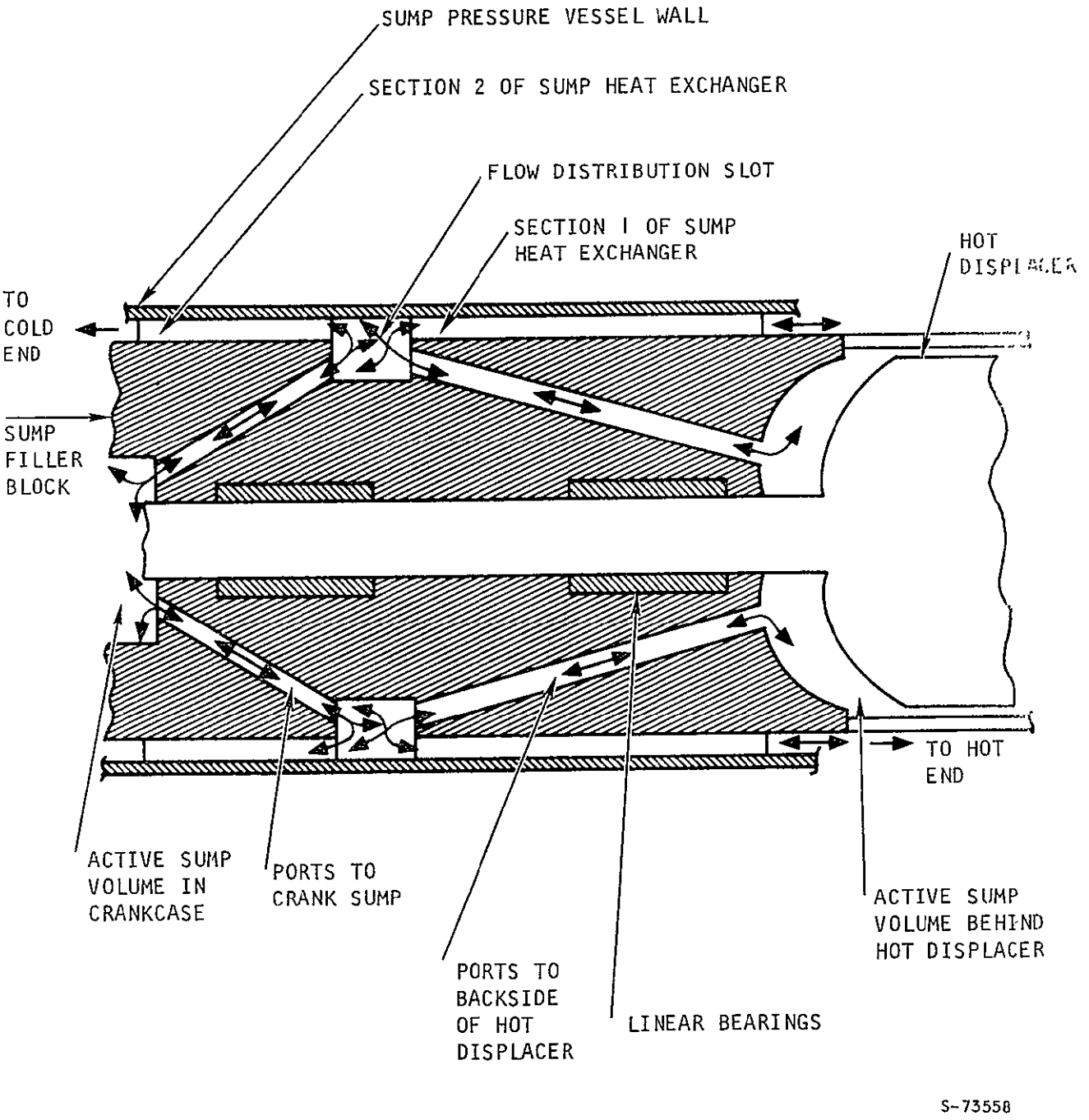

Figure 2-30. Configuration of Ports to Active Sump Volumes

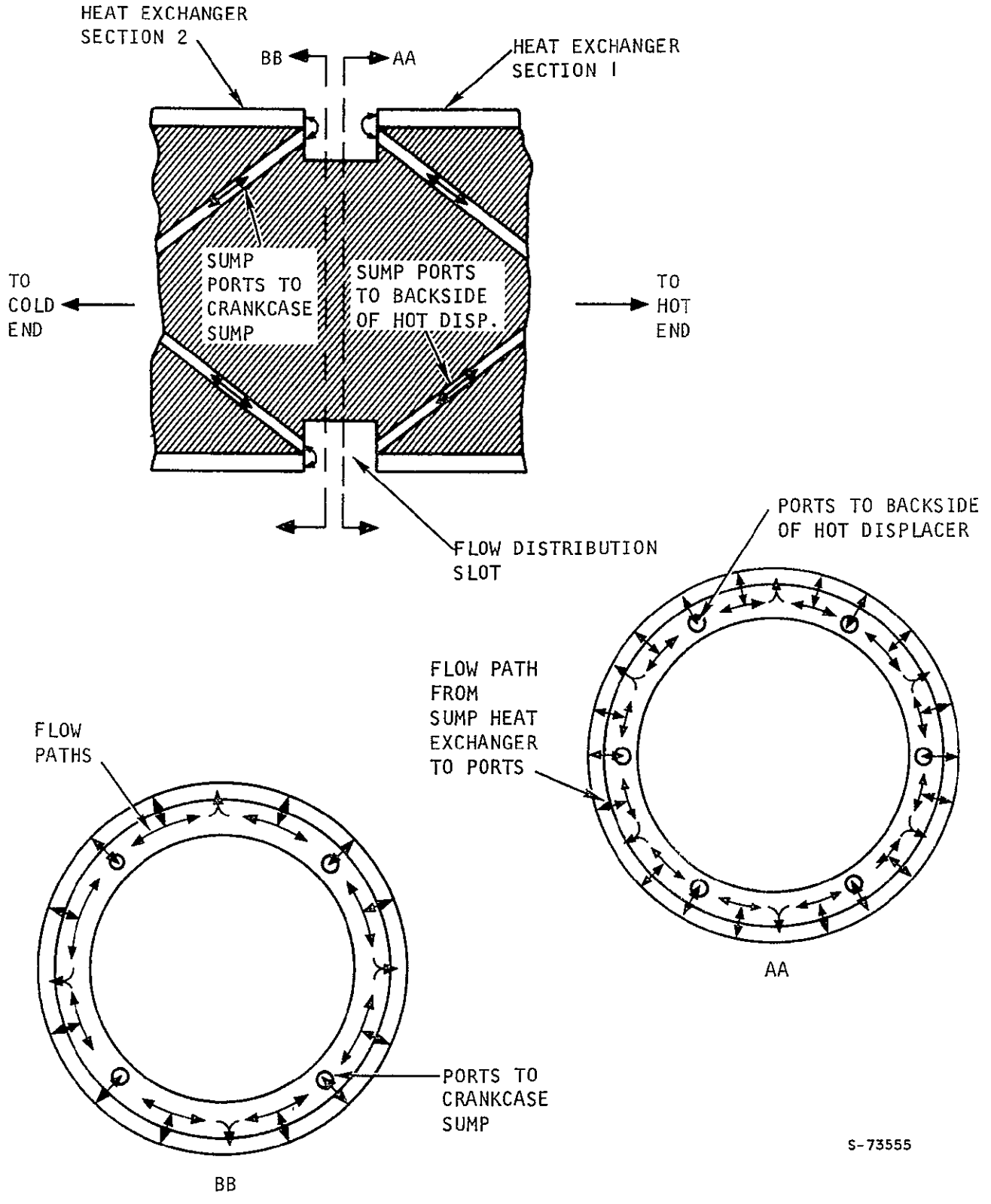

Figure 2-31. Sump Heat Exchanger Flow Distribution Slot

SECTION 3

TEST RESULTS

INTRODUCTION

Following fabrication and assembly, the VM refrigerator was instrumented for performance evaluation testing. Prior to performance testing, a bearing run-in period of approximately 100 hours was anticipated based on experience gained during the Task II testing with the bearing test rig. However, due to extremely low bearing wear characteristics, over 800 hours of operating time were accumulated and the bearings were still not completely run in. The long run-in period limited the range of operating parameters covered by the tests, but the refrigerator thermal performance during testing clearly exceeded all requirements.

At AiResearch, sixteen tests were performed on the VM refrigerator to determine refrigeration capacity at off-design conditions. Each test consisted of setting the desired operating conditions and then determining the cold finger temperature for a series of refrigeration heat loads. The refrigeration heat load was supplied by an electric heater attached directly to the cold finger. The following operating conditions were varied from test to test: (1) peak cycle pressure; (2) hot end temperature; (3) sump temperature; and (4) engine speed. The operating conditions for each test are summarized in Table 3-1.

BEARING RUN-IN PERIOD

The predicted long life of the VM refrigerator is primarily dependent upon low bearing wear. To achieve low bearing wear and in turn, the operating life required under this contract, bearings of Boeing Compact 6-84-1 in combination with tungsten carbide and chrome carbide, were chosen from materials evaluated during a test program described in the Task II summary report. Because these bearings demonstrated an extremely low wear rate, it was considered that a relatively long break-in period would be required in order to properly seat the bearing members.

Subsequent testing proved this to be exactly true; in fact, the bearing wear rate was so low that after 843 hours of testing, the bearings had not yet completed run-in even though the refrigerator performance requirements were fully satisfied. At this point, NASA accepted delivery of the machine.

TEST SETUP AND INSTRUMENTATION

The instrumentation as well as the control devices utilized during the performance test evaluations are shown schematically in Figure 3-1. Each of these devices and the associated instruments are discussed below.

Cold-End Temperature Instrumentation

The cold end of the engine was outfitted with six copper-constantan thermocouples located as shown in Figure 3-2. Each thermocouple was affixed to the engine by spotwelding directly to the structure of the pressure vessel, providing as accurate a temperature measurement as possible.

Cold-end thermocouples were located in the following positions:

T_1 on centerline of cold end

T_2 and T_3 on end of cold-end heat exchanger diametrically opposite to one another

T_4 and T_5 radially opposite one another in the center of the cold-end heat exchanger under the cold end thermal input heater strip

T_6 at the warm end of the cold regenerator at the sump input channel

Hot-End and Sump Temperature Instrumentation

Chromel-alumel thermocouples were installed at the hot-end and sump regions of the VM. As with the cold-end instrumentation, these devices were also spotwelded directly to the pressure structure. Figure 3-3 shows the location of these thermocouples. The individual location and function of the hot-end and sump thermocouples are as follows:

T_{11} was located at the sump-end of the hot regenerator and monitored input and exhausting gases from the hot generator.

T_{12} was mounted below the interface flange utilized to support the radiant input heating device.

T_{13} and T_{14} were situated diametrically opposite one another on the upstream side of the radiant input heater support flange. T_{13} served as the temperature controller reference.

T_{14}, T_{15}, T_{16} were located at different radial stations along the surface of the radiant energy input surface. T_{16} was mounted immediately adjacent to the hot-end support bearing base.

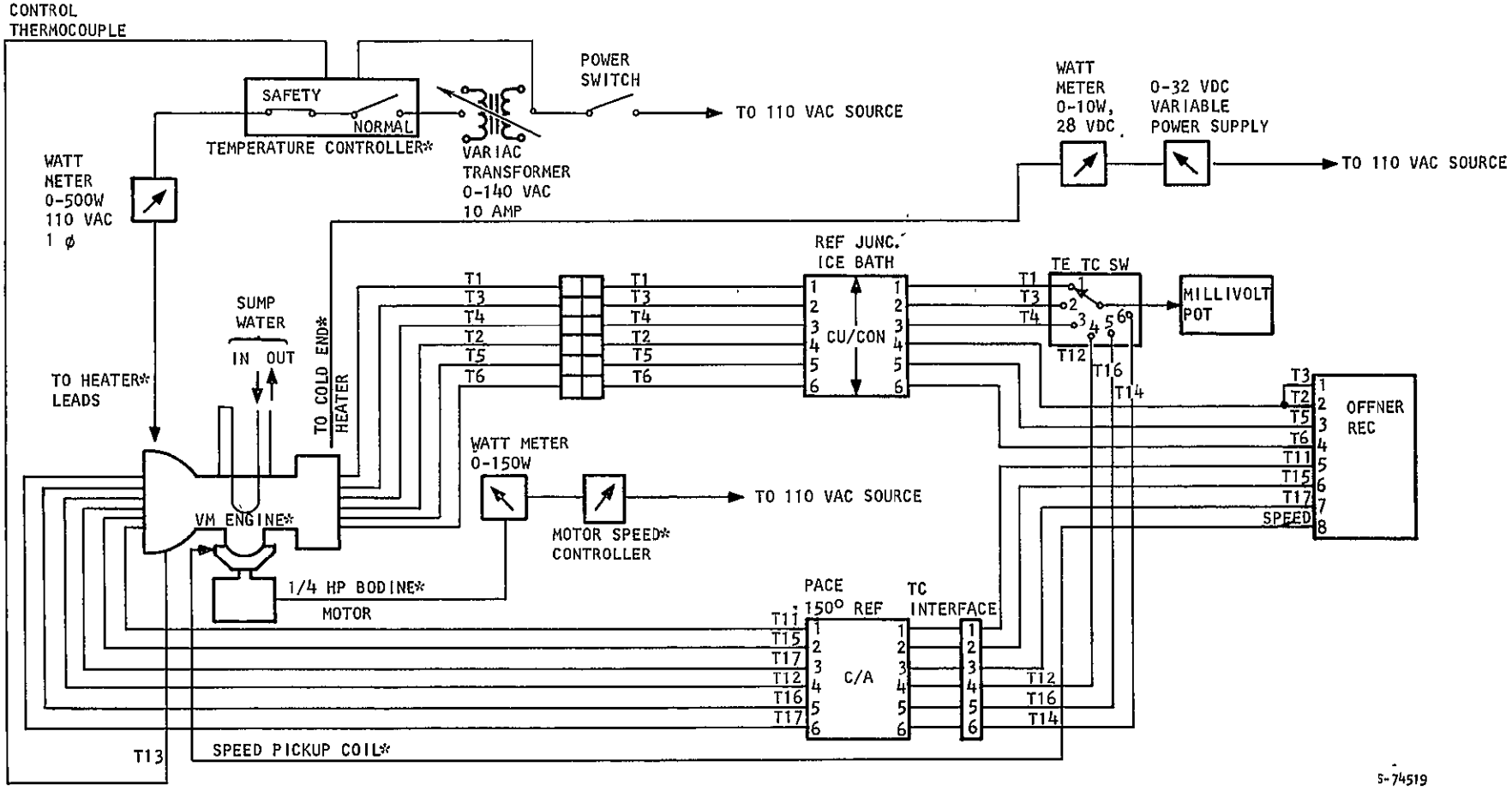

Figure 3-1. Instrumentation and Control Device Schematic

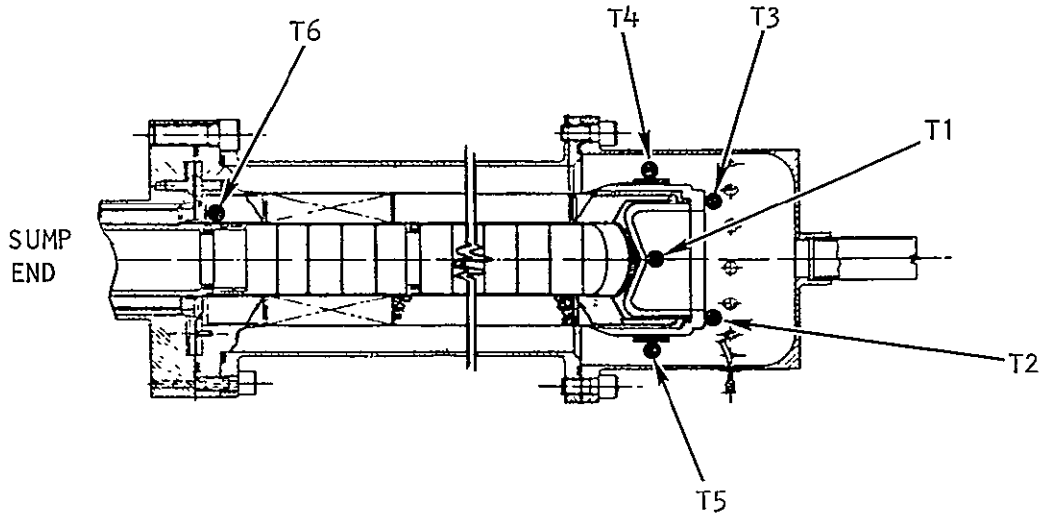

Figure 3-2. Cold-End Thermocouples

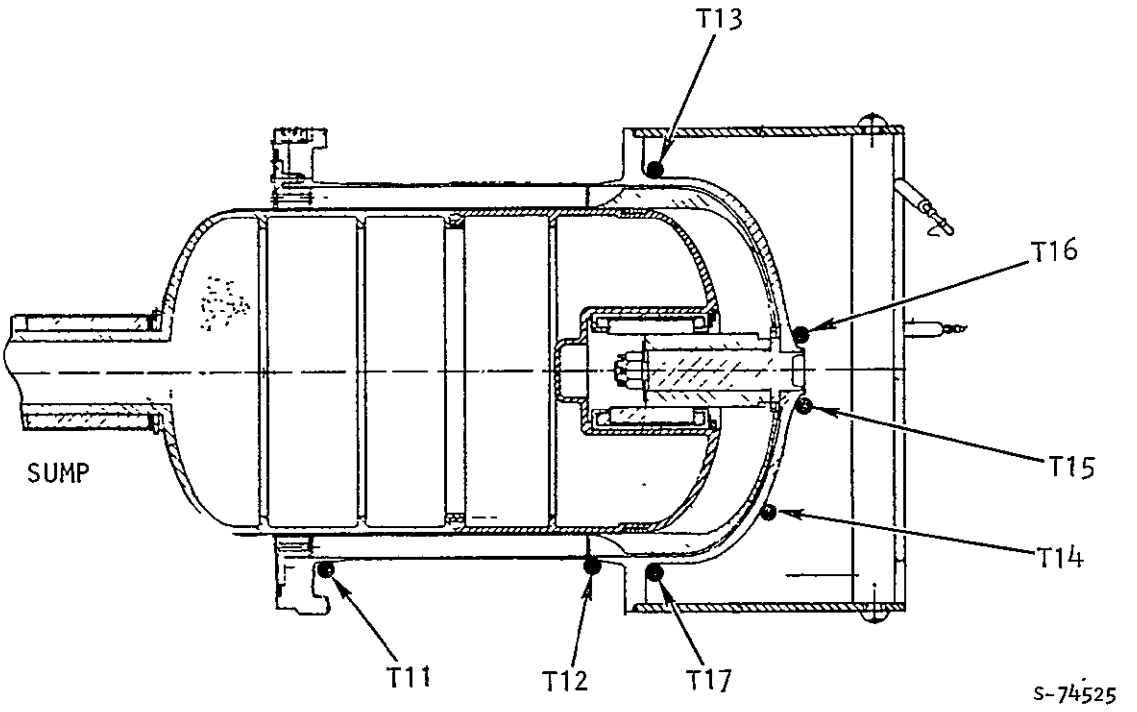

Figure 3-3. Hot-End Thermocouples

Two additional thermocouples (not shown in Figures 3-2 and 3-3) were located at each end of the ambient heat pipe collar in order to identify the sump temperatures immediately adjacent to the ambient temperature heat rejection collar.

Power Instrumentation

Figure 3-1 shows the method of controlling the hot-end temperature. The power used to raise the gas temperature was monitored by a single-phase watt meter. Controlled input power was routed through a temperature controller (not shown in Figure 3-1) equipped with safety shutoff devices in the event of failure of the controller or some other control function of the system (e.g. drive motor). Power input to the temperature controller was routed through a laboratory variable voltage transformer to allow precise power control. As noted earlier, thermocouple T_{13} was utilized as the temperature controller input reference.

Cold end power loading was accomplished with a resistive heating element mounted in intimate contact with the radial cryogenic heat pipe interface at the cold-end heat exchanger. Power to this device was provided by variable voltage d-c power supply and monitored on a d-c watt meter.

A final wattmeter was installed in the power-input line from the motor speed controller and laboratory drive motor used to rotate the crankshaft of the refrigerator.

A monopole magnetic pickup was placed in close proximity to a 60 tooth gear mounted directly on the input drive shaft to provide accurate indication of engine speed. The output of the pickup was then directed to an appropriate signal conditioning device and ultimately displayed on a digital readout instrument.

The critical instrumentation for evaluation of the performance of the VM refrigerator was monitored on a multichannel oscillographic recorder. The remainder of the temperature instrumentation was recorded periodically during testing.

TEST DATA

Data recorded for each of the 16 tests are presented in Appendix A and summarized in Table 3-1. Each test consisted of between 3 and 5 different refrigeration heat loads, for a total of 75 test points. The refrigeration heat loads imposed on the machine during each test ranged from approximately 0 to 7 watts.

Performance data plotted as refrigeration heat load versus cold finger temperature, are shown in Figure 3-4 through 3-19, one for each test performed. The test conditions are noted on each figure.

The curves indicate that the cold end temperature is a linear function of the refrigeration heat load imposed on the machine, subject to slight experimental data scatter.

DATA ANALYSIS

Design Point

Early in the program, it was decided to design the VM engine for a cooling capacity of 7 watts when new. Based on this capacity with new bearings, and correlated with bearing wear tests performed during Task II*, the predicted refrigeration at the end of a two year period of operation is 5 watts. Thus the design point operating conditions for a new machine are given in Table 3-2.

As previously discussed, very low bearing wear rates caused a lengthy bearing run in period which did not allow the machine to attain the design speed of 400 rpm for any of the 16 tests performed. Although the design point performance was not measured directly, performance data from Test No. 5 verifies better-than required thermal performance from the refrigerator.

The results from Test No. 5 show that the required 7-watt refrigeration capacity was attained at a cold-end temperature of 72°K, and a speed of 365 rpm and a hot-end temperature of 1000°F. These values are less than the design point conditions of 75°K, 400 rpm, and 1200°F respectively. All other operating conditions during Test No. 5 were the same as the design point requirements.

For purposes of comparison, two computer data outputs are given in Figures 3-20 and 3-21. Figure 3-20 presents the ideal cycle analysis program output for the machine design point. Figure 3-21 is the ideal cycle analysis program output for the operating conditions of Test No. 5 at a 7-watt refrigeration capacity. Comparing this data indicates that the refrigerator will produce 5 watts of refrigeration after 2 years of operation. This is discussed below.

In the Task II Final Report,* the total temperature drop from the cold end of the refrigerator to the cold gas was indicated to be 4.5°R at a 7-watt heat load. The corresponding hot-end and sump temperature drops are 30° and 20°R respectively. These temperature drops have been taken into account in producing the program data outputs of Figure 3-21. Figure 3-21 indicates an ideal refrigeration of 14.9 watts at the conditions of Test No. 5 and subtracting the 7 watts of net refrigeration from the ideal refrigeration (14.9 watts) indicates that cold end losses are approximately 7.9 watts in this case. This loss compares favorably with the calculated value of 10 watts for a new machine given in the Task II Final Report*; it should be noted that this calculation was based on conservative assumptions. When the experimental value of the cold-end loss (derived from Test No. 5) is subtracted from the ideal refrigeration at the design point (17.9516 watts from Figure 3-20) the expected net refrigeration is approximately 10 watts.

---

*C. W. Browning, V. L. Potter, Final Report for Task II, Analytical and Test Program for 75°K Vuilleumier Cryogenic Refrigerator

TABLE 3-1

SUMMARY OF TEST CONDITIONS

Test Number	Peak Cycle Pressure, psig	Sump Temperature, °F	Hot End Temperature, °F	Engine Speed, rpm
1	900	75	900	300
2	820	75	900	300
3	850	85	950	300
4	800	140	1000	300
5	800	140	975	365
6	800	140	1000	250
7	850	105	1000	300
8	750	135	1000	300
9	1025	140	1000	300
10	900	140	1000	300
11	725	140	1000	300
12	800	140	900	300
13	800	140	1050	300
14	800	140	800	300
15	800	110	1000	300
16	800	85	1000	300

TABLE 3-2

DESIGN POINT OPERATING CONDITIONS, 5 WATT VM WITH NEW BEARINGS

Hot end temperature, °F	1200
Sump temperature, °F	140
Cold end temperature, °K	75
Refrigeration, watts	7.0
Engine speed, rpm	400
Peak cycle pressure, psia	800

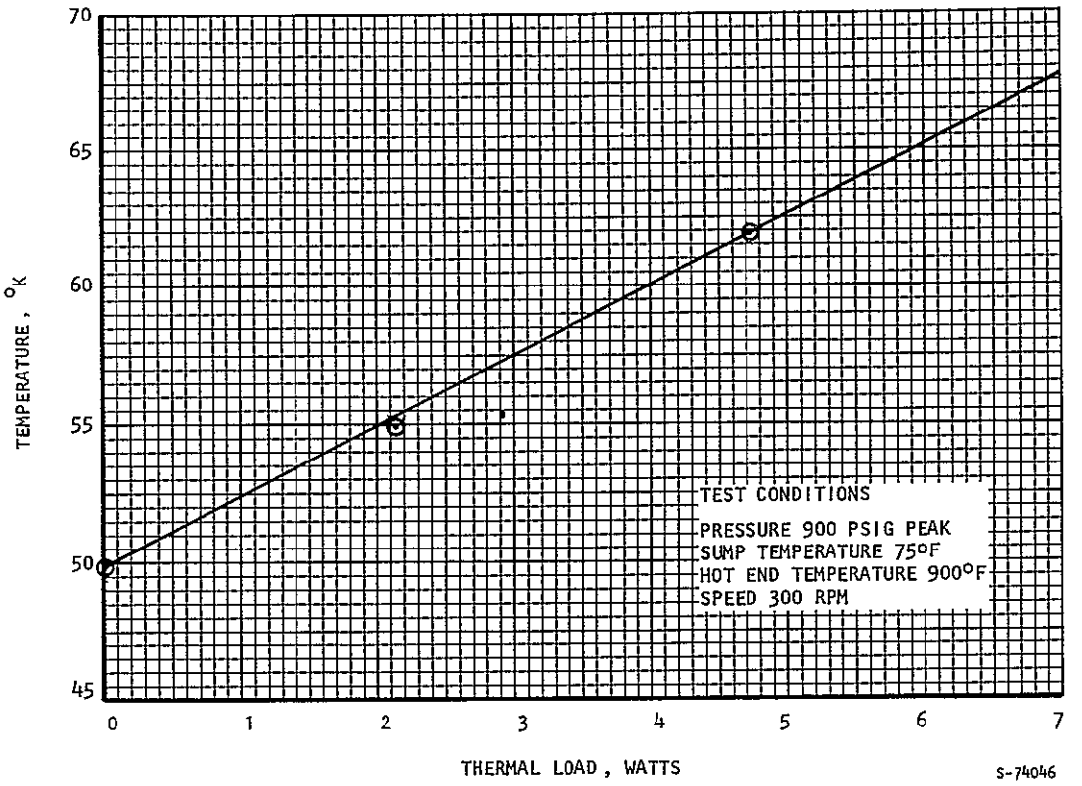

Figure 3-4. Performance Test No. 1

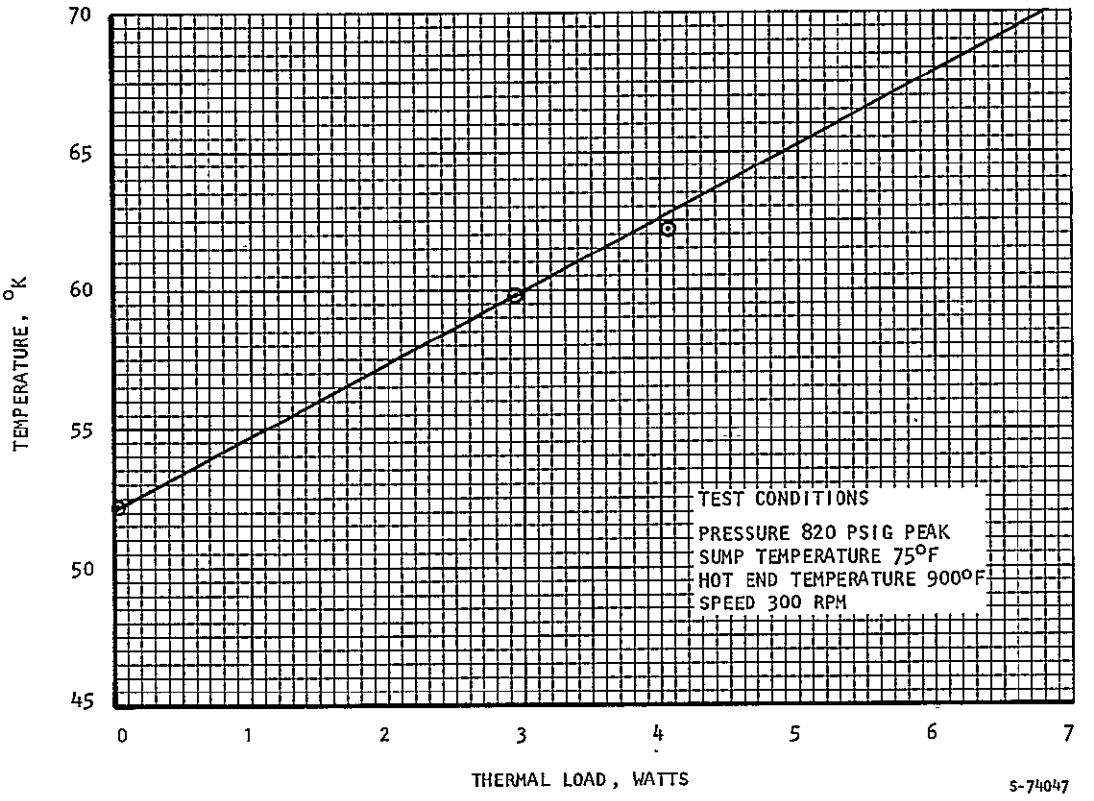

Figure 3-5. Performance Test No. 2

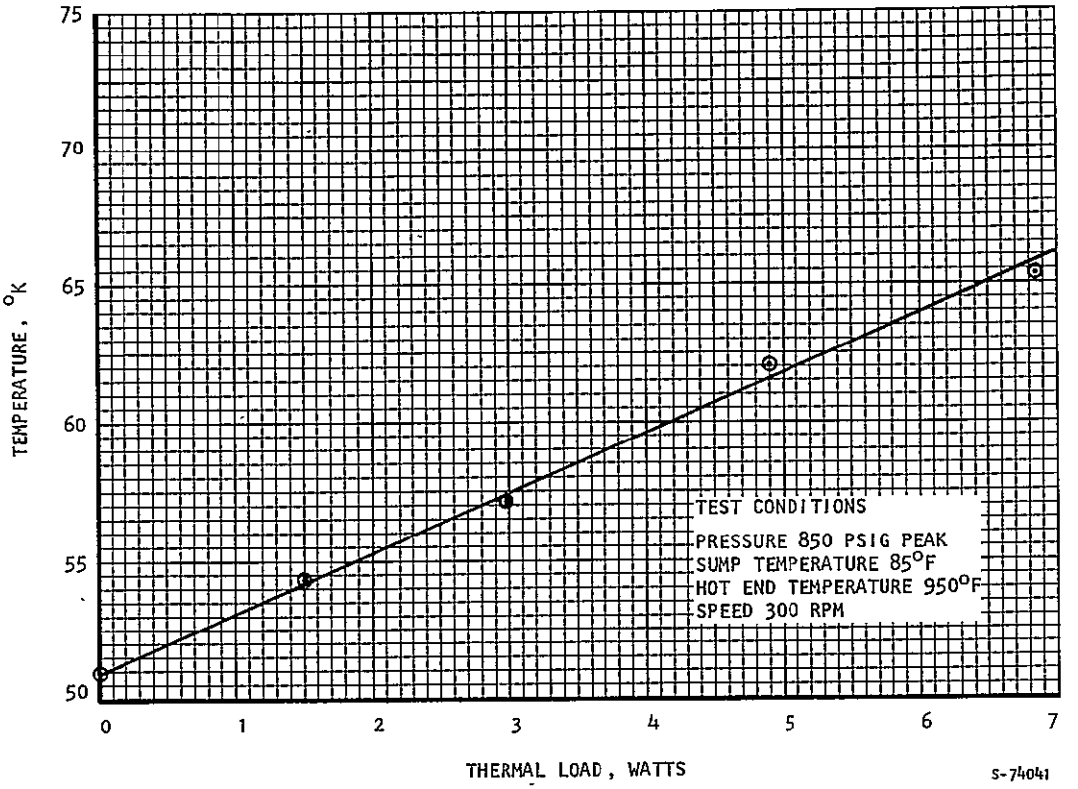

Figure 3-6. Performance Test No. 3

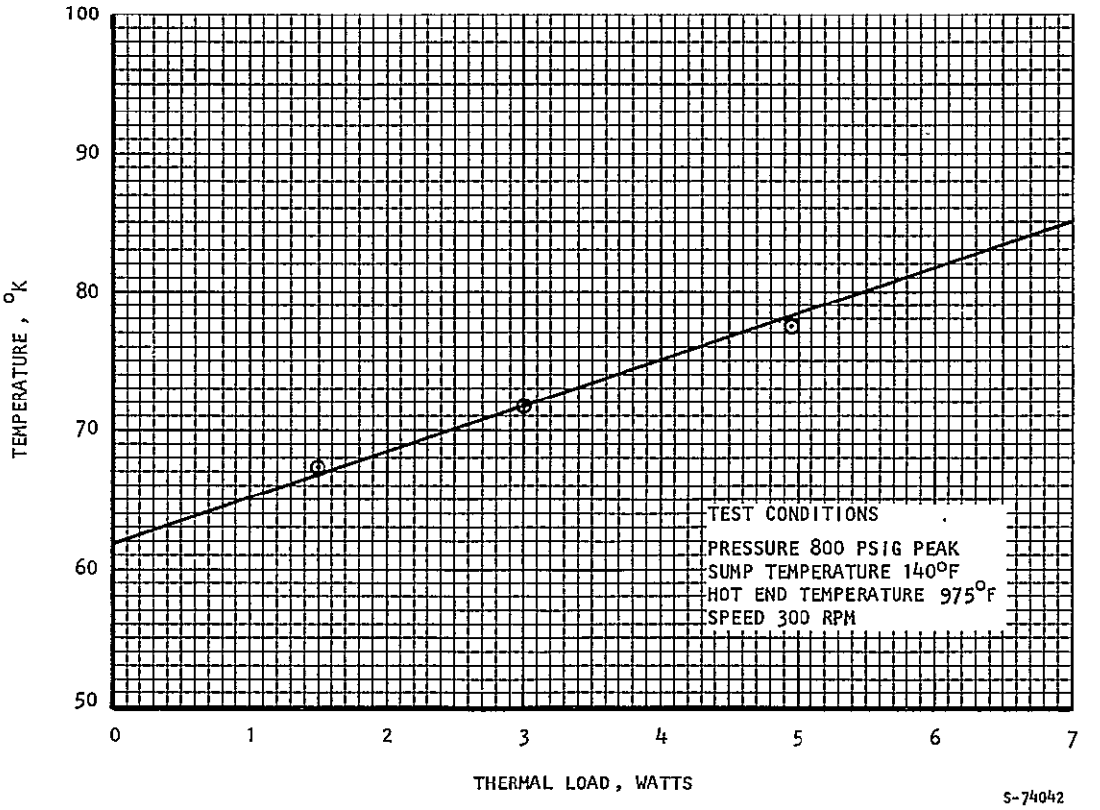

Figure 3-7. Performance Test No. 4

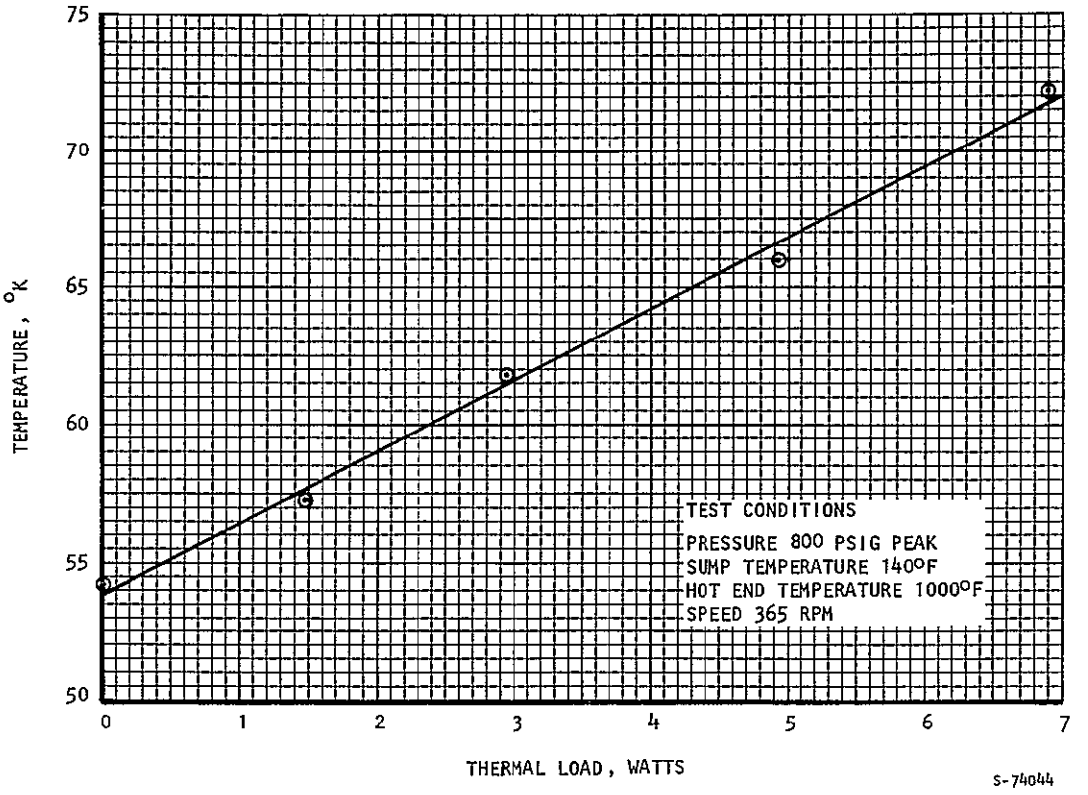

Figure 3-8. Performance Test No. 5

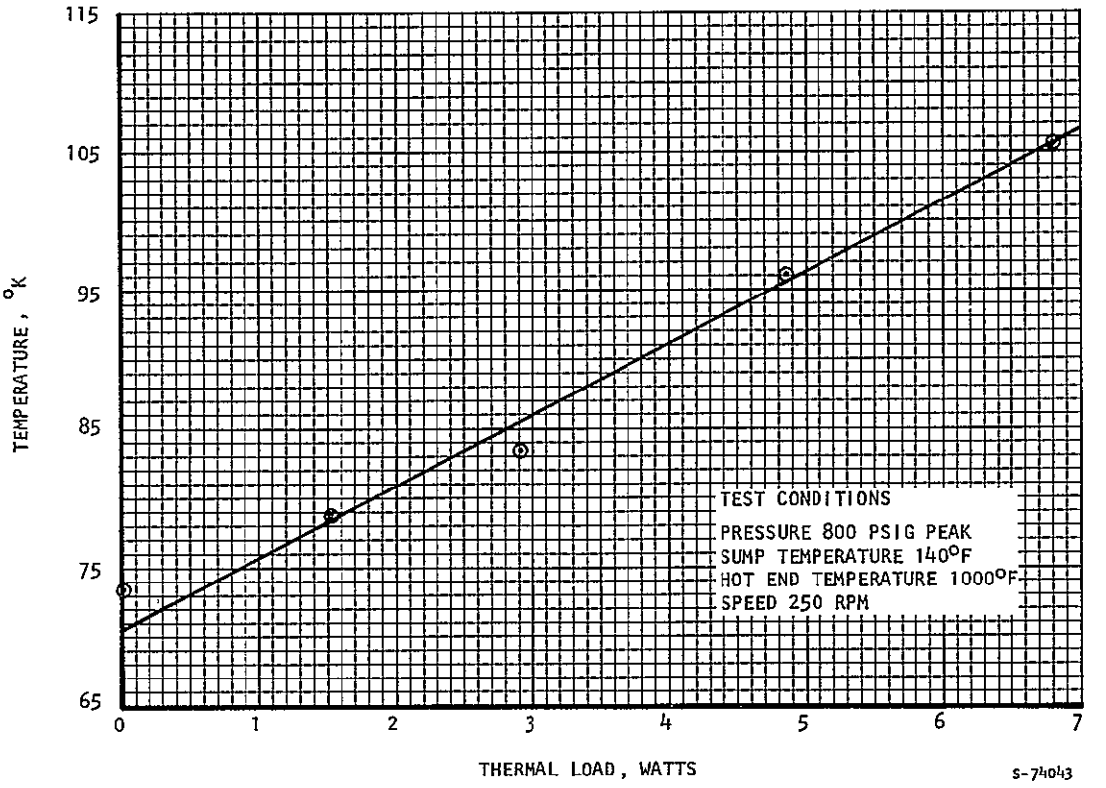

Figure 3-9. Performance Test No. 6

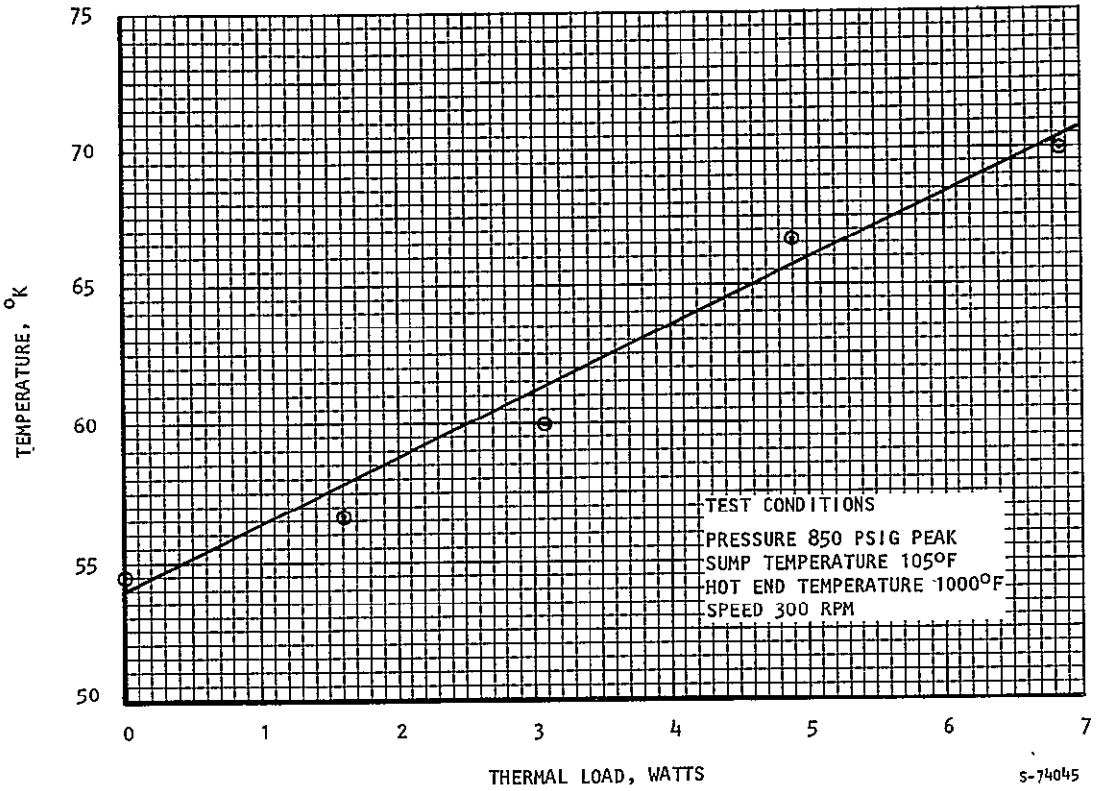

Figure 3-10. Performance Test No. 7

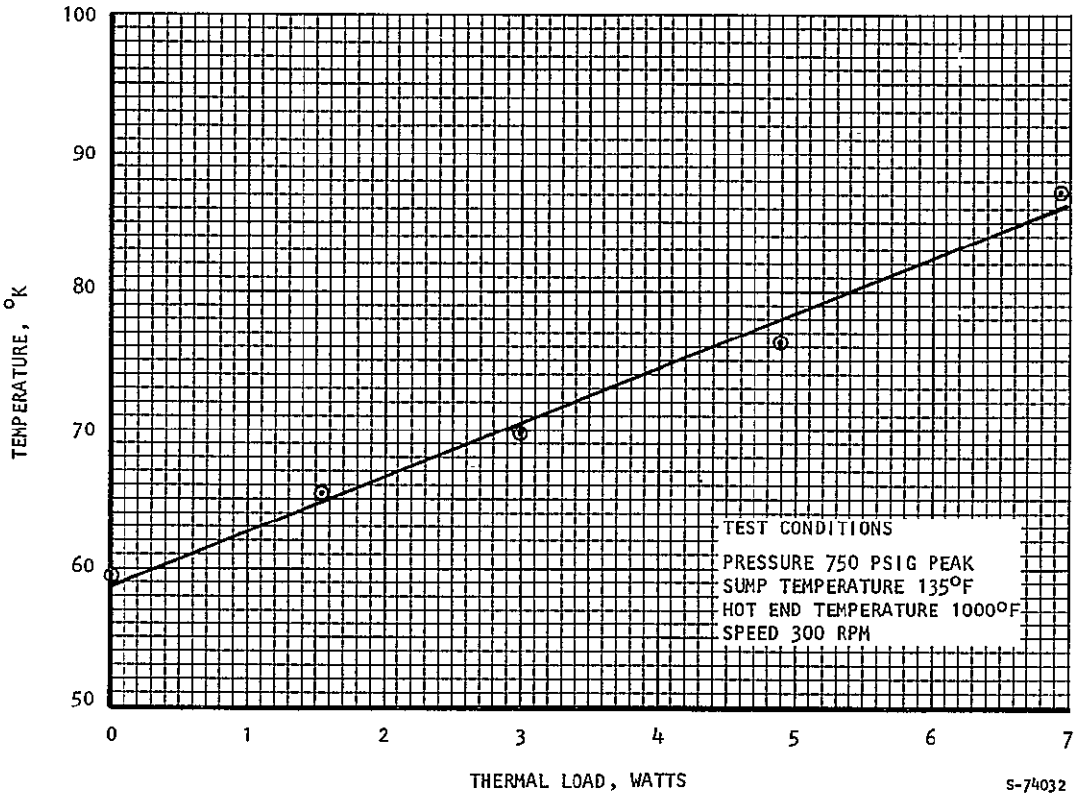

Figure 3-11. Performance Test No. 8

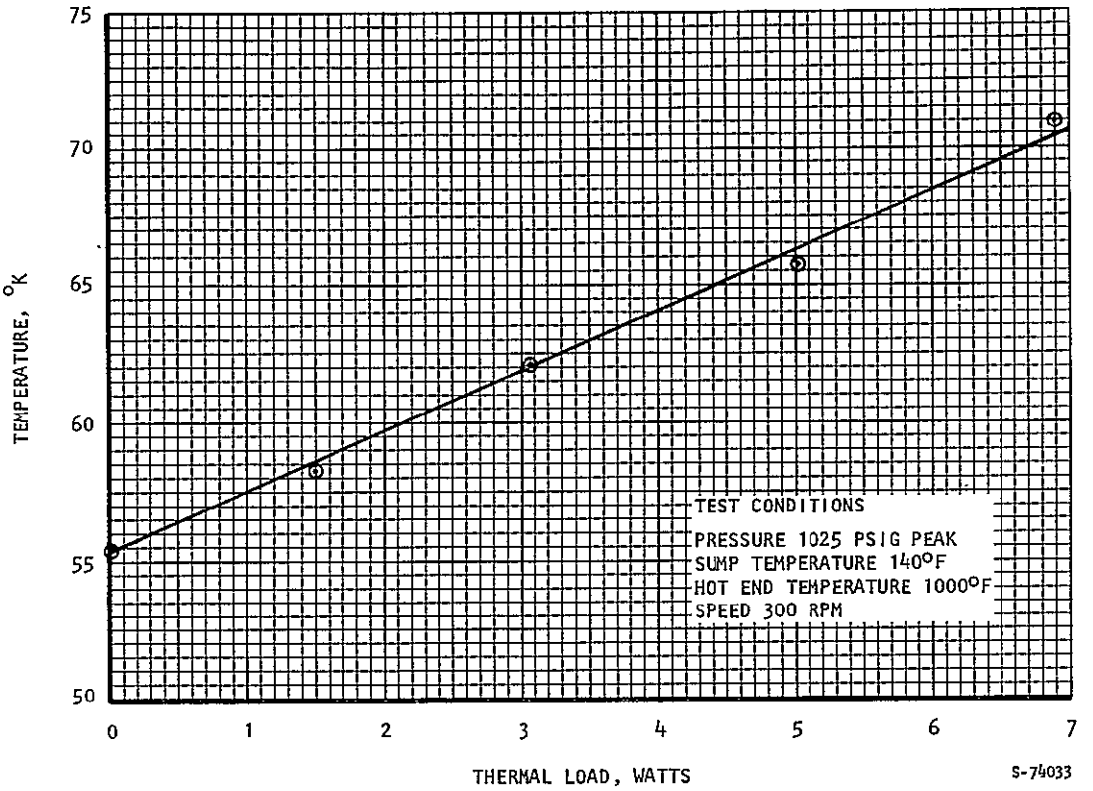

Figure 3-12. Performance Test No. 9

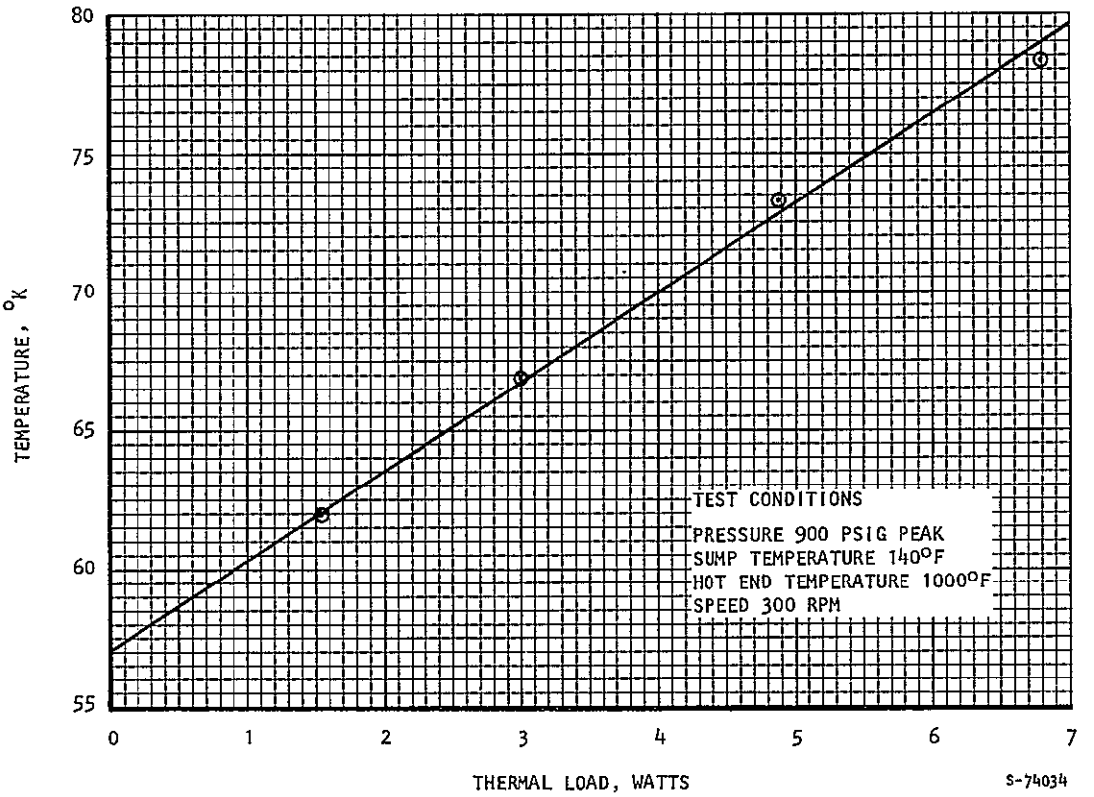

Figure 3-13. Performance Test No. 10

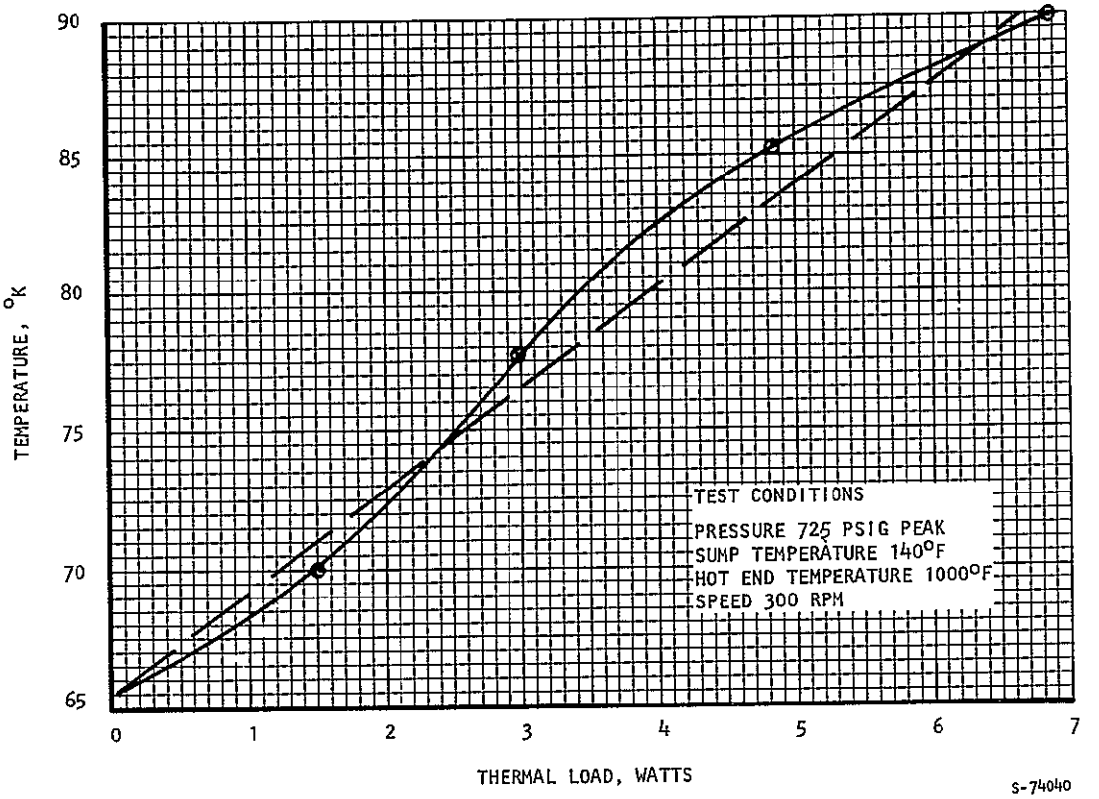

Figure 3-14. Performance Test No. 11

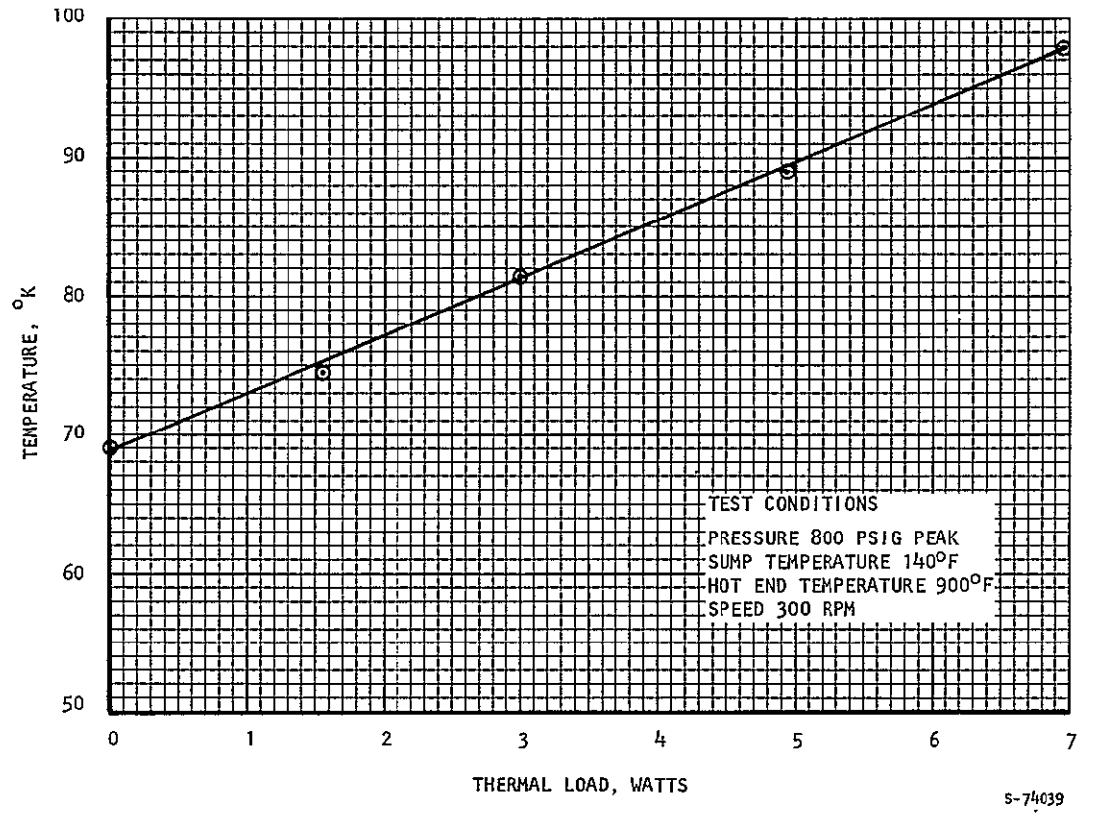

Figure 3-15. Performance Test No. 12

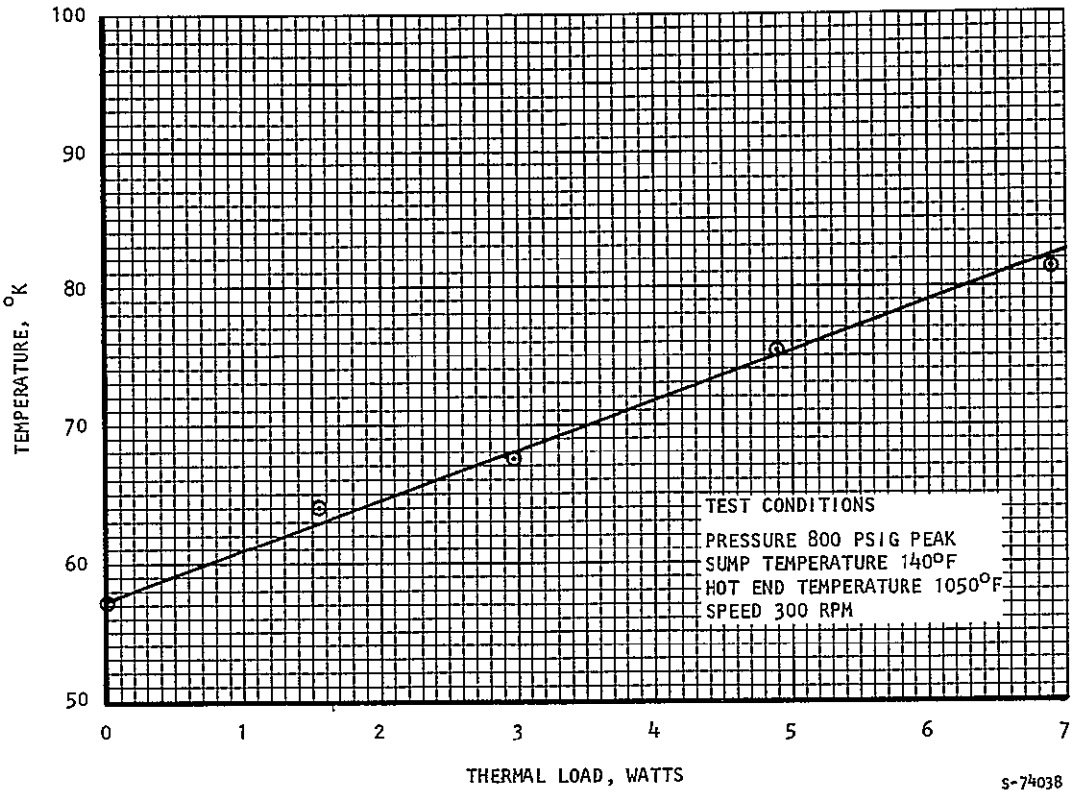

Figure 3-16. Performance Test No. 13

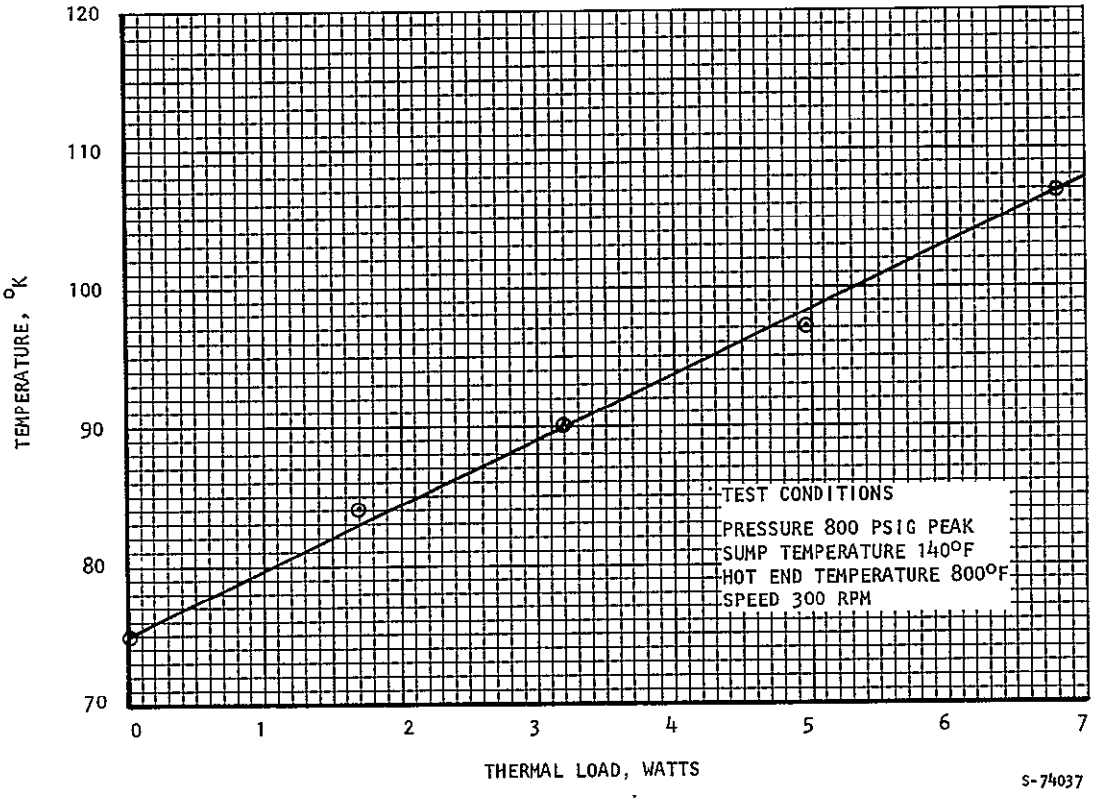

Figure 3-17. Performance Test No. 14

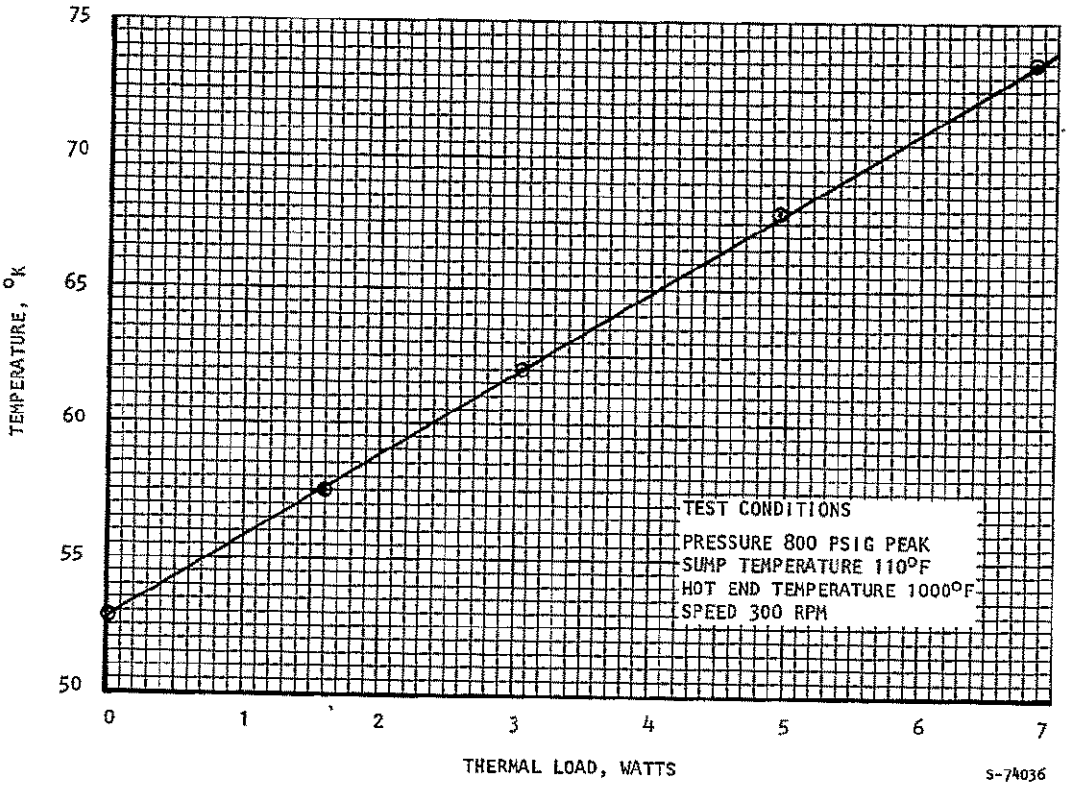

Figure 3-18. Performance Test No. 15

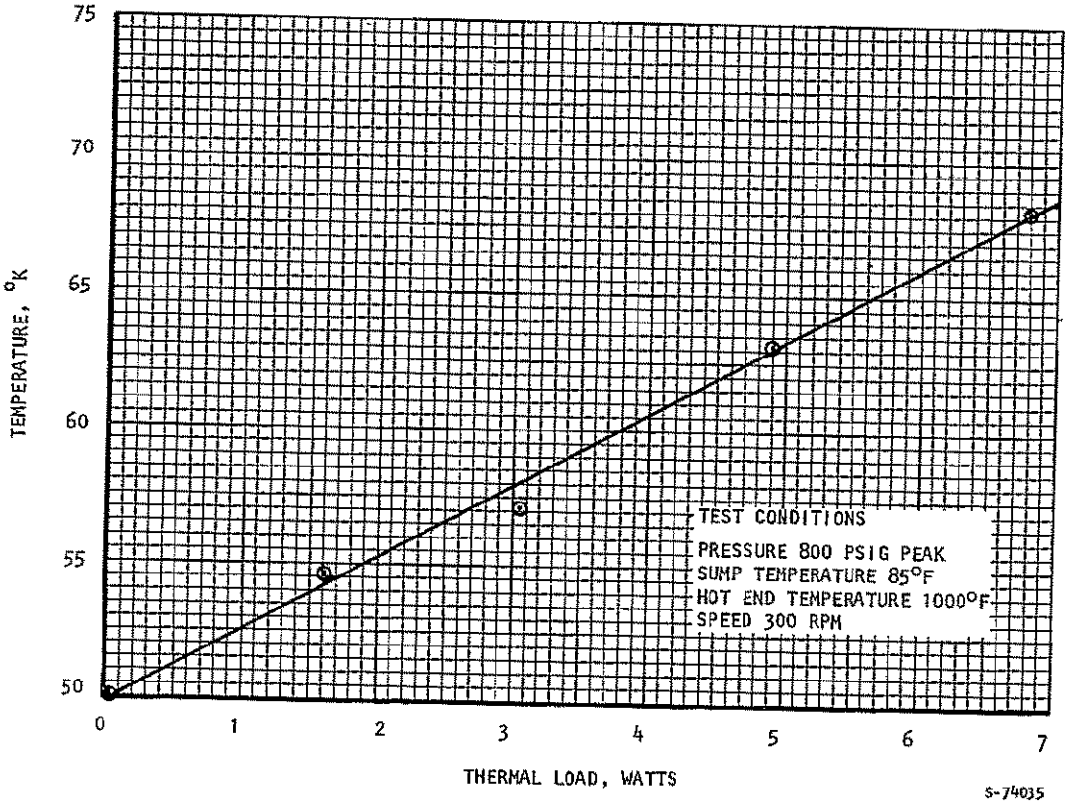

Figure 3-19. Performance Test No. 16

The Task II Final Report* also indicates a net refrigeration degradation over a two year operating period of 2.2 watts. This decrease is caused by cold end bearing wear, which allows increased working fluid leakage past the displacer. The bearing wear rates utilized in the leakage-calculation are also considered conservative. Thus it can be concluded that the refrigerator will produce greater than the required 5 watts of cooling after two years of continuous operation.

The hot-end heater control employed was of the on-off type, controlled by hot end temperature. Input power was measured during the "on" portion of the cycle. The hot-end temperature recording permits an estimation of the total amount of time the heater was on during the 7 watt portion of test 5, described above, and thus the average power input.

The VM was operated at this condition for 1-1/2 hours. The average hot-end heater input during this time period was 299 watts. This input, coupled with the 7 watts of refrigeration, yields a coefficient of performance of 0.0234. The hot-end heat input per watt of refrigeration is 42.7 watts at a refrigeration temperature of 72°K. This is believed to be the lowest value of heat input per watt of refrigeration ever attained with a Vuilleumier cycle refrigerator.

If the results of test number 5 are extrapolated to a refrigeration temperature of 75°K, the resulting cold end heat is 8.15 watts. This translates to a heat input per watt of refrigeration of 36.7 watts.

Off-Design Performance

The 16 tests performed on the GSFC 5-watt Vuilleumier cryogenic refrigerator (Figures 3-4 through 3-19) covered a wide range of operating conditions and show the linear dependence of cold-end temperature on refrigeration load. Results of these tests have been cross plotted to ascertain the effect of various operating parameters on performance. These cross plots are discussed in the following paragraphs.

1. Effect of Peak Cycle Pressure on Cold-End Temperature

The peak cycle pressure versus cold-end temperature plotted in Figure 3-22 is based on data from tests 4, 9, 10, and 11. The cold-end temperature is seen to decrease with increasing cycle pressure at a constant refrigeration level. The nonlinear relationship at low refrigeration levels is not as would be predicted from ideal considerations. Prediction of this peak pressure cold end

*C. W. Browning, V. L. Potter, Final Report for Task II, Analytical and Test Program for 75°K Vuilleumier Cryogenic Refrigerator

GSFC VM FINAL DESIGN PARAMLTERS 3 14 72 DATE = 14 MAR 72 TIME = 13:30:17

OPERATING PARAMETERS

COLD VOLUME TEMP.	= 125.00	R
SUMP VOLUME TEMP.	= 620.00	R
HOT VOLUME TEMP.	= 1630.00	R
COLD REGEN. TEMP.	= 372.00	R
HOT REGEN. TEMP.	= 1125.00	R
COLD DISPLACED VOL.	= .25110	CU-IN
HOT DISPLACED VOL.	= 6.84100	CU-IN
COLD DEAD VOL.	= .16438	CU-IN
SUMP DEAD VOL.	= 8.80395	CU-IN
HOT DEAD VOL.	= 2.05000	CU-IN
COLD REGEN. VOL.	= 3.11210	CU-IN
HOT REGEN. VOL.	= 8.14030	CU-IN
GAS CONSTANT	= 4634.40	IN-LB/LBM-R
SPEED	= 400.00	RPM
CHARGE PRESSURE	= 550.00	PSIA
CHARGE TEMPERATURE	= 535.00	R
MASS OF FLUID	= .0063	LBM
TOTAL VOLUME	= 29.36283	CU-IN

PRESSURE - MASS - FLOW PROFILE

ANGLE DEG	PC PSIA	PA PSIA	PH PSIA	VC CU-IN	VA CU-IN	VH CU-IN	MDOTC LB/SEC	MDOTA LB/SEC	MDOTH LB/SEC	MDOTRCA LB/SEC	MDOTRHA LB/SEC
24.	777.83	777.83	777.83	.1752	11.0737	6.8615	.00319	-.02614	.01545	.00716	.01899
48.	797.09	797.09	797.09	.2059	9.8925	8.0121	.00533	-.02187	.01168	.00790	.01397
72.	806.13	806.13	806.13	.2511	9.1360	8.7233	.00643	-.01264	.00517	.00698	.00566
96.	802.67	802.67	802.67	.3030	8.9350	8.8724	.00615	-.00055	-.00254	.00453	-.00398
120.	787.61	787.61	787.61	.3527	9.3244	8.4334	.00458	.01126	-.00946	.00120	-.01246
144.	764.61	764.61	764.61	.3915	10.2366	7.4823	.00221	.02004	-.01403	-.00214	-.01790
168.	738.65	738.65	738.65	.4127	11.5142	6.1835	-.00035	.02439	-.01565	-.00479	-.01960
192.	714.49	714.49	714.49	.4128	12.9362	4.7615	-.00260	.02431	-.01454	-.00639	-.01792
216.	695.75	695.75	695.75	.3916	14.2569	3.4619	-.00427	.02060	-.01134	-.00691	-.01369
240.	684.75	684.75	684.75	.3528	15.2480	2.5096	-.00525	.01423	-.00676	-.00642	-.00781
264.	682.65	682.65	682.65	.3032	15.7382	2.0690	-.00549	.00614	-.00140	-.00509	-.00105
288.	689.66	689.66	689.66	.2512	15.6428	2.2164	-.00498	-.00287	.00421	-.00305	.00592
312.	705.06	705.06	705.06	.2060	14.9782	2.9262	-.00374	-.01190	.00948	-.00048	.01238
336.	727.11	727.11	727.11	.1753	13.8593	4.0758	-.00182	-.01981	.01370	.00237	.01744
360.	752.78	752.78	752.78	.1644	12.4796	5.4664	.00061	-.02510	.01599	.00511	.01999

IDEAL REFRIGERATION AND HEAT INPUT

REFRIGERATION	= 17.9516	WATTS
THERMAL HEAT	= 108.5229	WATTS
MAX. PRESSURE	= 806.4589	PSIA

Figure 3-20. Ideal VM Cycle Computer Program Output for Nominal Design Conditions

GSFC 5 WATT VM, CONDITIONS OF TEST NUMBER 5 AT 7 WATTS

DATE = 18 AUG 72 TIME = 10:29:16

OPERATING PARAMETERS

COLD VOLUME TEMP,	= 125,20	R
SUMP VOLUME TEMP.	= 620,00	R
HOT VOLUME TEMP,	= 1430,00	R
COLD REGEN, TEMP.	= 372,60	R
HOT REGEN, TEMP,	= 1025,00	R
COLD DISPLACED VOL,	= ,25110	CU-IN
HOT DISPLACED VOL,	= 6,84100	CU-IN
COLD DEAD VOL,	= ,16438	CU-IN
SUMP DEAD VOL,	= 8,80395	CU-IN
HOT DEAD VOL,	= 2,05000	CU-IN
COLD REGEN, VOL,	= 3,11210	CU-IN
HOT REGEN, VOL,	= 8,14030	CU-IN
GAS CONSTANT	= 4634,40	IN-LB/LBM-R
SPEED	= 365,00	RPM
CHARGE PRESSURE	= 583,13	PSIA
CHARGE TEMPERATURE	= 535,00	R
MASS OF FLUID	= ,0067	LBM
TOTAL VOLUME	= 29,36283	CU-IN

PRESSURE - MASS - FLOW PROFILE

ANGLE DEG	PRESS PSIA	VC CU-IN	VA CU-IN	VH CU-IN	MDOTC LB/SEC	MDOTA LB/SEC	MDOTH LB/SEC	MDOTRCA LB/SEC	MDOTRHA LB/SEC
20.	786.26	,1719	11,2983	6,6402	,00251	-,02566	,01644	,00590	,01975
40.	802.01	,1937	10,2479	7,6688	,00430	-,02309	,01378	,00683	,01626
60.	812.01	,2271	9,4509	8,4324	,00555	-,01702	,00898	,00681	,01022
80.	814,58	,2681	9,0035	8,8389	,00600	-,00828	,00273	,00577	,00251
100.	809.26	,3117	8,9595	8,8392	,00556	,00166	-,00390	,00388	-,00554
120.	796,99	,3527	9,3244	8,4334	,00434	,01104	-,00976	,00149	-,01253
140.	779,78	,3861	10,0540	7,6704	,00258	,01842	-,01397	-,00097	-,01745
160.	760,19	,4079	11,0605	6,6421	,00062	,02294	-,01611	-,00314	-,01979
180.	740,83	,4155	12,2224	5,4725	-,00128	,02439	-,01618	-,00478	-,01960
200.	723,89	,4079	13,3998	4,3027	-,00290	,02304	-,01444	-,00578	-,01726
220.	711.02	,3862	14,4505	3,2737	-,00412	,01938	-,01132	-,00612	-,01326
240.	703,54	,3528	15,2480	2,5096	-,00489	,01396	-,00720	-,00583	-,00813
260.	701,41	,3118	15,6961	2,1025	-,00516	,00731	-,00248	-,00500	-,00232
280.	705,39	,2682	15,7408	2,1014	-,00495	-,00007	,00250	-,00367	,00374
300.	714,97	,2273	15,3766	2,5066	-,00423	-,00765	,00737	-,00195	,00960
320.	729,41	,1938	14,6475	3,2691	-,00303	-,01481	,01171	,00007	,01474
340.	747,42	,1720	13,6414	4,2970	-,00141	-,02079	,01503	,00222	,01857
360.	767,14	,1644	12,4796	5,4664	,00050	-,02469	,01677	,00426	,02043

IDEAL REFRIGERATION AND HEAT INPUT

REFRIGERATION = 14,9054 WATTS
THERMAL HEAT = 97,5156 WATTS
MAX, PRESSURE = 814,7000 PSIA AT ANGLE = 76,46 DEGREES

Figure 3-21. VM Cycle Computer Program Output for 7-Watt Design Conditions

TABLE 3-3

IDEAL VUILLEUMIER CYCLE ANALYSIS
NOMENCLATURE KEY

Symbol	Definition
PC	Pressure in cold displaced volume
PA	Pressure in ambient volume
PH	Pressure in hot displaced volume
VC	Cold displaced volume
VA	Ambient displaced volume
VH	Hot displaced volume
MDOTC	Flow rate into cold volume
MDOTA	Flow rate into ambient volume
MDOTH	Flow rate into hot volume
MDOTRCA	Flow rate into cold regenerator at the end toward the sump
MDOTRHA	Flow rate into hot regenerator at end toward the sump

temperature characteristic which accounts for all internal losses, requires use of a computer program such as the one possessed by GSFC.* Prediction of this characteristic was not attempted for this report.

2. Effect of Hot-End Temperature on Cold-End Temperature

The hot-end temperature versus cold-end temperature plotted in Figure 3-23 is based on data from tests 4, 12, 13, and 14. As expected, cold-end temperature decreases as hot-end temperature increases.

3. Effect of Refrigerator Speed on Cold-End Temperature

The refrigerator speed versus cold-end temperature plotted in Figure 3-24 is based on data from tests 4, 5, and 6. Cold-end temperature increases with decreasing speed, but not linearly. The figure illustrates, especially at higher heat loads, that a further decrease in refrigerator speed (below 250 rpm) would result in drastically reduced performance. As discussed earlier, bearing run-in friction prevented attainment of the 400 rpm design speed.

4. Effect of Sump Temperature on Cold-End Temperature

The sump temperature versus cold-end temperature plotted in Figure 3-25 is based on data from tests 4, 15, and 16. The cold-end temperature at a given refrigeration heat load increases with increasing sump temperature.

5. Test Data Deviation

Figure 3-23 indicates that test 4 (1000°F hot end) deviates from a linear relationship of cold end temperature vs hot end temperature. This deviation becomes greater at increasing refrigeration heat loads and indicates that the slope of the cold end temperature vs heat load characteristic, shown in Figure 3-7, is different from those of the other tests used in the preparation of Figure 3-23. This discrepancy is also evident in Figure 3-22. In view of this apparent discrepancy in the test data, it is recommended that the data of test 4 be verified by performing a test at duplicate conditions. It should be noted that the results of test 4 have been used in the preparation of Figures 3-22 through 3-25. Therefore all of these curves should be used with discretion until test 4 is verified.

Conclusions

The test results demonstrate conclusively that the refrigerator exceeds the required design point performance. The tests were performed during the bearing run in period, and exact duplication of the design point was thus not

---

*Mathematical Analysis of a Vuilleumier Refrigerator, by Allan Sherman NASA/GSFC. ASME Publication 71-WA/HT-33

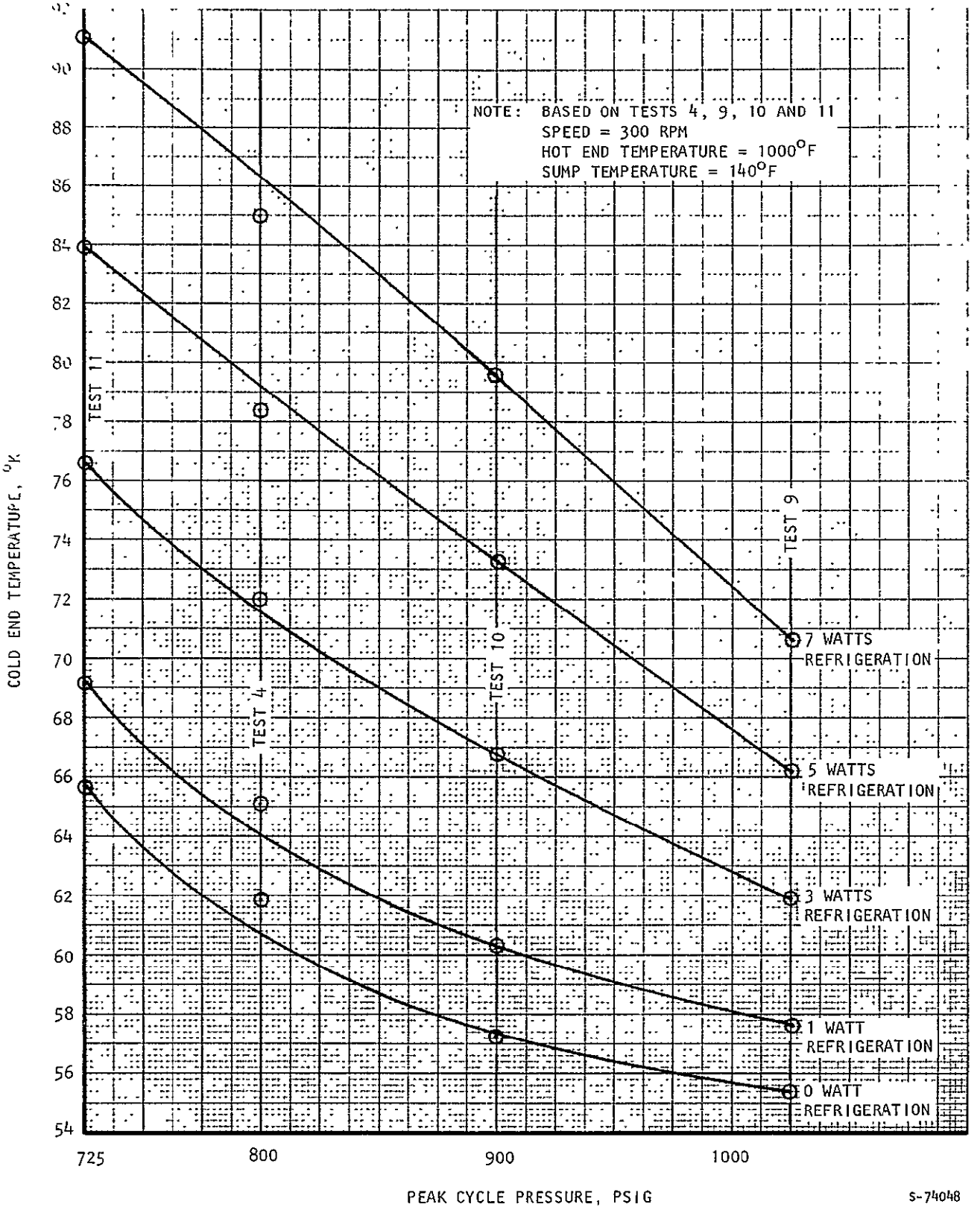

Figure 3-22. Effect of Peak Cycle Pressure on Cold-End Temperature

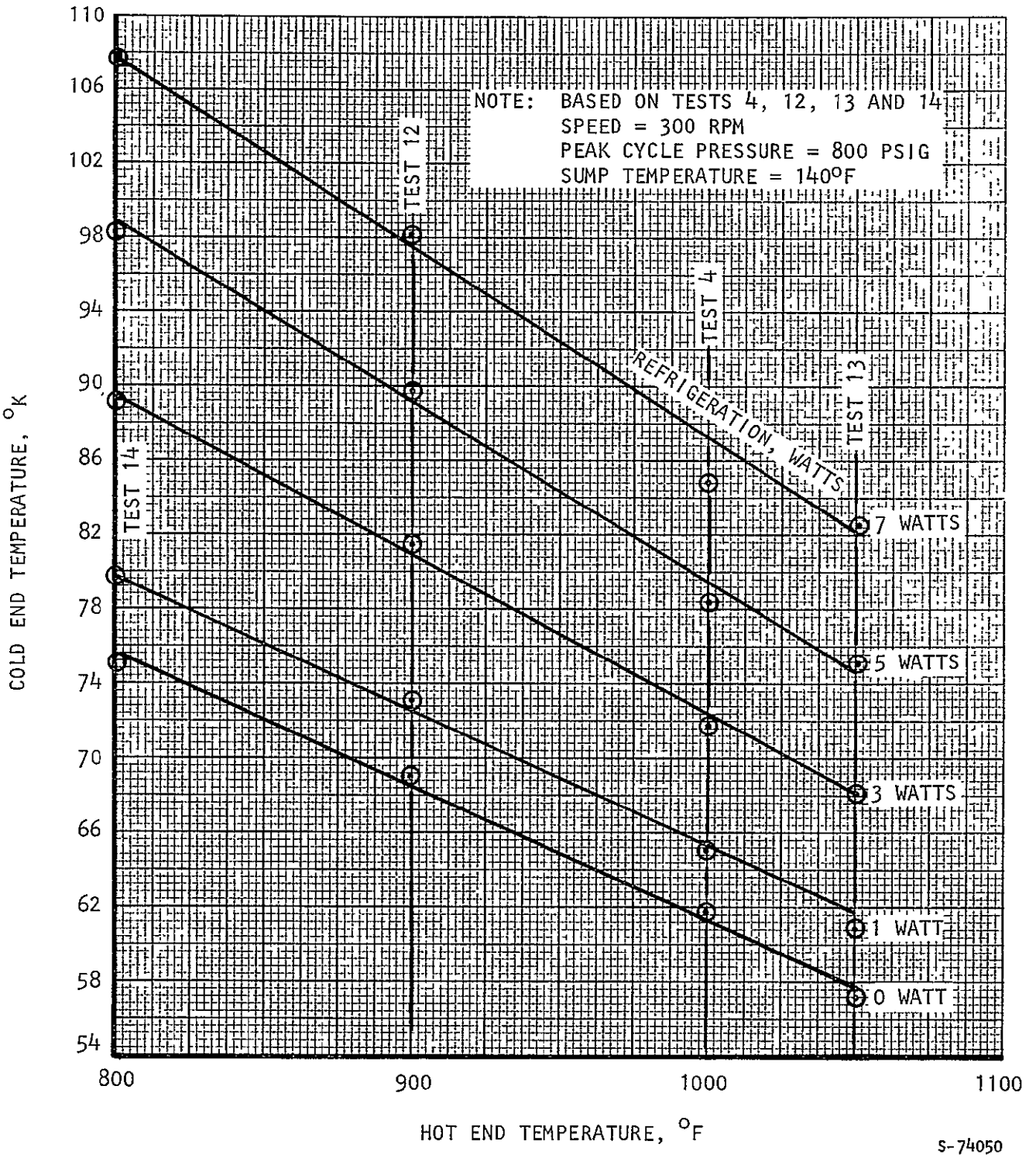

Figure 3-23. Effect of Hot-End Temperature on Cold-End Temperature

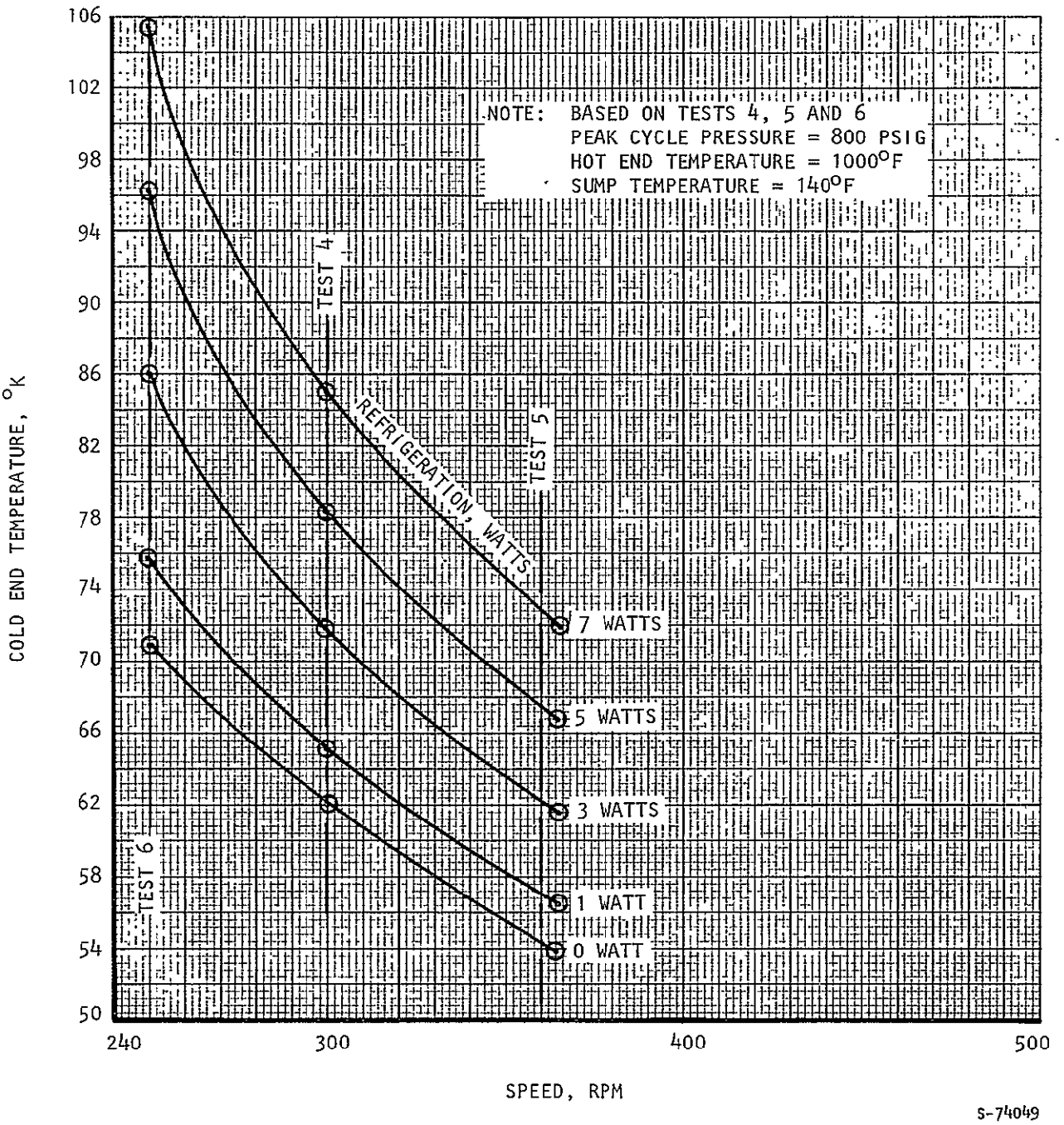

Figure 3-24. Effect of Speed on Cold-End Temperature

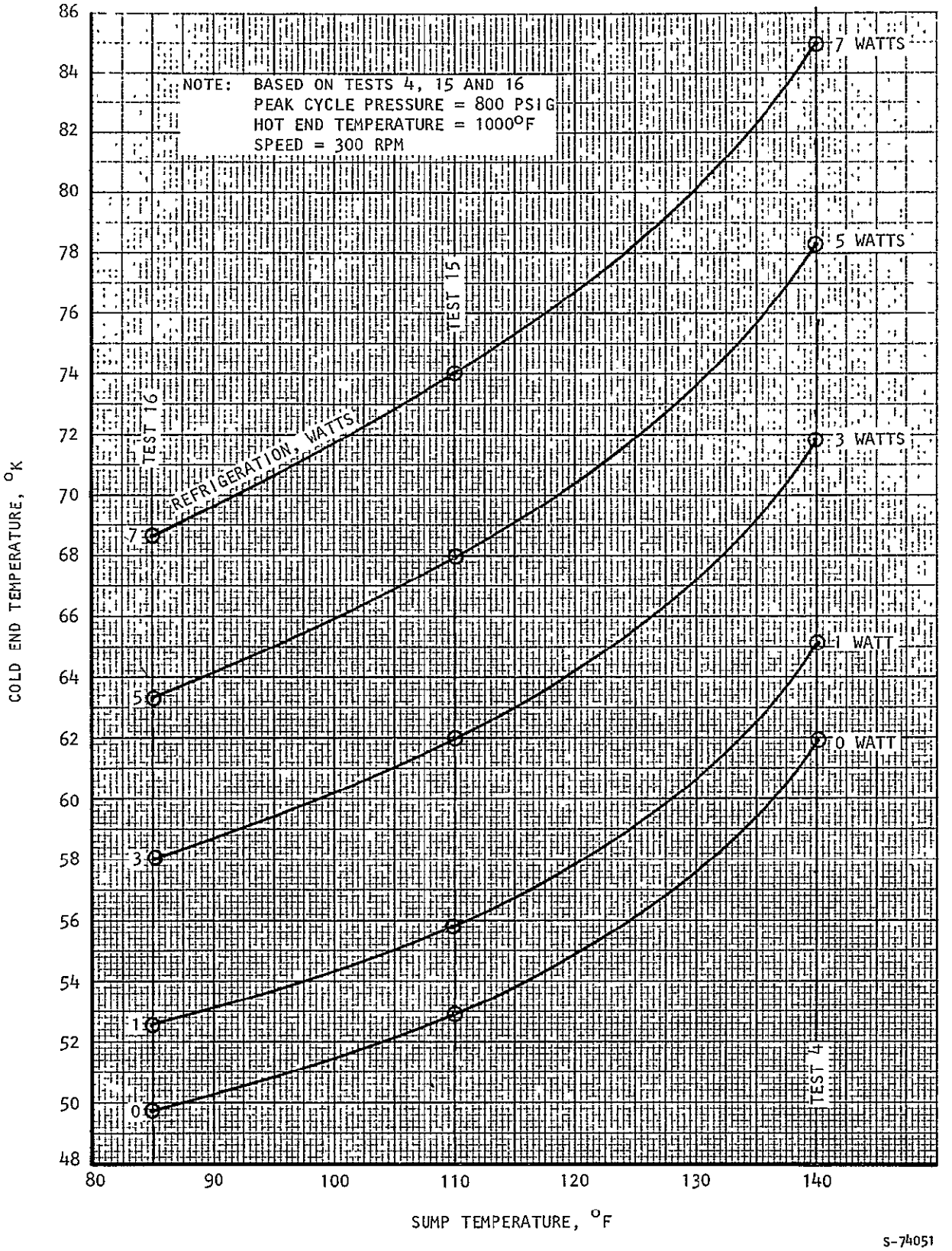

Figure 3-25. Effect of Sump Temperature on Cold-End Temperature

possible. However, one test conducted with engine speed, hot end temperature and cold end temperature below design values produced design point refrigeration. It is estimated that the machine is capable of producing approximately 10 watts of refrigeration at the design point. AiResearch has full confidence that the required 5-watt refrigeration capacity after 2 years of operation will also be exceeded. The thermal efficiency is believed to be the maximum ever attained with a Vuilleumier cycle-refrigerator.

The test results allow determination of performance over a wide range of VM operating parameters. The off-design performance curves presented in this report should be used with caution until the results of the one questionable test are verified.

The internal cold end losses of the machine are also less than calculated. This was expected since conservative assumptions were used in the loss calculations.

AiResearch has full confidence in extending the technology developed under this contract to a flight-type Vuilleumier cryogenic refrigerator.

APPENDIX A

GSFC 5 WATT VUILLEUMIER REFRIGERATOR TEST DATA

TABLE A-I
TEST DATA SUMMARY
VM PERFORMANCE DURING BREAKIN PERIOD

Test No.	Date 1972	Total Time, hr	Motor		Hot End		Cold End		Pressure		Nominal Sump Temperature, °F	Remarks
			rpm	watts	°F	watts	°K	watts	Peak psig	ΔP psig		
	3/7	1	100	Wattmeter readings incorrect	R.T.			0	200		≈75°F - Temperature Not Monitored	
	3/7	3	140		R.T.			0	200			
	3/8		250		R.T.			0	200			
	3/14		300		400	200 cycled		0	200			
	3/15		300	44	400	200	200	0	300	40		
	3/15		300	50	600	200	160	0	300	40		
	3/16		350	54	700	200	133	0	300	45		
	3/17		300	52	900	200	115	0	300			
	3/18		300	51	950	275	101	0	300	45		
	3/20	100	360	57	950	250	119	0	300	45		
	3/20		300	66	975	250	119	0	300	45		
	3/21	118	300	40	980	275	150	0	200			
	3/22	127	300	40	900	275		0	325			
	3/23	135	300	40	900	275	66	0	550	85		
	3/24		300	39	900	275	54	0	700	110		
	3/27											
	3/28	184.8	300	32	900	225	72	0	500	80		
	3/29	208.5	300	30	900	260	55.5	0	685	100		
	3/30	232.5	300	32	900	275	53.4	0	700	110		
	3/30		300	35	900	275	50.5	0	800	110		
	4/3	291.0	300	29	925	250	80.5	0	400	70		
	4/4	298.0	300	36	900	250	55.5	0	625	100		
	4/5	315	300	36	900	260	51.4	0	685	110		
	4/5	318.5	300	42.5	900	280	48.0	0	840	150		
	4/5	320.5	300	42	900	280	48.4	0.5	840	150		
	4/5	321.4	300	41.5	900	280	49.6	1.0	840	150		
	4/5	322.9	300	42	900	280	51.45	2.0	840	150		
	4/5	323.8	300	42	900	280	56.1	3.0	840	150		
	4/5	324.8	300	42	900	280	63.0	4.0	840	150		
	4/5	325.7	300	40	900	280	78.0	5.0	840	150		Data point questionable
	4/6	338.7	300	37.5	900	280	47.8	0	815	150		Data point questionable
	4/6	340.2	300	37.5	900	280	59.7	3.75	815	150		Data point questionable
	4/6	342.2	300	37.5	900	280	64.0	4.875	825	150		Data point questionable
	4/6	343.5	300	40	900	280	68.6	6.85	825	150		Data point questionable
1	4/7	363.2	308	45	900	300	50	0	900	160		
	4/7	369.7	300	43	900	300	55	2.10	900	160		Potentiometer recalibrated
	4/7	371.1	295	41	900	300	62.1	4.70	900	160		
	4/7	373.1	306	43	900	300	64.2	6.70	900	160		
2	4/6	345.9	300	40	900	280	56.1	2.825	800	150		
	4/6	346.9	300	37.5	900	280	60.0	2.9	800	150		
	4/6	348	300	39	900	280	71	6.95	800	150		
	4/6	349.5	300	39	900	280	62.1	4.02	800	150		Questionable cold end temp
	4/6	353.5	300	36	900	280	52.2	0	800	150		

TABLE A-1

TEST DATA SUMMARY
(Continued)

Test No.	Date 1972	Total Time, hr	Motor		Hot End		Cold End		Pressure		Nominal Sump Temperature, °F	Remarks
			rpm	watts	°F	watts	°K	watts	Peak psig	ΔP psig		
3	5/18	874.8	300	42.5	926	300	51	0	850	175	85	
	5/18	875.2	300	42	933	300	54.4	1.5	850	175	85	
	5/18	875.7	300	45	946	300	57.2	2.98	850	175	85	
	5/18	876.4	300	43	958	300	62.2	4.9	850	175	85	
	5/18	876.8	300	45	964	300	65.4	6.85	850	175	85	
4	5/4	803.2	300	42	961	300	71.75	3.0	800	150	140	
	5/4	804.8	300	45	979	300	77.4	4.95	800	150	140	
	5/4	805.4	300	44.5	980	306	85.0	7.1	800	150	140	
	5/4	807.8	300	40.5	983	298	67.2	1.5	800	150	140	
5	5/5	825.5	365	52.5	989	375	54.4	0	800	150	140	
	5/5	826.2	370	52.0	988	375	57.2	1.5	800	150	140	
	5/5	826.8	370	51.0	948.5	375	61.7	2.94	800	150	140	
	5/5	827.7	360	55.5	985	372	66.1	4.95	800	150	140	
	5/5	829.1	355	51.0	996	375	72.2	6.90	800	150	140	
6	5/26	1008.4	250	25	999	240	74.4	0	800	150	140	
	5/26	1009.9	250	25	999	245	80.9	1.48	805	155	140	
	5/26	1010.9	250	25.5	1001	240	87.9	3.1	820	170	140	
	5/26	1012.6	250	25	1009	250	97.2	4.95	830	180	140	
	5/26	1013.9	250	26	1004	245	108	6.85	840	170	140	
7	5/18	878.1	300	38	992	300	54.4	0	850	175	105	
	5/18	878.5	300	44	972	300	56.7	1.6	850	175	105	
	5/18	878.9	300	40	979	300	60	3.08	850	175	105	
	5/18	879.4	300	40	987	300	66.7	4.9	875	175	105	
	5/18	880.1	300	42.5	984	300	70	6.85	875	175	105	
8	5/18	880.9	300	35	975	295	59.5	0	750	125	135	
	5/18	881.3	300	36	989	296	65.5	1.55	750	125	135	
	5/18	881.9	300	36	983	300	70.0	3.0	750	125	135	
	5/18	882.6	300	37	984	302	76.7	4.90	750	125	135	
	5/18	883.6	300	35	992	301	87.2	6.95	750	125	135	
9	5/19	897.7	300	40	979	330	55.5	0	1000	200	140	
	5/19	898.3	300	36	992	330	58.4	1.5	1000	200	140	
	5/19	898.8	300	36	997	330	62.2	3.08	1000	200	140	
	5/19	899.3	300	37	997	330	65.8	5.02	1025	200	140	
	5/19	899.8	300	39	987	330	71	6.9	1025	200	140	
10	5/19	901.5	300	35.5	988	315	54.6	0	900	175	140	
	5/19	902.1	300	35	992	315	62	1.55	900	175	140	
	5/19	902.6	300	35	996	315	67	3.0	900	175	140	
	5/19	903.7	300	35	996	315	73.4	4.9	900	175	140	
	5/19	903.8	300	34	999	315	78.4	6.8	900	175	140	

TABLE A-I

TEST DATA SUMMARY
(Continued)

Test No.	Date 1972	Total Time, hr	Motor		Hot End		Cold End		Pressure		Nominal Sump Temperature, °F	Remarks
			rpm	watts	°F	watts	°K	watts	Peak psig	ΔP psig		
11	5/22	915.3	300	36	987	300	65.5	0	725	150	140	
	5/22	916.4	300	37	998	300	70	1.5	725	150	140	
	5/22	917.7	300	36	1000	290	77.8	2.98	725	150	140	
	5/22	918.8	300	36	989	292	85.3	4.85	750	150	140	
	5/22	920.1	300	36	990	293	90	6.90	750	150	140	
12	5/23	941.1	300	35	903	300	69.2	0	800	150	140	
	5/23	941.9	300	34	899	300	74.8	1.55	800	150	140	
	5/23	943.3	300	36	906	300	81.7	3.0	800	150	140	
	5/23	944.5	300	36	903	300	89	4.95	800	150	140	
	5/23	946	300	37	891	300	98	6.95	800	150	140	
13	5/23	935.1	300	40	1038	330	57.1	0	820	170	140	
	5/23	936.8	300	37.5	1053	330	64	1.55	825	175	140	
	5/23	937.7	300	39	1042	330	67.8	2.97	825	175	140	
	5/23	939	300	33	1040	330	75.5	4.9	825	175	140	
	5/23	940	300	38	1047	330	81.6	6.9	840	190	140	
14	5/24	960.2	300	33	802	245	75	0	800	150	140	
	5/24	962.5	300	33	803	230	84	1.70	800	150	140	
	5/24	963.9	300	33	800	235	90	3.18	810	160	140	
	5/24	965.4	300	32	799	230	97.2	4.98	820	170	140	
	5/24	966.4	300	32	799	230	107	6.8	810	160	140	
15	5/25	989.3	300	34	998	310	52.8	0	800	150	110	
	5/25	989.9	300	35	1003	290	57.5	1.6	800	150	110	
	5/25	990.5	300	38	1003	290	62.2	3.05	815	165	110	
	5/25	991.5	300	39	1007	290	68.0	4.95	820	170	110	
	5/25	992.3	300	39	1009	300	73.6	6.88	820	170	110	
16	5/25	983.8	300	35	996	320	50	0	800	150	85	
	5/25	984.7	300	36	995	325	54.7	1.6	800	150	85	
	5/25	985.7	300	38	1002	295	57.2	3.05	805	150	85	
	5/25	986.5	300	37	997	300	63.3	4.9	820	170	85	
	5/25	987.8	300	38	1001	300	68.3	6.8	820	170	85	